

Model for turbine B

Sandia Vertical-Axis Wind Turbine Program Technical Quarterly Report

October - December 1975

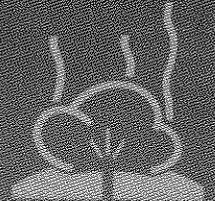
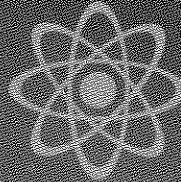
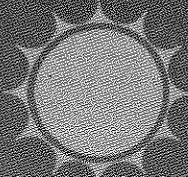
Advanced Energy Projects Division 5715
James F. Banas, William N. Sullivan, Editors

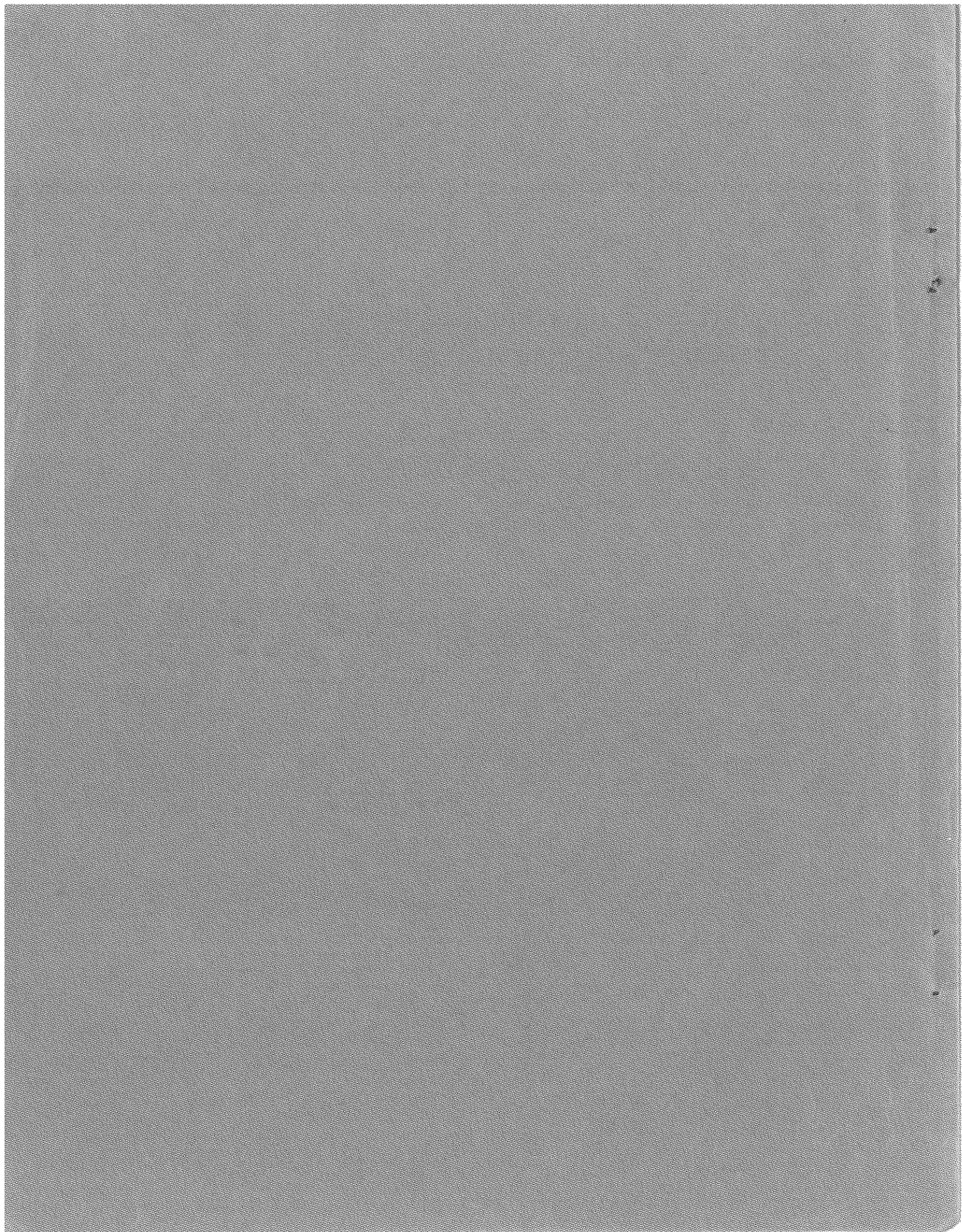
Prepared by Sandia Laboratories, Albuquerque, New Mexico 87115
and Livermore, California 94550 for the United States Energy Research
and Development Administration under Contract AT(29-1)-789

Printed April 1976



Sandia Laboratories
energy report





SANDIA VERTICAL-AXIS WIND TURBINE PROGRAM
TECHNICAL QUARTERLY REPORT
October-December 1975

Advanced Energy Projects Division 5715

Edited By

James F. Banas
Systems Analysis Division II, 5742

William N. Sullivan
Applied Mechanics Division III, 1284
Sandia Laboratories
Albuquerque, New Mexico 87115

ABSTRACT

This quarterly report describes the activities within the Sandia Laboratories Vertical-Axis Wind Turbine Program during the second quarter of fiscal year 1976. Included are the highlights of the quarter; review of the status of general design efforts in the areas of aerodynamics, structures, systems analysis, and testing; summary of preliminary design details of the proposed 17-m turbine/60-kW generator system for power grid application; and structural analysis and operational test results for the existing 5-m turbine.

Printed in the United States of America

Available from
National Technical Information Service
U. S. Department of Commerce
5285 Port Royal Road
Springfield, Virginia 22161
Price: Printed Copy \$6.50; Microfiche \$2.25

FOREWORD AND ACKNOWLEDGMENTS

The work covered in this quarterly report was performed by Sandia Laboratories under a contract administered by the Wind Energy Conversion Branch (Division of Solar Energy) of the Energy Research and Development Administration. The time period is primarily September 1, 1975, to December 31, 1975; however, some previously unreported efforts are also included.

The report was edited from the individual contributions of the following Sandia staff members:

J. F. Banas (Systems Studies, Aerodynamics)
B. F. Blackwell (Aerodynamics)
L. V. Feltz (Mechanical Design)
E. G. Kadlec (Test Facility)
R. C. Reuter (Tower Analysis, Blade RFQ)
R. E. Sheldahl (Wind Tunnel Tests)
W. N. Sullivan (Structural Loads, Synchronous Tests)
A. F. Veneruso (Electrical Design, Asynchronous Tests)
L. I. Weingarten (Blade Analyses)

Acknowledgment is also due the following Sandia personnel who contributed significantly to the hardware development aspects of this program:

R. C. Anderson
K. G. Grant
C. E. Longfellow
D. F. McNeill
R. S. Rusk

CONTENTS

	<u>Page</u>
FOREWORD AND ACKNOWLEDGMENTS	5
SUMMARY	7
PART I - GENERAL APPLICATIONS EFFORTS	9
Aerodynamic Studies	9
Aerodynamic Performance Models	10
Influence of Airfoil Properties	13
Structural Analysis	14
Blade Analyses	15
Tower Analysis	16
Systems Studies	19
System Application for the VAWT	19
Comparison of Wind Turbine Performance Characteristics	20
Synchronous Power Grid Application	24
Performance and Economic Evaluation of Synchronous Systems	26
Toward Economic Optimization	28
Test Program	33
Test Facility	33
Wind Tunnel Tests	36
PART II - SPECIFIC APPLICATIONS EFFORTS	41
The 17-m Turbine	41
Introduction	41
Performance Predictions	42
Structural Analysis	48
Structural Load Requirements	57
Mechanical Design	67
Electrical Analysis and Design	71
The 5-m Turbine	76
Introduction	76
Blade Structural Analysis	77
Synchronous Test Program	79
Asynchronous Test Program	83
References	86
APPENDIX A - 17-m Turbine Blade Request For Quotation (RFQ)	87
APPENDIX B - Synchronous Generator Request for Quotation (RFQ)	99
APPENDIX C - Sandia Publications and Presentations	107

SUMMARY

The basic concept of the Darrieus vertical-axis wind turbine¹ (VAWT) consists of fixed-pitch blades attached to a central, torque-transmitting shaft, as shown by the artist's conception. Preliminary investigations of this device²⁻⁴ have noted a number of potential advantages* over more conventional horizontal-axis systems. These advantages provided the motivation for establishing a program at Sandia to further investigate the feasibility of this turbine, particularly when used as an augmenting device to pump energy into an existing synchronous electrical network.

Based on the notion that feasibility can best be established through a balanced program of hardware and analytical development, a twofold interactive approach has been adapted. This technical approach involves: (1) the development of the necessary analyses and empirical experience to design large, megawatt-range turbine systems which are economically optimized; and (2) the use of this technical background as it is developing, in conjunction with the experience and manufacturing facilities of private industry, to design and construct a series of large, VAWT power generating systems. This series is to begin with a 17-m diameter turbine connected to a 60-kW synchronous generator.

This quarterly report will review the status of the major program activities as of December 31, 1975. The program highlights during this period may be briefly summarized:

A blade design and manufacturing request-for-quotation (RFQ) for the 17-m turbine was submitted to 58 potential suppliers. The response to the RFQ indicates that an aerospace company will be able to supply turbine blades meeting the necessary performance requirements on schedule.

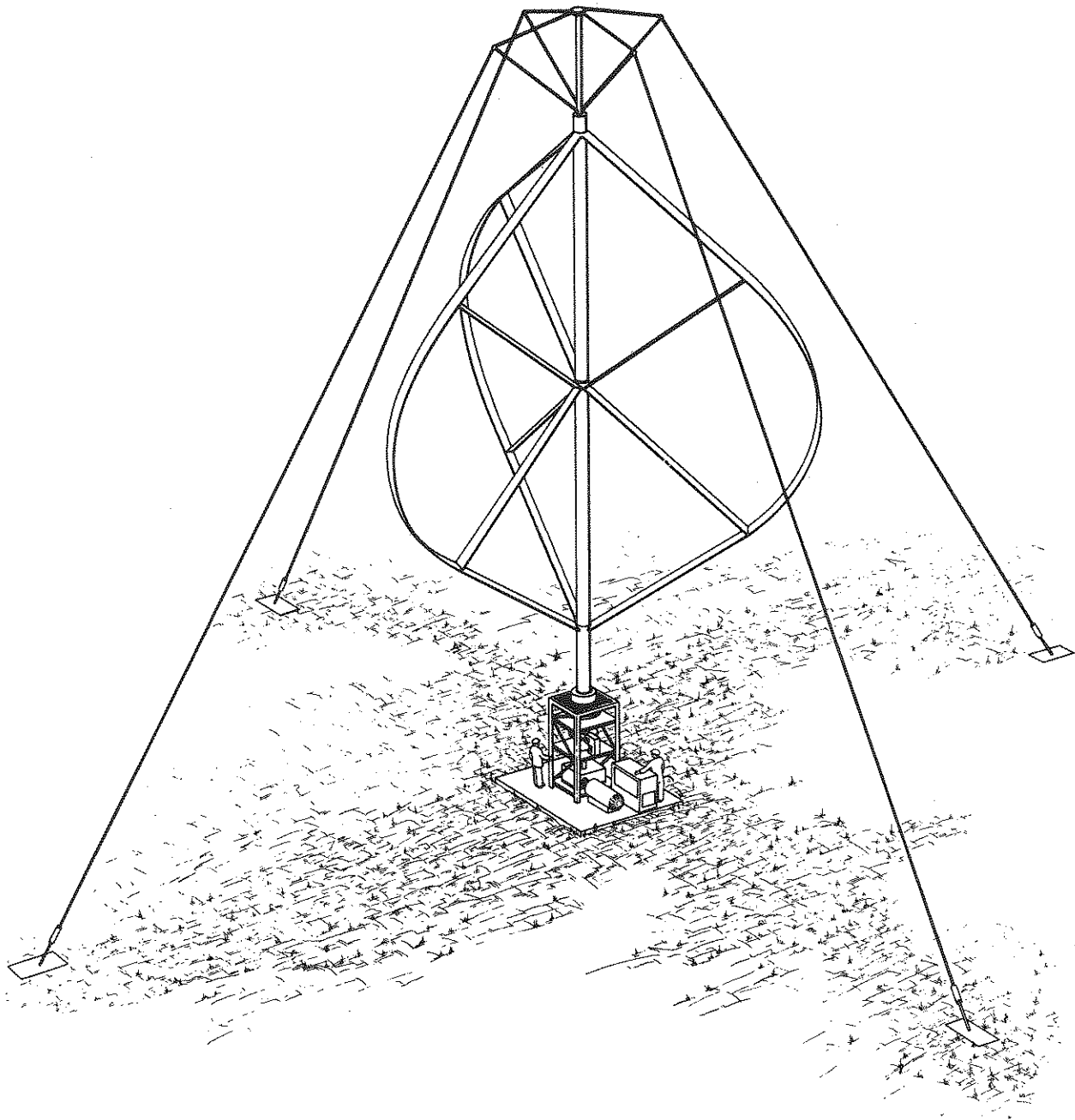
Preliminary structural analysis of the 17-m turbine has indicated that the design is structurally feasible. No insoluble structural design problems have yet been encountered.

Wind tunnel testing of 2-m model turbines has been completed. The results of these tests form a data base which is greatly expanded over that previously available and which has been invaluable for the verification of the aerodynamic performance models used in this program.

An outdoor wind energy test facility is now operational and is collecting field data on the Sandia 5-m test turbine.

For discussion of specific aspects of this program, this report is divided into two major sections. The first section, entitled "General Application Efforts," deals with the aerodynamic, structural, systems and testing programs which are intended to be of general use for designers of vertical-axis turbine power systems. A second section, "Specific Application Efforts," discusses the details of design and testing which are currently being carried out on the proposed 17-m and the existing 5-m turbines. Finally, Appendix A contains a copy of the blade RFQ, Appendix B contains a copy of the generator RFQ, and Appendix C provides a list of Sandia reports and presentations relevant to the program.

*These advantages are: yaw control is eliminated; the power production equipment can be placed at ground level; the machine is self-regulating when operated at constant rotational speed, and the structure is potentially lighter and thus probably lower in cost.



The 17-m Turbine - An Artist's Conception

SANDIA VERTICAL-AXIS WIND TURBINE PROGRAM
TECHNICAL QUARTERLY REPORT

PART I
GENERAL APPLICATIONS EFFORTS

Aerodynamic Studies

The primary goal of this effort is to establish a capability to reliably predict the aerodynamic performance of a wide variety of vertical-axis wind turbines. Aerodynamic blade loads are important inputs to the structural analysis and design of both the wind turbine blades and the supporting tower. Furthermore, the identification of optimum system designs requires knowledge of the effects on power coefficient by such parameters as turbine solidity and configuration, type of airfoil, and Reynolds number.

The aerodynamic studies can be conveniently divided into wind tunnel testing and development of analytic models. Wind tunnel testing is a relatively inexpensive and rapid means to obtain experimental performance data for a limited selection of turbines in order to verify and/or redirect the analytic models. Due, however, to physical limitations imposed by the size of available wind tunnels, rotational speed constraints imposed by turbine structures, and the need to examine a multitude of parameter variations, the design of large turbines must rely on predictions from analytic models. The following sections summarize analytic efforts to date.

The first section describes the single-streamtube and multiple-streamtube⁵ aerodynamic models. Both of these models are based on blade-element/momentum theory. The single-streamtube model presumes a uniform induced velocity to exist across the turbine disc, while the multiple-streamtube model allows for variations in the induced velocity. A fair agreement is found with experimental data, although several areas needing improvement are indicated.

The second section discusses the relative influence of airfoil properties on turbine performance. It is observed from using approximate airfoil data that minimum drag coefficient and maximum lift coefficient can substantially affect turbine efficiency, thereby providing some basis for the selection of candidate airfoils. Performance is significantly improved with increasing Reynolds number, which suggests the need for airfoil data at Reynolds numbers appropriate to larger turbines. Inherent Reynolds number variations along a blade and as a blade rotates appear to affect performance only moderately when approximate airfoil data is given a Reynolds number dependence.

Aerodynamic Performance Models

There are several models, ranging from very complex to reasonably simple, to investigate the aerodynamic performance of the VAWT. For example, a model could be based on vortex theory, which has been successfully used in propeller and wing design. However, because of the complicated structure of the resulting vortex system associated with the VAWT configuration, computer time required to carry out a solution appears to be excessive. This is an important consideration due to the desire to treat a large number of parameter variations.

Another approach is to visualize that the turbine is enclosed in a single streamtube. The wind velocity is assumed to be everywhere constant within the turbine. A relationship between the wind velocity in the streamtube through the turbine and the undisturbed freestream wind velocity can be established by equating the drag force on the turbine to the change in momentum of the fluid moving through the turbine. Using the induced velocity, that is, the combination of the streamtube velocity and the rotational velocity of the turbine, the forces on the blades can be computed. This single-streamtube model is basically the same as a model developed by R. J. Templin of the National Research Council of Canada.⁶ A solution can be found in a straightforward manner by choosing a value for the streamtube velocity; this allows the simultaneous computation of a power coefficient and a freestream velocity. While this approach is somewhat elegant in its simplicity and predicts overall performance rather well for lightly loaded blades, it is incapable of adequately predicting information which requires a more precise knowledge of wind velocity variations across the rotor. These variations become increasingly large as blade solidities and blade tip speeds increase. In addition, it does not appear that wind shear effects can be incorporated into the model.

A somewhat more sophisticated model than the single-streamtube model is one in which a number of streamtubes are assumed to pass through the rotor. The same basic principles which were applied to the single streamtube are now applied to each of the multiple streamtubes. The multiple-streamtube model gives rise to a velocity distribution through the rotor which is a function of the two spacial coordinates perpendicular to the streamwise direction. The multiple-streamtube model, while still somewhat inadequate in its description of the flow field, does predict overall performance very well, yields a more realistic distribution of blade forces, and has been used to study wind shear effects. The velocity in a given streamtube is found by means of an iterative numerical technique. Computing times for these models are small and comparable.

Figure 1 shows a comparison among the single-streamtube model, the multiple-streamtube model, and some early experimental data obtained with a 2-meter-diameter turbine. At low tip speed ratios where the turbine does not significantly disturb the air flow, the induced velocity is uniform and the two models give identical results. At high tip speed ratios, the induced velocity becomes nonuniform across the turbine disc and considerable differences appear. The results from the multiple-streamtube model are, in general, much closer to the experimental data. The remaining discrepancy can possibly be explained by Reynolds-number effects and the interference that an

upwind blade has on a downwind blade. An interference effect similar to that for a tandem rotor is being developed for future investigation. The section lift and drag characteristics are input in tabular form as a function of angle of attack. At the present time, the entire blade is assumed to operate at a constant Reynolds number. As additional section data become available, the code will be modified to handle the Reynolds-number variation (both as a function of blade position and location along the blade) by inputting tabular section data for several discrete Reynolds numbers and interpolating for intermediate values.

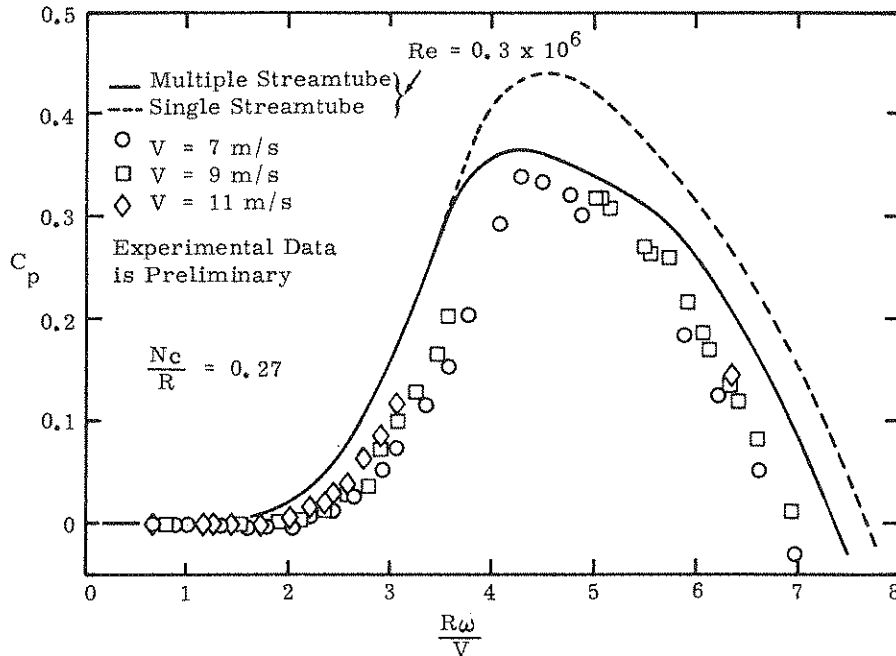


Figure 1. Comparison of Single-Streamtube Model and Multiple-Streamtube Model with Experimental Data

Figure 2 depicts an example of the variation of streamtube velocities across the turbine disc at a tip speed ratio of 3.5. The single-streamtube model for comparative purposes predicts a constant value for the ratio of streamtube velocity to freestream velocity of 0.756.

Figure 3 shows a comparison between power coefficients for a turbine with or without wind shear included. To account for wind shear, the common 1/7 power freestream velocity profile was used. The difference between the two curves is small when the centerline or equatorial freestream velocity is used as the basis for computing the power coefficient.

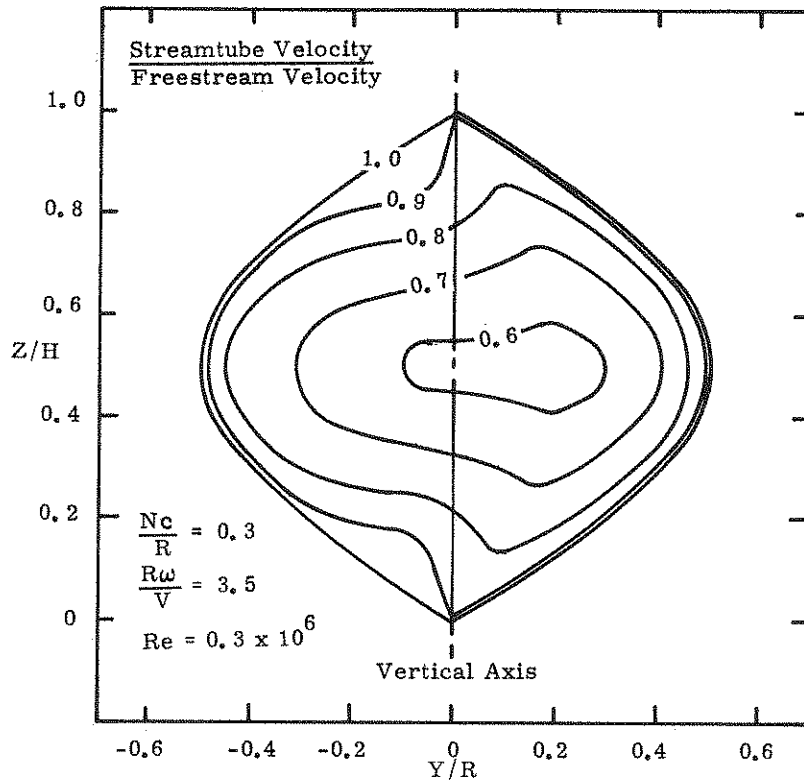


Figure 2. Variation of Streamtube Velocities Through the Rotor (view looking upstream through the rotor)

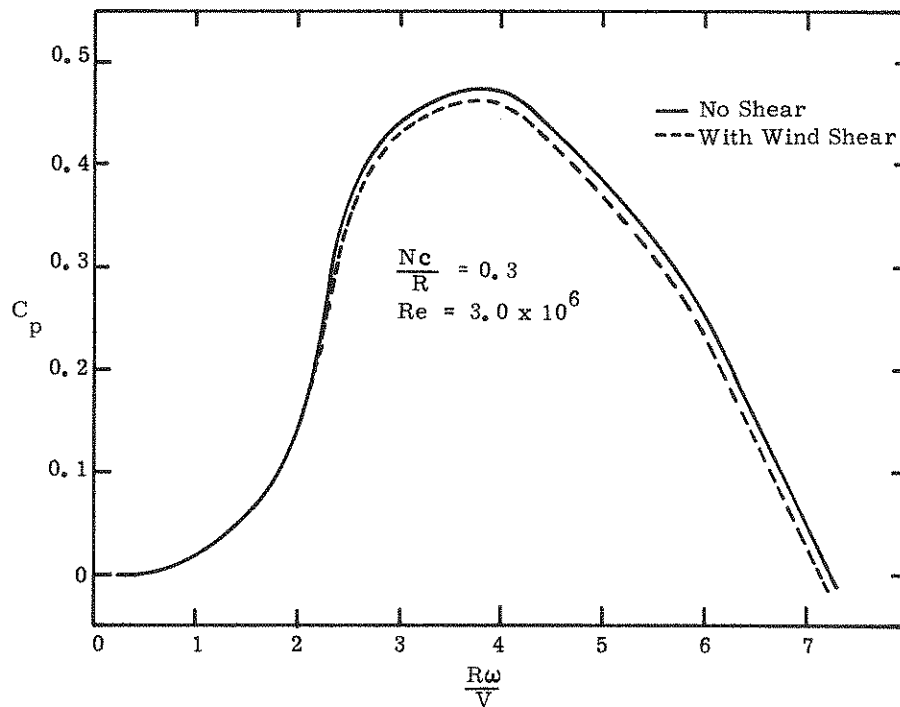


Figure 3. Effect of Wind Shear on Rotor Performance

Influence of Airfoil Properties

The aerodynamic performance models require airfoil lift and drag coefficients as functions of angle of attack and Reynolds number. Such information is not, however, generally available over a sufficient range of the input variables. The vertical-axis turbine blades can achieve angles of attack approaching 180 degrees, for example, while data are more typically not tabulated beyond the stall angle. Although the wind tunnel can be used to obtain the necessary data, this procedure is expected to be limited to a few selected airfoils. Use of approximate airfoil data, while not appropriate to absolute predictions of turbine performance, is convenient in judging relative effects.

Two important airfoil properties are minimum drag coefficient, $C_{D_{min}}$, and maximum lift coefficient, $C_{L_{max}}$. In order to study the effect of these characteristics, drag coefficient was assumed to be constant and lift coefficient was assumed to be of constant slope (0.1/degree) up to the stall angle of attack; past stall, lift and drag properties similar to a flat plate were used. Figure 4 shows the power coefficient for a variety of values for $C_{D_{min}}$ and $C_{L_{max}}$, using the multiple-streamtube model. These results suggest that candidate airfoils might be initially selected by searching for low-drag, high-lift sections.

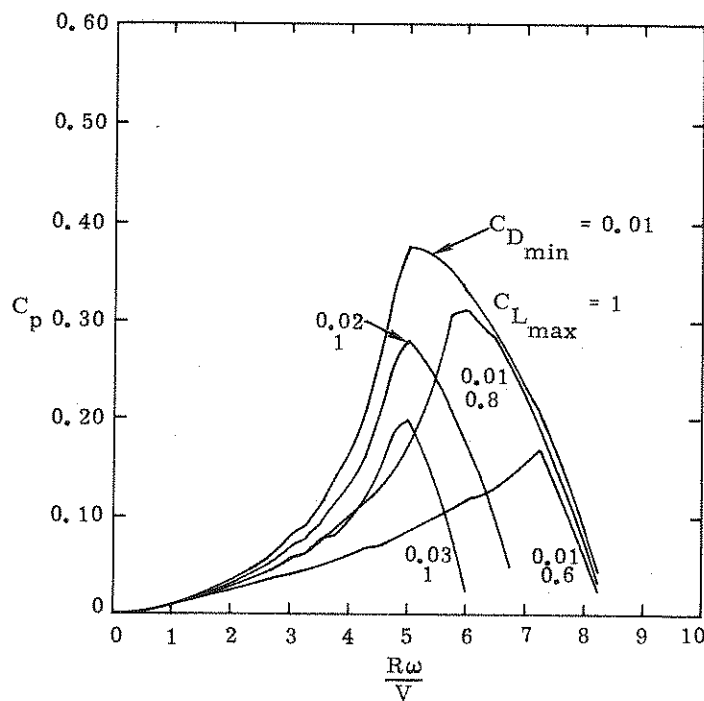


Figure 4. Effect of $C_{D_{min}}$ and $C_{L_{max}}$ on Turbine Performance

Turbine performance improves with increasing Reynolds number. Figure 5 shows results from the single-streamtube model using NACA 0012 airfoil data at Reynolds numbers of 3×10^5 and 3×10^6 . Such a trend has also been observed from wind-tunnel testing of the 2-m turbine. This Reynolds number effect influences the design of large turbines, such as the 17-m turbine.

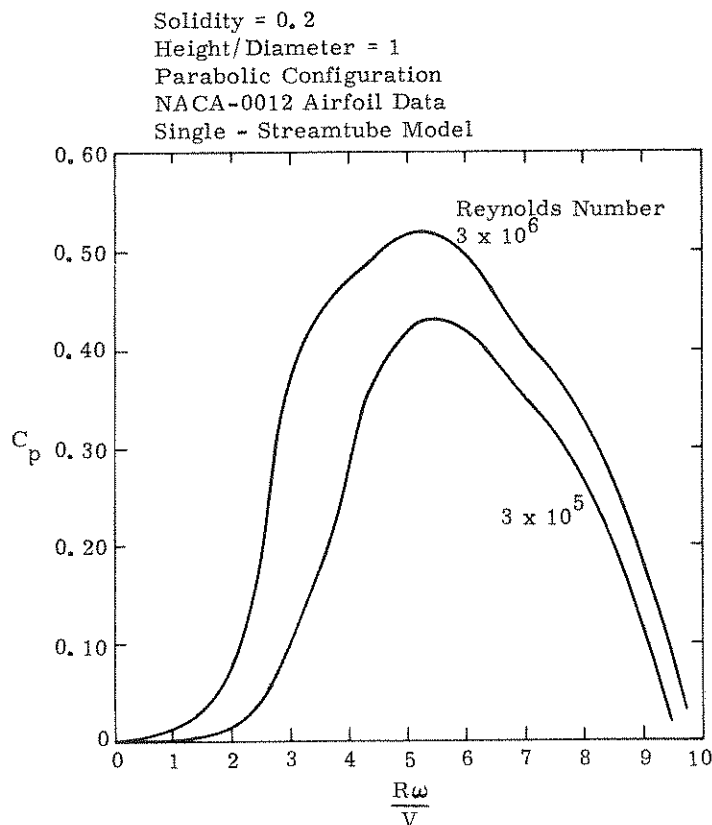


Figure 5. Effect of Reynolds Number on Turbine Performance

Model results and experimental data appear to agree quite well, even though, as previously mentioned, the models do not currently account for Reynolds-number changes along a blade or as the blade rotates. Approximate airfoil data were used in an attempt to investigate these variations. Minimum drag coefficient and maximum lift coefficient were made functions of Reynolds number. It was found that only a small difference in power coefficient is obtained by accounting for Reynolds-number variations along the blade. A possible explanation is that, since the performance models integrate blade forces with respect to position along the blade and rotational position, variations tend to be averaged. As additional section data become available from wind tunnel testing, the effect of Reynolds number variations will be evaluated in more detail.

Structural Analysis

There has been considerable emphasis in the wind power program to develop general methods for assessing the static and dynamic structural performance of Darrieus-type vertical-axis wind turbines. This effort has so far provided techniques which can analyze the static response of the blades and tower to the major applied loads. As regards dynamic effects, methods to calculate the resonant frequencies of the major turbine components are now available.

It is believed that the current static analysis forms a reasonable basis for the design of turbine components provided the resonant frequencies of these components are separated from the expected

load excitation frequencies. The use of this static analysis to design "softer" turbines with low-frequency, closely spaced resonances, would be with some additional risk. It may be desirable from a cost standpoint to consider such soft systems in the future. Thus, it is an eventual goal of the structural analysis to include more dynamic effects, coupled with physical experience gained from operating research turbines.

The structural analysis has been separated into individual studies of the blades and tower. The following sections will summarize the major features of these analyses.

Blade Analyses

The major tool used for blade analyses is a general-purpose, nonlinear, dynamic, finite element structural code. Applications to date have used a two-node, isoparametric curved beam element with bending in one plane only. Geometrical nonlinearities are accounted for with this element.

The curved beam element has been applied to study the so-called flap degree of blade motion, i. e., motion in the plane defined by the blade center and the turbine axis. The blade loadings include centrifugal, gravitational, and aerodynamic forces, the latter being calculated with the single streamtube aerodynamic model. The analysis generates the flap deformation, along with bending and tensile stresses. An example output for blade deformation is shown in Figure 6. In addition, the first few natural frequencies and associated mode shapes are calculated. These frequencies account for the structural deformations which may be present due to the applied loading. The effects of flap-restricting blade support struts have been estimated by eliminating blade motion normal to the strut at the strut attachment point.

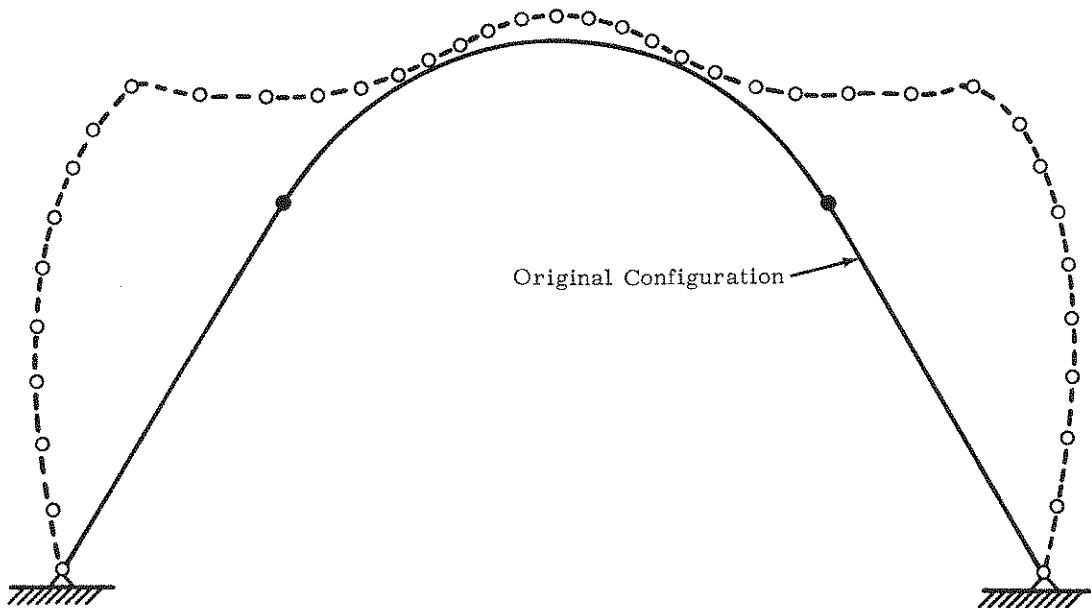


Figure 6. Calculated Blade Deformations (10X)

The curved-beam analysis has been applied to study flap motion of the 2-m, 5-m, and 17-m turbines. As the 2-m and 5-m turbines are operational turbines, a limited amount of experimental verification of the analysis has been obtained. In particular, the first two flap natural frequencies of the 2-m turbine at zero RPM have been measured and found to agree within 5 percent of the calculations. A prediction of high bending stresses at high RPM leading to permanent deformation of the straight blade sections on the 5-m turbine has also been verified.

More recent efforts in blade analysis have been initiated to account for more degrees of freedom in blade motion. Inclusion of the lead-lag deformations (involving combined bending and twist of the blade) due to aerodynamic loads, is the first priority. The effect of blade twist on the aerodynamic loading is of particular interest. An attempt is planned to couple the aerodynamic models with the calculated twists so that aerodynamic loads can be appropriately adjusted.

Aside from the finite-element analyses being pursued, there has been some investigation of turbine scaling phenomena because of its obvious implications for the design of large turbine blades. It has been found that, to a first approximation, the stresses due to centrifugal and aerodynamic forces, and the resonant frequencies (relative to the rotational frequency), are invariant while geometrically scaling a turbine. Gravitational stresses, alternatively, increase linearly with size. This implies that large blade designs may need particular attention to cope with gravitational loads.

Tower Analysis

A linear elastic analysis of the tower/tiedown system, using simple beam theory, has been completed. The analysis considers either a pinned or moment transmitting condition at the bottom of the tower and an elastic tie-down configuration at the top. The tie-down configuration consists of elastic cables extending from rigid "outriggers" at the top of the tower to the ground, similar to the system used on the 5-m turbine. These boundary conditions are an important part of the overall tower design because of their effect on local bending moments, bending frequencies and tower stiffness requirements. The tie-down bears upon tower design insofar as tie-down loads must be transmitted through the tower, affecting its load carrying capability and bending frequencies. The analysis developed so far permits calculations of tower deflections and stresses due to the loads applied by the blades. Development is continuing on means to calculate the tower/tie-down resonant frequencies.

To provide technical support to aid in the decision on the type of towers most suitable for this application, analyses have been developed which permit a comparison of polygonal, prismatic trusses and tubular or cylindrical shell-type towers.* The analysis consists of, in part, derivations of expressions which relate tower stiffness properties to tower geometry and material parameters. In the case of the truss-type tower, the necessary parameters are: (1) bay length (a bay is that portion of the tower which is repeated, lengthwise), (2) cross bracing configuration, (3) the number of sides in the polygonal cross section, (4) element diameter (and wall thickness, if hollow), (5) truss radius

* To date only constant section towers have been considered.

(radius of circumscribing circle), (6) truss length, and (7) the extensional and shear moduli. The tubular, shell-type tower is characterized by: (1) overall diameter, (2) wall thickness, (3) tube length, and (4) the extensional and shear moduli. Clearly the truss towers offer a greater design challenge than the tubular towers because of the larger number of parameters involved and the necessity to characterize the dependent interaction of the truss elements. The latter can be exemplified by the torsion problem where it is found that, due to element interaction, torsional resistance in each bay is developed by twisting, bending, shear, and extensional deformation in the truss elements. Stiffness properties used in the comparison exercises between trusses and shells are the axial, torsional, and bending components. Results indicate that, for specified torsional and bending stiffness values, a truss-type tower will yield the lightest weight structure, while, for a specified axial stiffness value, a tubular-type tower will be the most weight effective.

An example of this type of comparison is provided in Figure 7, where the ratio of the weight of the tubular tower to the weight of a truss tower is shown versus the ratio of the truss radius to bay length. Each curve represents results for a specified inside-to-outside tubular tower diameter ratio and truss element diameter. These results suggest that, except for very long, slender bay geometries, truss towers can be made lighter than tubular towers that have the same value of bending stiffness. Further, the most weight effective truss towers will occur when $R/L = 0.52$ which corresponds to a diagonal element angle of approximately 42 degrees with the tower axis. These results are for triangular towers with one diagonal cross-brace member in each bay face.

Similar comparative analyses have been conducted for the torsional and axial problems and for general and local (truss element) buckling. These comparative relationships, coupled with minimum tower performance requirements, tower cost, and availability factors will be used for the design of future tower tie-down configurations.

Another analysis is available which considers the turbine/generator dynamic coupling problem. This study was initiated to examine the effect on the system of cyclic torque variations applied to the tower by the blades. It was found that the resulting torque variations at the motor were generally several orders of magnitude lower than the variations applied to the blades, depending upon turbine size and operating speed. This smoothing effect occurs for both two- and three-bladed systems* and is due principally to the fact that the high inertia of the blades retards turbine rotational response to applied torque variations. With reduced oscillatory rotational response of the turbine, oscillatory torques transmitted to the generator are also reduced. Since torque variations at the generator, even for a two-bladed system, are so small relative to the maximum acceptable level of 5 percent at the generator, it is concluded that shaft torque variations do not present insurmountable design problems.

* Two-bladed systems produce stronger torque variations than three-bladed systems (Reference 2).

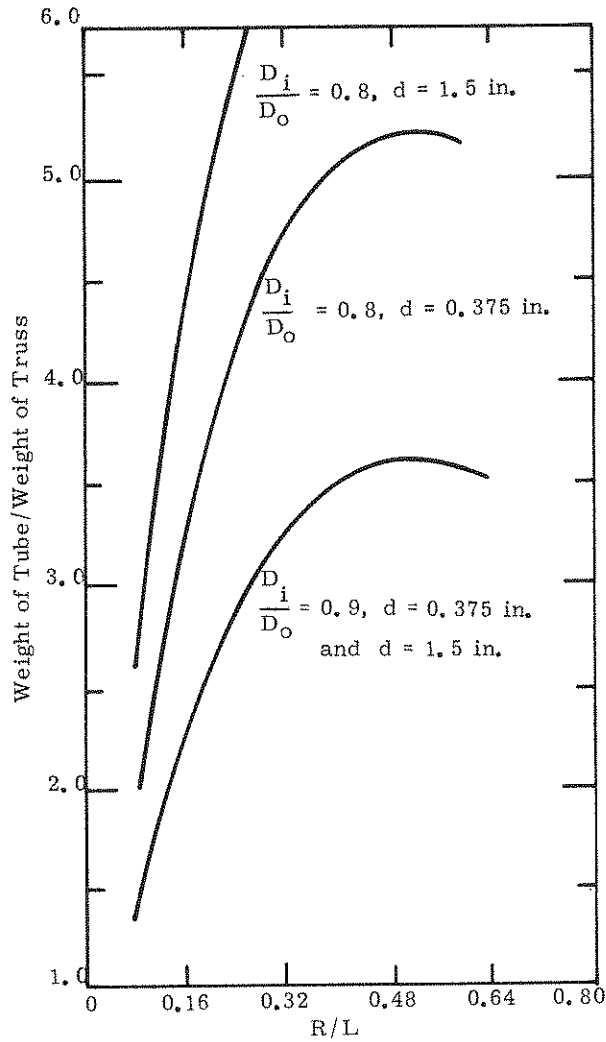


Figure 7. Relative Weights of Tubular and Truss Towers

This analysis led to the discovery of a possible problem related to torsional vibrations of the system. When the turbine-generator interface is fairly stiff, as in the case of a synchronous generator, torque variations at the generator fall off suddenly at a particular frequency. This frequency corresponds to a "dipole" torsional oscillation of the tower where the oscillating portion of the motion causes the bottom of the tower to rotate one way and the top the other way. At this frequency, energy is trapped in the turbine where it is stored as elastic strain energy and kinetic energy. This resonant phenomenon can, however, be avoided by designing the tower with torsional resonances above the known excitation frequency, corresponding to two or three per revolution for two- or three-bladed turbines, respectively.

Systems Studies

The purposes, in general, of systems studies are to identify attractive system applications for the vertical-axis wind turbine and provide assessments of both performance and cost for those applications in order to establish overall system design goals. The following sections summarize systems studies efforts to date.

The first section describes the considerations leading to the selection of the synchronous power grid application utilizing the Darrieus VAWT. Operational differences between various turbine/load combinations suggest that compatibility depends strongly on both the characteristics of the load and the aerodynamic behavior of the turbine; each given load prescribes a set of desirable properties that the driving turbine should possess. In this regard, the Darrieus VAWT appears particularly well-suited to drive a constant-speed load such as a synchronous generator in that, with proper design, no mechanism need be provided on the turbine to regulate operation for high wind speeds.

The second section describes methods for performance and economic evaluation of synchronous systems. Early results suggest that VAWT systems are cost competitive with more conventional horizontal-axis wind turbine systems. Further efforts, however, are required to develop a turbine cost model appropriate to the VAWT.

The third and final section discusses economic optimization through the use of a turbine efficiency characteristic which has variable features. Using this approach, some intuition and trends have been obtained. More obvious conclusions are that maximum efficiency and efficiency "broadness" should be large, which results in higher energy output. Furthermore, the tip speed ratio at maximum efficiency should be large, which results in lower transmission cost due to a decreased torque rating. Perhaps a less obvious conclusion is that the tip speed ratio which corresponds to the beginning of high wind speed performance should assume a particular value, depending on the relative costs of the turbine and transmission. Since aerodynamic design parameters produce efficiency characteristics which substantially trade off these features in a complicated manner, further effort will be required to achieve the goal of identifying optimum system designs.

System Application for the VAWT

A wind energy system consists basically of a turbine which extracts energy from the wind and a load which converts this energy to do useful work. The complexity of the performance characteristics of wind turbines suggests that careful attention be given to the selection of an application in which a given wind turbine may be particularly well-suited. System simplicity, performance, reliability, and cost are some of the considerations important to the selection process. This section briefly traces the evolution of the synchronous power grid application for the Darrieus vertical-axis wind turbine.

Comparison of Wind Turbine Performance Characteristics

The shaft power of a wind turbine is expressed by

$$P = \frac{1}{2} \rho AV^3 C_p \quad , \quad (1)$$

where ρ is the air density, A is the area of the turbine projected in the direction of the wind, i. e., the swept area, V is the wind speed, and C_p is the conversion efficiency, referred to as the power coefficient. The power coefficient is a function of the tip speed to wind speed ratio (tip speed ratio) $\frac{R\omega}{V}$, where R is the maximum turbine radius measured from the rotational axis and ω is the rotational speed. For example, Figure 8 shows the power coefficient as a function of tip speed ratio for a number of wind turbines. Although historically the power coefficient has been important in describing the performance of a wind turbine, the nondimensional nature of efficiency and tip speed ratio does not allow a straight-forward assessment of turbine performance when coupled to a load. A more appropriate form, in this case, is actual turbine shaft torque as a function of rotational speed. Utilizing Equation (1), turbine shaft torque is given by

$$T = \frac{P}{\omega} = \frac{\frac{1}{2} \rho AV^3 C_p \left[\frac{R\omega}{V} \right]}{\omega} \quad (2)$$

(1.225 kg/m³)
(0.02378 slug/ft³)

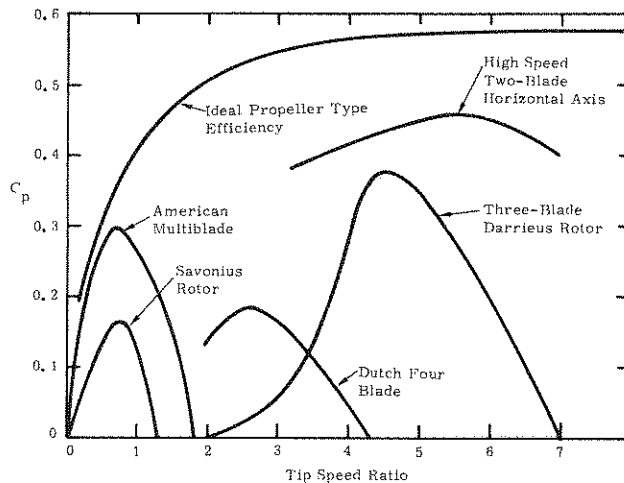


Figure 8. Efficiency Characteristics for a Selection of Wind Turbines

Figures 9 and 10 depict torque as a function of rotational speed for certain values of wind speed. The performance curves for an American Multiblade turbine, shown in Figure 9, and for a Darrieus turbine, shown in Figure 10, are based on a maximum diameter of 15 feet for illustrative purposes.

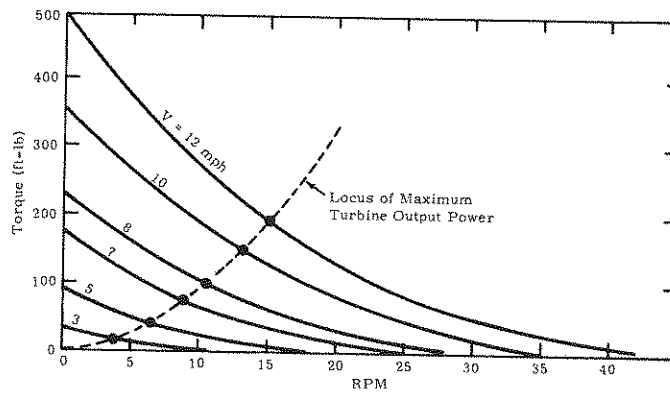


Figure 9. Performance Characteristics of an American Multiblade Turbine

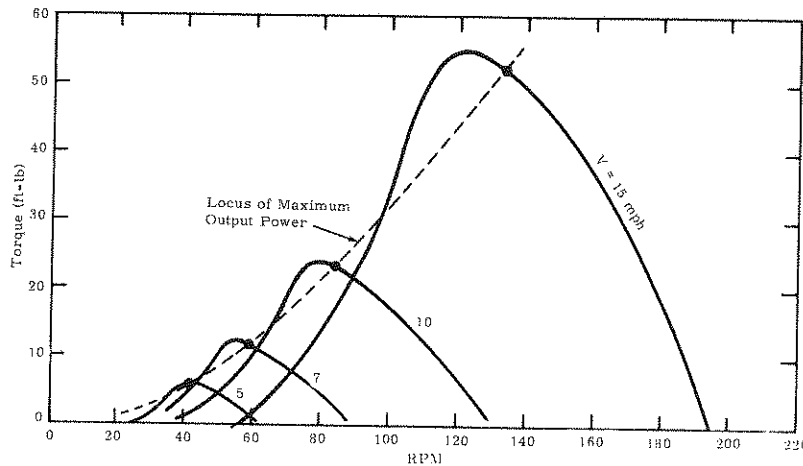


Figure 10. Performance Characteristics of a Darrieus Turbine

Comparison of Figures 9 and 10 indicates a performance characteristic not readily apparent from examination of the efficiency curves. For the American Multiblade turbine, as the wind speed increases, more torque is obtained at any given rotational speed. Power coefficients leading to this behavior will be referred to as "nested" since the torque versus RPM curves for various wind speeds do not intersect each other. The performance curves for the Darrieus, alternatively, have the property that torque continuously decreases with a sufficient increase in wind speed at any given rotational speed; therefore, its power coefficient will be referred to as "unnested." The notions of nested and unnested power coefficients are introduced because, as will be indicated, these properties can considerably influence system behavior in various applications.

Applications with a Speed-Dependent Load -- For certain types of energy conversion devices, the input shaft torque and device output depend primarily on the input shaft RPM. By rigidly connecting such a load through a fixed-gear-ratio transmission to the output shaft of the wind turbine, a particularly simple variable speed wind energy system results. Examples of this type of system include wind-powered water pumps and DC generator/regulator/storage battery combinations. The operating point of a wind turbine connected to a variable RPM load is determined by the intersection

of the torque versus RPM curves for the turbine and load. Figure 11 shows the superposition of the torque versus RPM curves for a nested power coefficient turbine and typical speed-dependent load.

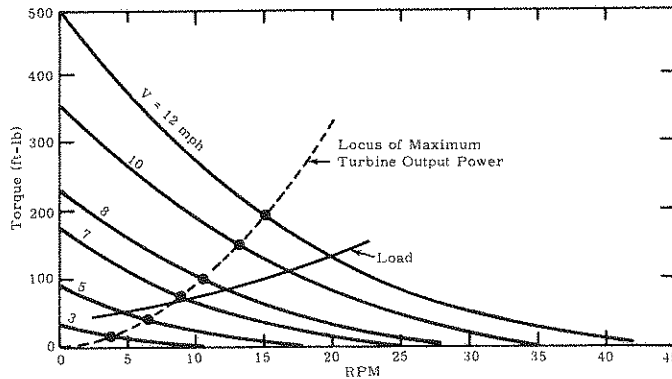


Figure 11. Operating Characteristics of a Nested Power Coefficient Turbine with Speed-Dependent Load

When a selected turbine/load configuration is placed in a wind environment which varies rapidly with time, the machine will not operate exactly at the equilibrium points of Figure 11. The degree to which the system "follows the wind" depends on the component inertias and the gustiness of the wind. It is, however, apparent from Figure 11 that in a changing wind environment, system operation will persist with a nested power coefficient turbine.

Figure 12 shows the superposition of the torque versus RPM curves for a Darrieus turbine and a typical speed-dependent load. The property of having an unnested power coefficient can lead to problems in a changing wind environment. Suppose, for example, the system is operating at the stable point corresponding to a wind speed of 10 mph. A sudden gust to 15 mph leads to a reduction in turbine torque and hence a reduction in turbine RPM. Should the wind speed remain at 15 mph, the system will continue to slow down until it stops. In fact, if the turbine slows enough during the transient, the wind speed could return to 10 mph and the turbine speed would still continue to drop. This stalling effect is difficult to generalize, as it depends on many factors, including the gustiness of the local environment, the system inertia, and the specific shape of the load curve. It is clear, however, that the problem becomes more acute as the load approaches the maximum torque output of the turbine. This problem can be alleviated to some extent. Since the Darrieus turbine is not self-starting, some means must be provided. Use of a Savonius rotor mounted on the same shaft has been suggested for this purpose. Rather than stalling, the system will tend to operate at equilibrium points due to the Savonius rotor, that is, the load operates "on the Savonius." Such operation involves considerably less output than corresponding operation "on the Darrieus," but is preferable to the alternative of system stall.

In summary, it is clear that there are pitfalls associated with the use of an unnested power coefficient coupled to a speed-dependent load which require careful engineering to avoid. The principal problem appears to be the tendency of the system to stall during wind transients, particularly if loads approach the peak output of the turbine. The problem is alleviated if applied loads

are a small fraction of the turbine capacity. Or, if the machine is placed in a very steady wind environment, e. g., a trade wind, acceptable performance for loads near the peak turbine capacity may be realized.

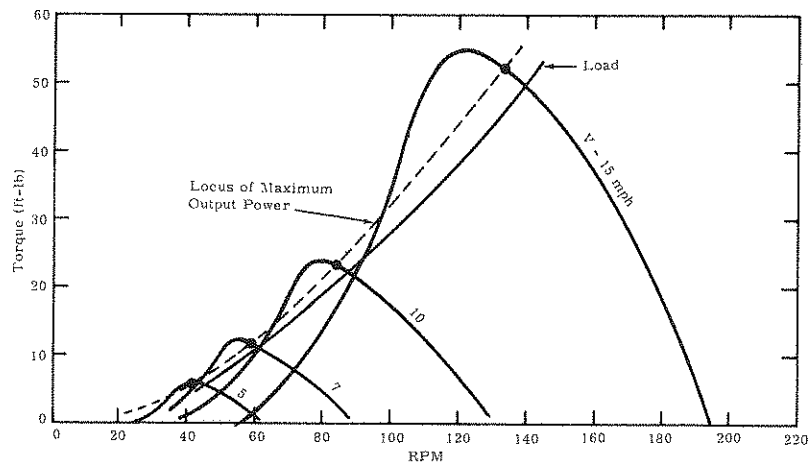


Figure 12. Operating Characteristics of an Unnested Power Coefficient Turbine with Speed-Dependent Load

Applications with a Constant-Speed Load -- A system in which the turbine and load are operated at constant rotational speed is of both historical and current interest for large-scale electrical power production. Such a load can be represented by a torque versus RPM curve which is vertical and has a limiting value of torque associated with it, e. g., the pullout torque of a synchronous generator.

Figure 13 shows the superposition of the torque versus RPM curves for a nested power coefficient turbine and a constant-speed load. If wind speed exceeds that value corresponding to the maximum load, the load will be lost and the turbine will become free-running. Thus, for a nested power coefficient turbine, some form of regulation is required. The regulator, typically a blade pitch mechanism, contributes significantly to system complexity and cost.

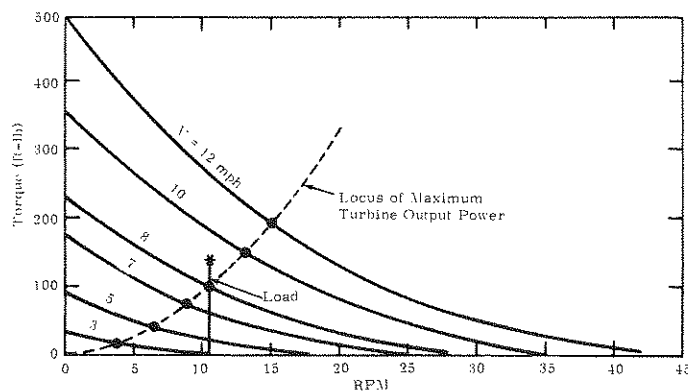


Figure 13. Operating Characteristics of a Nested Power Coefficient Turbine with a Constant-Speed Load

Figure 14 shows the superposition of the torque versus RPM curves for the Darrieus turbine and a constant-speed load. The feature to note is that, with proper sizing of the load, the rating will never be exceeded, due to the unsted property of the turbine. Thus, no regulator need be provided on the turbine. This suggests utilizing the Darrieus vertical-axis wind turbine in a synchronous power grid application.

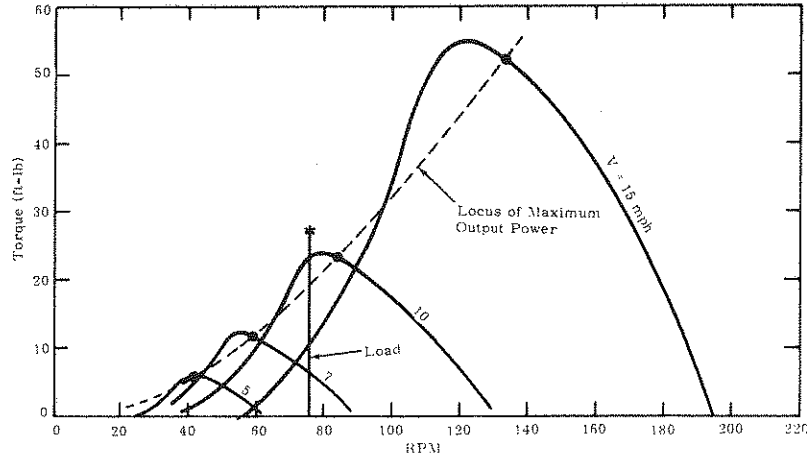


Figure 14. Operating Characteristics of an Unsted Power Coefficient Turbine with a Constant-Speed Load

Synchronous Power Grid Application

Figure 15 shows in block diagram form the basic elements of a wind energy system for synchronous electrical power generation. A turbine rotating at constant speed is connected to a synchronous generator through a transmission. The transmission typically includes a fixed gear-ratio speed increaser to better match the turbine to a practical generator. The generator in turn is connected to an electrical power network which determines the synchronous frequency. It should be noted that the network capacity must be large relative to the wind energy system capacity so that it is the network which fixes the frequency and thereby the generator and turbine rotational speed.

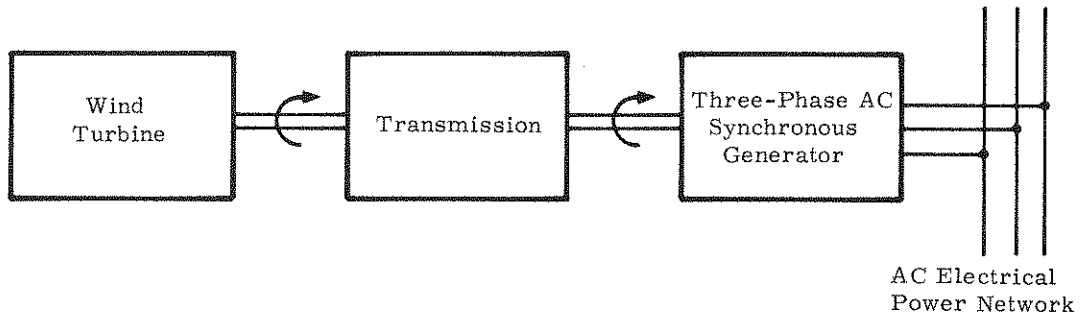


Figure 15. Synchronous System Diagram

If the turbine rotational speed is fixed, then shaft torque (or power) becomes a function only of wind speed. Thus, for synchronous power generation, the appropriate performance characteristic to describe system operation is torque (or power) versus wind speed for fixed values of rotational speed, which can be derived from Equation (2). Figure 16 depicts the performance at constant rotational speed for a Darrieus turbine which has a maximum diameter of 15 feet and a power coefficient shown in Figure 8.

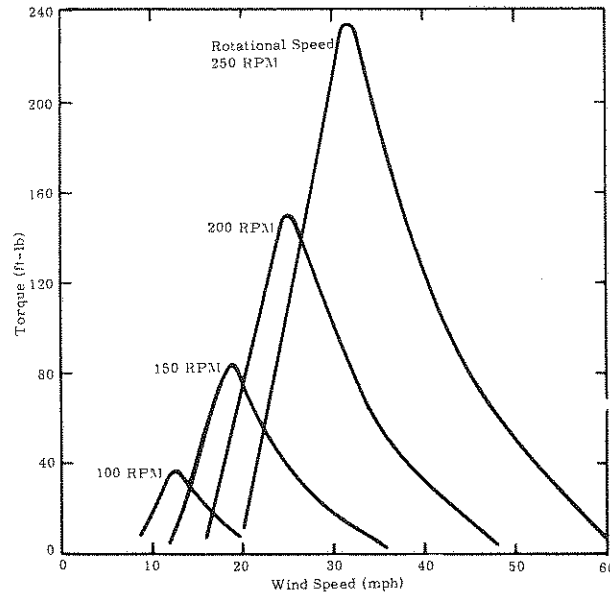


Figure 16. Performance Characteristics for a Darrieus Turbine at Constant Rotational Speed

Note that torque reaches a maximum with respect to wind speed. If the generator rating is chosen to correspond to this maximum, then no regulation mechanism need be provided on the turbine and presumably a substantial cost savings to the system can be accrued.

The performance characteristics indicate that, for sufficiently high wind speeds, torque becomes negative, that is, the synchronous machine becomes a motor to maintain constant rotational speed, and, in so doing, draws energy from the grid. This potential loss of energy might be avoided in several ways:

1. By selecting the turbine rotational speed so that motoring only occurs rarely at a given site;
2. By shutting down the system if the condition persists;
3. By tailoring the aerodynamic performance of the turbine in order to make the torque versus wind speed characteristics remain close to the maximum.

Performance and Economic Evaluation of Synchronous Systems

The economics of large-scale production of electrical energy involves a tradeoff between both component costs and annual energy output of the system. Calculation of energy output accounting for the wind speed statistics at a site, turbine power output, and component efficiencies can be accomplished by using the following expression

$$\text{Annual Energy} = \int_0^{\infty} \eta [P_T] P_T [V, \omega, R] f [V] dV \quad , \quad (3)$$

where P_T is the turbine output power (a function of the wind speed V , the fixed rotational speed ω , and the radius R), η is the efficiency of the transmission and generator (which may be characterized as a function of the turbine output power), and f is the annual wind speed frequency distribution for the site. An equivalent graphical procedure is illustrated in Figure 17, which qualitatively illustrates the power duration curve and, for increasing values of rotational speed, the system power output.

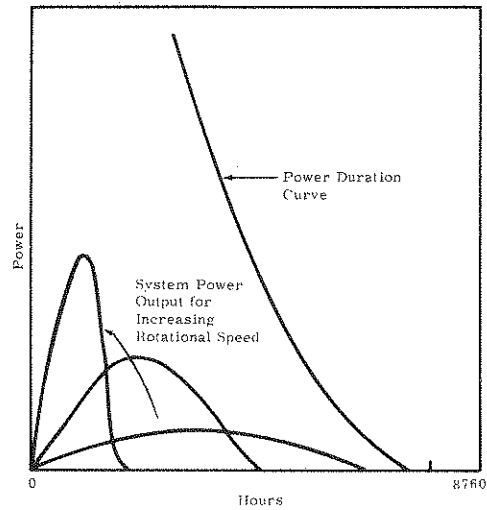


Figure 17. Estimation of Annual Energy for an Unnested Power Coefficient Turbine

The power duration curve for a site shows the number of hours in a year for which the power in the wind exceeds a specified value. This curve is converted to a system power output curve by accounting for efficiencies of the turbine, transmission, and generator. Figure 17 indicates again that, for a system with an unnested power coefficient turbine, rating can be chosen to equal the maximum power output at a given rotational speed, thereby eliminating the need for any regulation mechanism on the turbine. The area under each power output curve represents the annual energy for the corresponding rotational speed. Annual energy approaches zero for both large and small values of rotational speed. Thus, annual energy is maximized at some intermediate value of rotational speed.

Performance, however, is not the only consideration in analyzing the economics of wind energy systems. Economic optimization which attempts to minimize cost per unit of energy must also include component costs. Tradeoffs between costs and energy production tend to identify systems which do not necessarily maximize energy output.

The flow chart shown in Figure 18 indicates the procedure adopted to identify, for a given rated power, the system which minimizes cost per unit of energy.

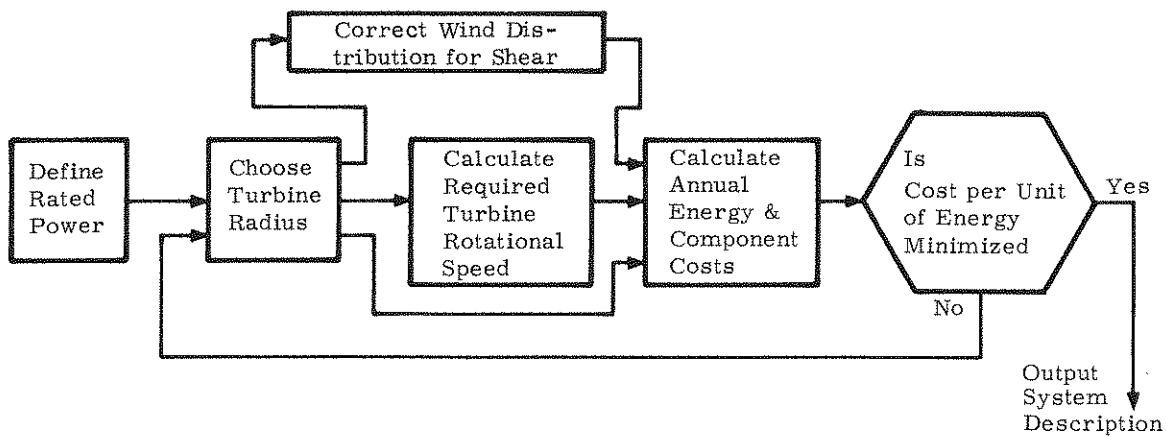


Figure 18. Flow Chart for Economic Analysis

Component cost formulas have been taken directly from the conceptual design study performed by General Electric.⁷ A modification was made to the rotor cost formula to reflect the elimination of the torque regulation mechanism (i.e., blade pitch control); the rotor cost was taken to be half that for horizontal-axis turbines, since GE estimates that about half of the rotor cost is for the regulation mechanism. It is expected that as structural, fabrication, and manufacturing studies progress, a turbine cost model more appropriate to the Darrieus turbine will become available to the systems studies.

Figure 19 shows production cost per unit of energy as a function of rated power for VAWT systems and, due to GE, horizontal-axis systems. Also indicated in Figure 19 are turbine size and rotational speed for selected values of rated power. The minimum cost VAWT system with respect to rated power occurs at about one megawatt. Analysis has indicated that this conclusion is quite sensitive to variations in the cost and performance models. For example, with increasing turbine size, Reynolds number is increasing, leading to improved aerodynamic performance. This tendency is illustrated in Figure 19 by using performance data at Reynolds numbers of 3×10^5 and 3×10^6 .

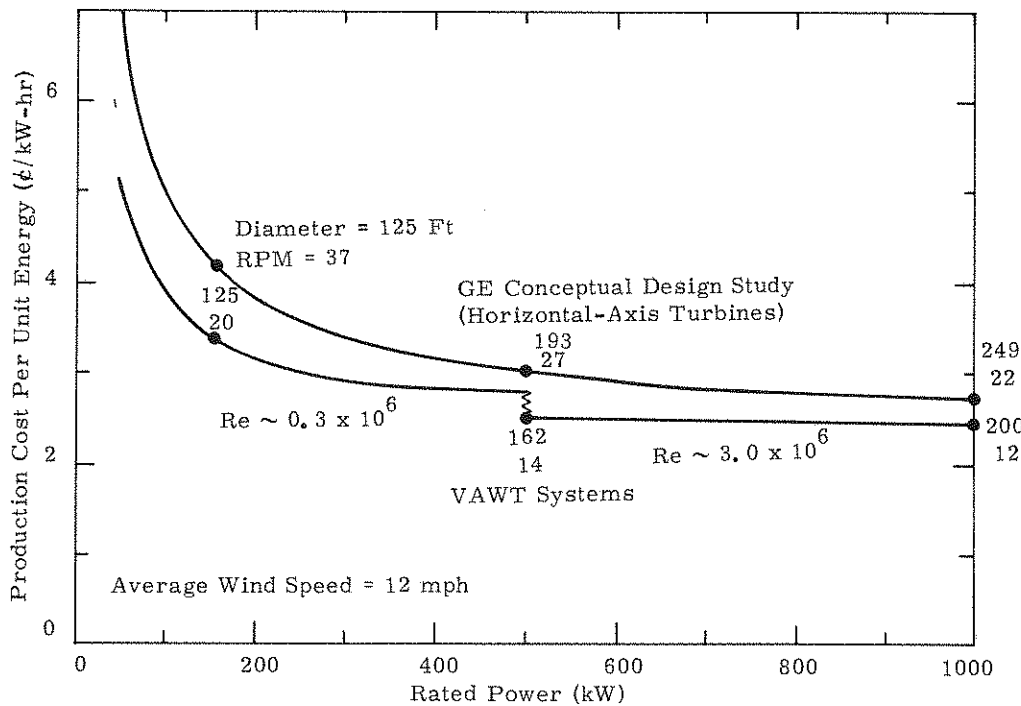


Figure 19. Wind Energy System Economics

From the results of this early economic analysis, VAWT systems appear cost competitive with horizontal-axis systems. It should be noted, however, that drawing conclusions more detailed than this may not be justified within the framework of the current assumptions.

Toward Economic Optimization

The economics of synchronous power generation systems involve a complex interplay of both cost and performance parameters. For example, aerodynamic studies indicate that parameters such as solidity, height-to-diameter ratio, and turbine configuration can produce a wide variety of performance characteristics. A major objective of the systems studies is to identify parameter values which lead to economically attractive systems. In an attempt to build intuition to achieve this goal, simple economic indicators have been defined and the effect of various features of the power coefficient on them are being investigated.

The economic analysis mentioned in the previous section has indicated that turbine cost and transmission cost are the two major contributors to total system cost. Turbine cost can, to some degree, be related to the swept area of the turbine. Transmission cost is related to the rated output torque of the turbine. Thus, it would appear reasonable to use as measures of energy per unit of production cost the terms E/A and E/T_R where E is the annual energy output, A is the swept area, and T_R is the rated torque. These "economic indicators" are relatively easy to evaluate and, therefore, a wide range of postulated systems can be investigated.

A particular functional form for the turbine power coefficient has been selected and is depicted in Figure 20. Features of interest are the maximum power coefficient $C_{p_{max}}$, the tip speed ratio corresponding to the maximum efficiency λ_m , the tip speed ratio at zero efficiency λ_r , the tip speed ratio at which power reaches a maximum with respect to wind speed λ_k , and an exponent n which defines the turbine power output for high wind speeds. For example, a horizontal-axis turbine with blade pitch control can be modeled by choosing $n = 3$ so that power is constant with respect to wind speeds for tip speed ratios less than λ_k .

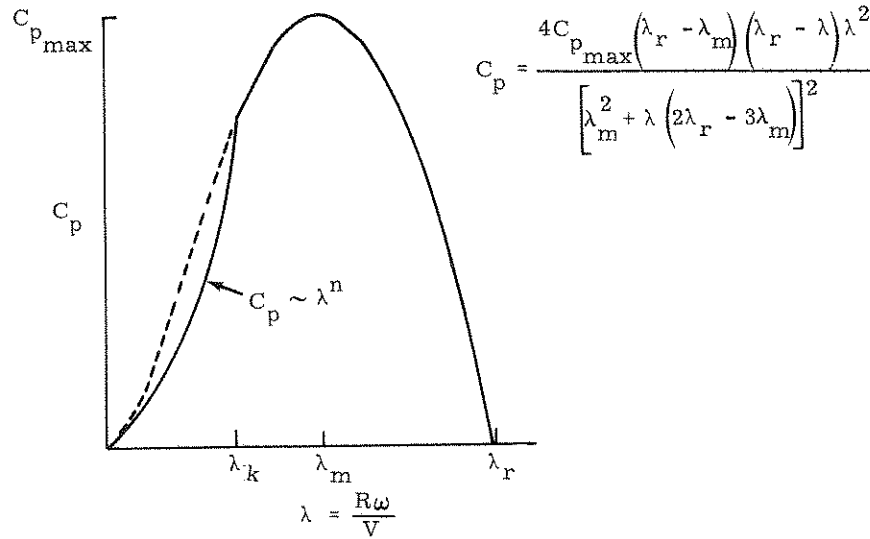


Figure 20. Model Power Coefficient

A particular functional form for the wind speed frequency distribution has also been selected. This distribution, which is to some extent representative of real wind statistics, is given by

$$f[V] = \frac{52560 V (V_{max} - V)}{V_{max}^3}, \quad 0 \leq V \leq V_{max} \quad (4)$$

where V_{max} is the maximum wind speed. The average wind speed is $1/2 V_{max}$.

Figures 21a and 21b show a typical result from computations of E/A and E/T_R as functions of the variables $R\omega/\lambda_m$ and λ_k/λ_m . The parameters X and η noted on these figures are used to characterize the efficiency of the transmission and generator. Several observations can be made as follows:

1. E/A and E/T_R increase with $C_{p_{max}}$; that is higher efficiency means more energy extracted from the wind;
2. E/T_R increases with λ_m , that is, rated torque (for a given rated power P_R) can be decreased by increasing λ_m , which is a measure of turbine rotational speed;
3. E/A and E/T_R reach maxima with respect to $R\omega/\lambda_m$; that is, as discussed previously, there is a particular rotational speed for which energy is maximized.

As illustrated in Figures 21a and 21b, E/A and E/T_R are substantially dependent on λ_k/λ_m . Figures 22a and 22b further demonstrate this dependence by showing E/A and E/T_R (maximized with respect to $R\omega/\lambda_m$) as a function of λ_k/λ_m for various values of n and λ_r/λ_m .

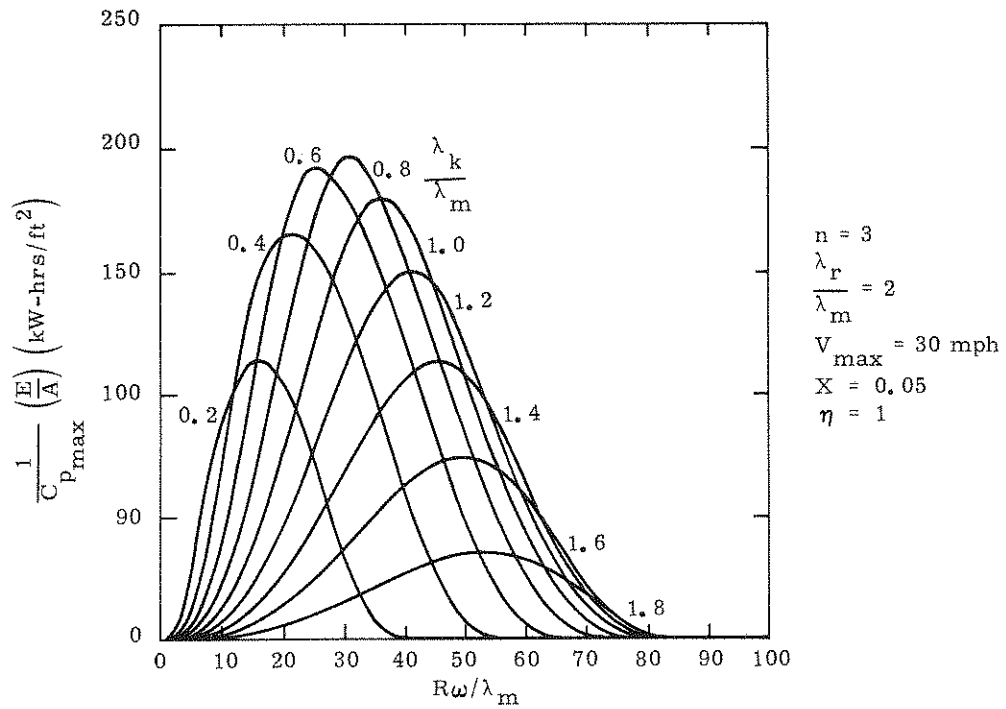


Figure 21a. Annual Energy per Unit Swept Area

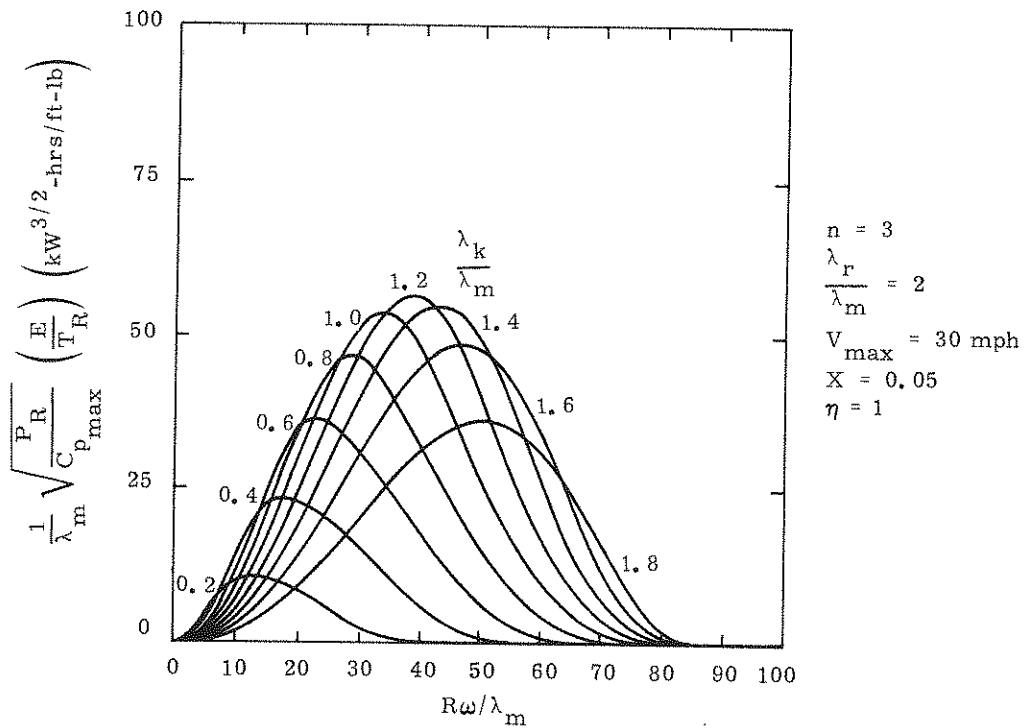


Figure 21b. Annual Energy per Unit Rated Torque

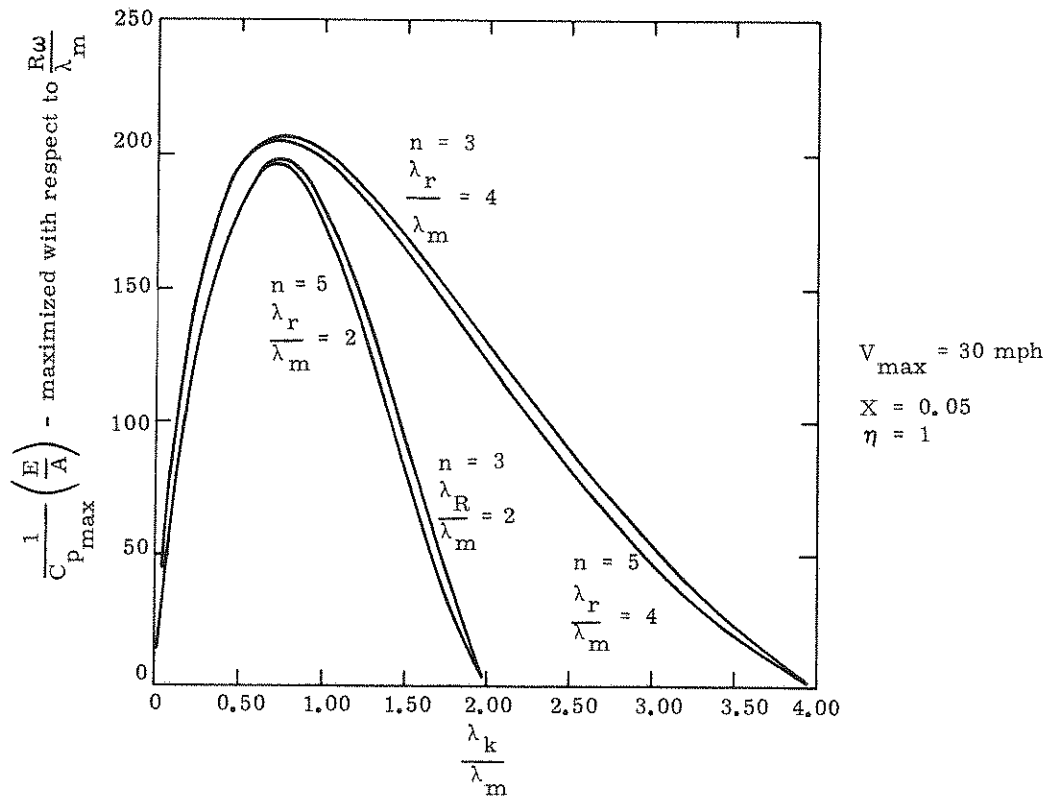


Figure 22a. Maximized Annual Energy per Unit Swept Area

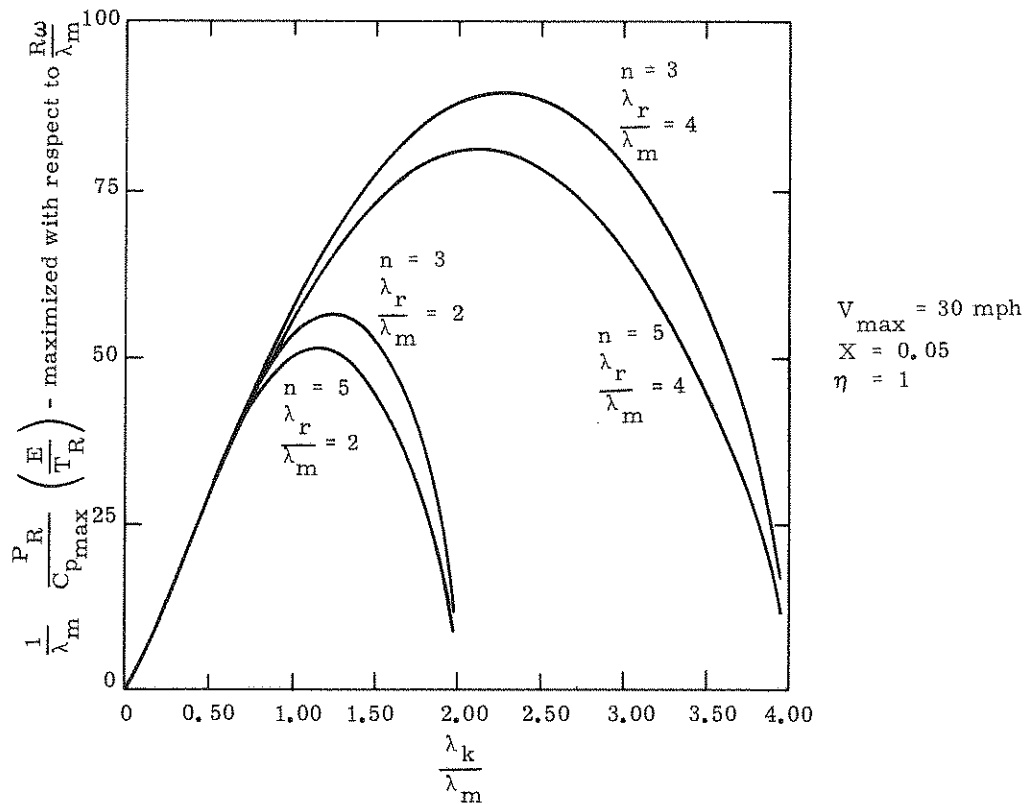


Figure 22b. Maximized Annual Energy per Unit Rated Torque

Thus, for a $\lambda_r/\lambda_m = 2$, the largest value of E/A occurs for $\lambda_k/\lambda_m \sim 0.7$ and $R\omega/\lambda_m \sim 30$, while the largest value of E/T_R occurs for $\lambda_k/\lambda_m \sim 1.2$ and $R\omega/\lambda_m \sim 40$. When $\lambda_r/\lambda_m = 4$, E/T_R is maximized with $\lambda_k/\lambda_m = 2.2$ and $R\omega/\lambda_m = 75$.

Since total system cost is approximately the sum of turbine and transmission costs, the economic analysis described previously can be used to combine the effects of these indicators. Figure 23 shows production cost per unit energy as a function of rated power when minimized with respect to λ_k/λ_m , R , and $R\omega/\lambda_m$. It appears that the optimization procedure chooses a value of λ_k/λ_m intermediate to values indicated in Figures 22a and 22b.

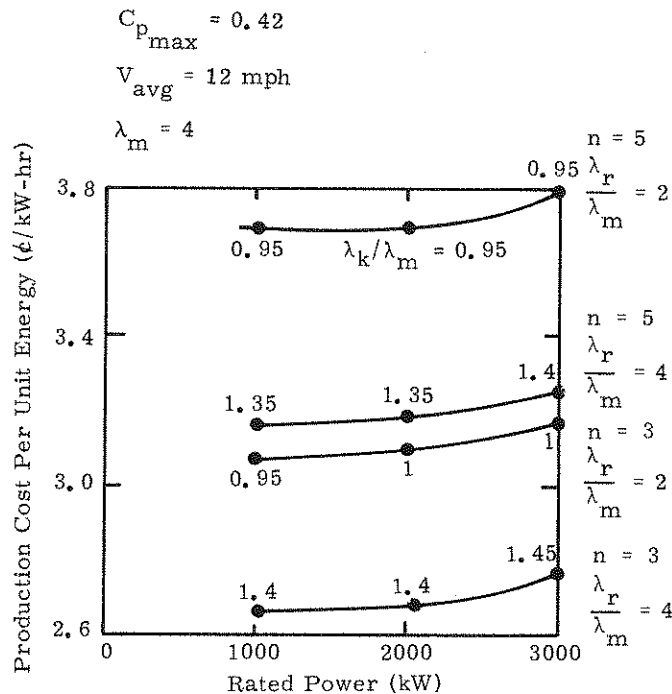


Figure 23. Economics Using Model Power Coefficient

The foregoing discussion has indicated that several features of the power coefficient can influence the economics of synchronous systems. Results from aerodynamic studies suggest, however, that these features cannot be varied independently. For example, Figure 24 shows power coefficients for several values of turbine solidity (blade area/swept area) calculated using the single-streamtube aerodynamic performance model. While the feature λ_m is increasing, as desired, with decreasing solidity, the feature $C_{p_{max}}$ is decreasing. Coupling of the features is similarly obtained from variations in other aerodynamic parameters, such as height-to-diameter ratio, turbine configuration, and Reynolds number. Thus, more effort is required to understand the relative influence of the features on economics in order to identify future wind turbine system designs.

Parabolic Configurations
Height/Diameter = 1.5
Reynolds Number = 3×10^6

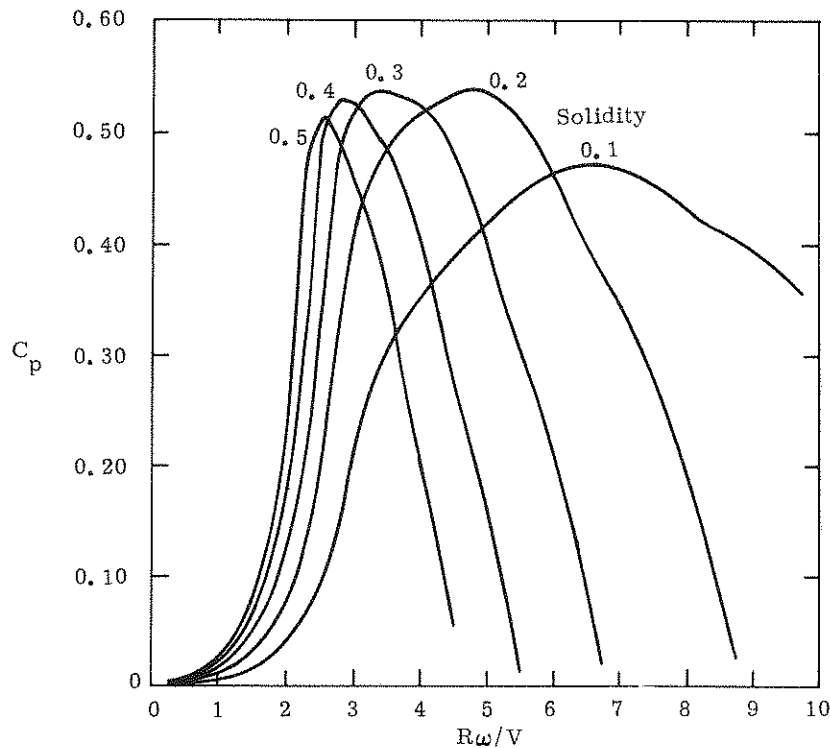


Figure 24. Effect of Solidity on Power Coefficient

Test Program

Test Facility

Concurrent with wind turbine design activities, a test facility is being prepared for use with both the 5-m and 17-m turbines. The facility is a general-purpose type, capable of collecting both turbine performance and wind statistical data. The anemometry system, the 5-m turbine, and preliminary instrumentation and controls have been installed and will be briefly discussed. It should be emphasized that the capabilities discussed are not complete or final, as it is anticipated that the facility will be continuously updated as the needs imposed by the test program become clear.

The test facility is located approximately one-half mile east of Tech Area I of Sandia Laboratories, Kirtland Air Force Base, East. An existing building (350 ft^2), Building 899, is being used for the control and instrumentation center. The building is located (Figure 25) at the edge of the 35-acre test area. An anemometer tower is located at the western edge of the test area. The surrounding terrain is generally flat so that terrain influence on wind patterns is minimized.

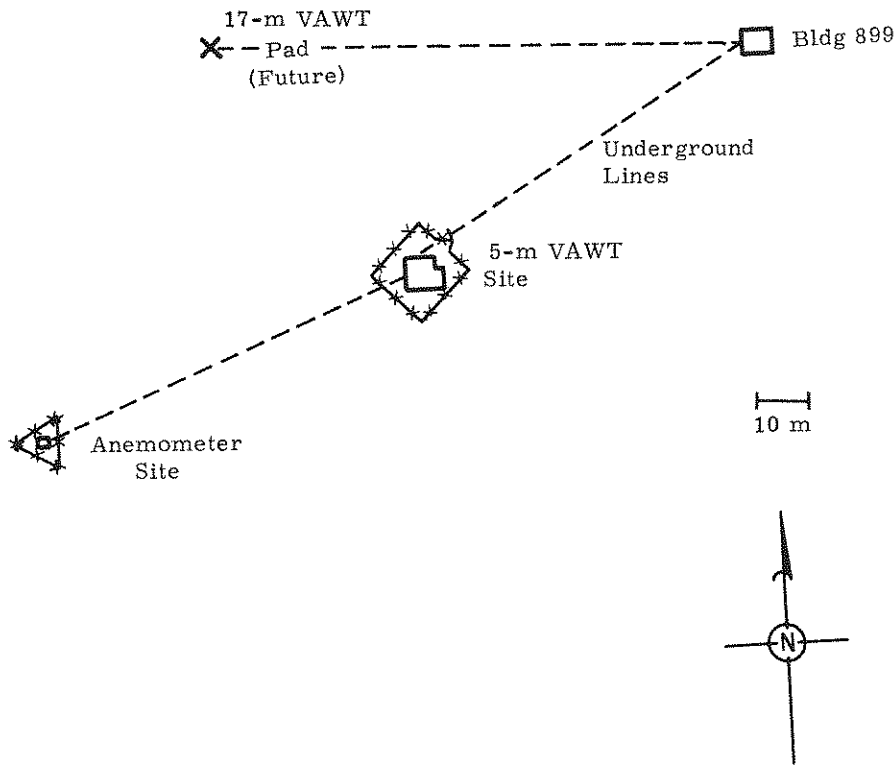


Figure 25. Test Facility Layout

Anemometry -- Most of the facility's anemometers are located on a 36-m telescoping tower. This tower has four sets of anemometers and direction indicators set at heights of 3, 10, 17, and 30 meters. The signal lines are fed through underground conduit to Building 899. The anemometers are Model 1564B, manufactured by Teledyne-Geotech, capable of maximum wind speed of 90 mph. The direction indicators are Model 1565B by the same manufacturer.

The anemometer tower will be used primarily for the statistical characterization of the wind at this site. An additional portable anemometer is available which can be mounted within 10 m of the 5-m turbine. This portable unit is now being used for correlating wind speed data with turbine output.

5-m Turbine^{*} -- The 5-m wind turbine has been installed at the test location shown in Figure 25. The current configuration is a two-bladed turbine coupled to a 3600-rpm, 5-hp, 220-volt, single-phase induction motor/generator using timing belts and pulleys as a speed increaser. Several turbine rotational speeds between 100 and 225 rpm are available. The induction machine acts as both a starter and as a generator returning generated power to the electrical grid. The turbine is operated at constant rotational speed except as dictated by the slip of the induction machine.

^{*}This turbine was originally designed as a 15-foot-diameter unit. In the interest of using consistent units in this report, it will be referred to as the 5-m turbine.

After three-phase power is made available at the test site (approximately April 1976), the turbine will be operated with a three-phase induction generator. The three-phase generator can be used in conjunction with a commercial speed controller, thereby increasing the number of available operational speeds.

Instrumentation and Controls -- The instrumentation readout and control functions are located in Building 899 (Figure 26).



Figure 26. Test Facility Instrumentation Rack

In addition to wind speed and wind direction signals, torque and rotational speed signals are available. These are displayed on digital voltmeters and strip charts and can be recorded on magnetic tape.

The starter/generator controls are located on a panel adjacent to the instrumentation readouts. These consist of a manual stop/start and brake control. The brake control is battery-operated and is fail/safe, i. e., if line voltage is lost, the brake is applied. In addition, if the turbine overspeeds, the brake is applied. A local brake control is also available at the turbine.

The microprocessor system consists of an Intellect 8 microprocessor, an MITS ALTAIR 8800 microprocessor, a Doric 210 A/D converter, Remix paper tape reader, Remex paper tape punch, an Icom disc memory and a Texas Instrument Silent 700 teleprinter. It is intended to use the microprocessor to reduce anemometer data from the weather tower to a more manageable statistical form, to carry out real-time reduction of turbine performance data, and to provide logic for the automatic control of turbine functions. The programming and use of these devices has only begun, and will be reported on in detail next quarter.

Wind Tunnel Tests

Two series of wind-tunnel tests have been performed on models of Savonius and Darrieus rotors. These tests took place in the 15- x 20-foot test section of the LTV Low Speed Wind Tunnel in Dallas, Texas. The first series of tests were done in May 1975 in which several Darrieus rotor tests were performed and all Savonius rotor tests were completed. A photograph of a two-bucket Savonius rotor in the LTV Low Speed Wind Tunnel is shown in Figure 27. Two- and three-bucket configurations with various gap openings between the buckets were tested.

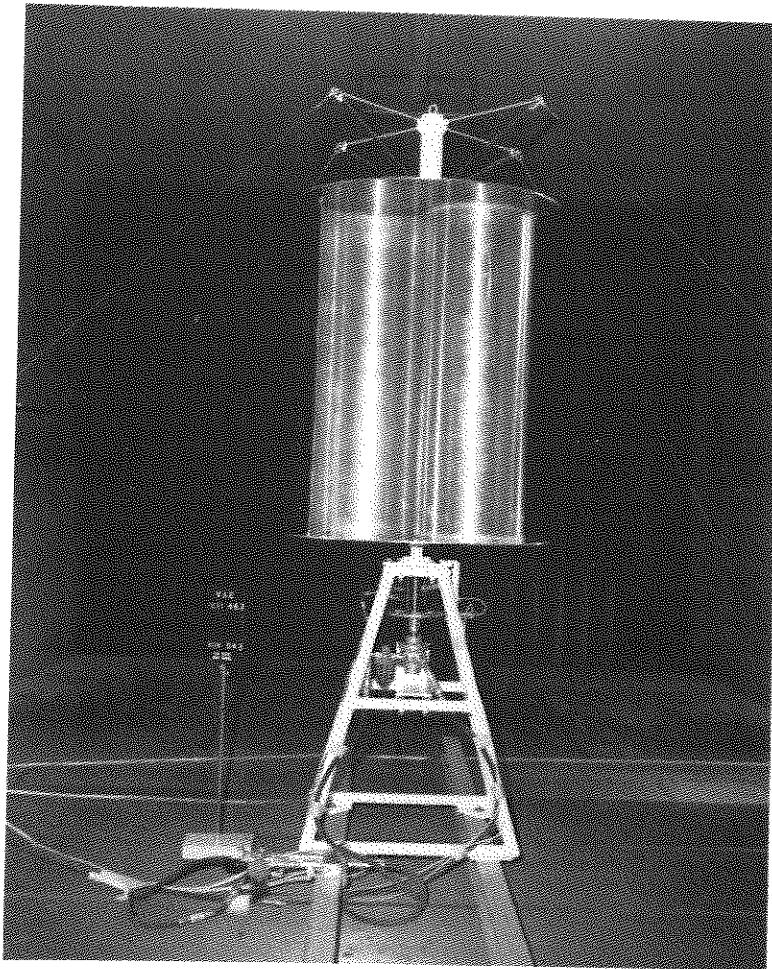


Figure 27. Photograph of a 2-Bucket Savonius Rotor in the LTV 15- x 20-foot Low-Speed Wind Tunnel

The power coefficient for a wind turbine is given by the equation:

$$C_p = \frac{T\omega}{1/2 \rho V^3 A_s}$$

where

T = shaft torque, n-m

ω = shaft rotational speed, rad/s

ρ = free stream air density, kg/m³

V = free-stream velocity, m/s

A_s = projected swept area of the rotor, m²

This power coefficient is the ratio of the turbine power output to the total power in the air stream tube of area A_s . The power coefficient is a measure of the efficiency of the turbine. The tip speed ratio, λ , is the ratio of the velocity of the outermost blade or bucket tip at radius R , to the velocity of the free stream.

$$\lambda = \frac{R\omega}{V}$$

A plot of the power coefficient as a function of tip speed ratio for the most efficient Savonius rotor tested is shown in Figure 28. The most efficient configuration was the rotor with two buckets and a small gap opening between the buckets. The gap dimension, s/d , is the actual gap width, s , divided by the diameter d , of the buckets. All two-bucket configurations approached a peak power coefficient of 0.25 with only a slight effect of the gap dimension with the best performance given by the smallest gap (not zero) tested. All three-bucket configurations gave peak power coefficients in the range of 0.14 to 0.17, which were consistently lower than any two-bucket configuration. The peak power coefficients occurred within a tip speed ratio range of 0.75 to 1.0 for all configurations.

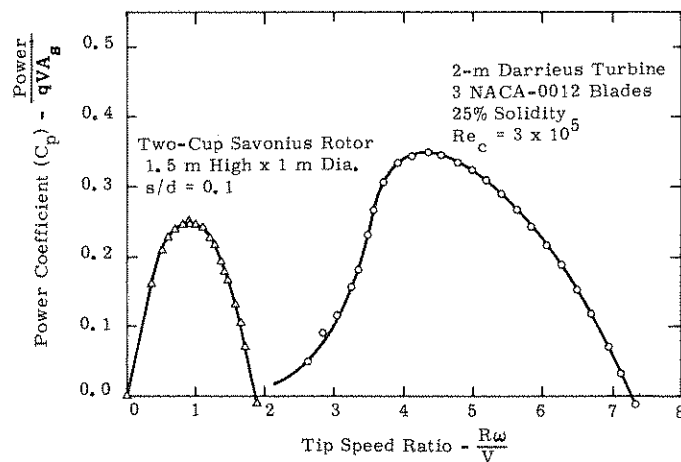


Figure 28. Performance Data for Two Wind Turbines Obtained at the LTV 15- x 20-foot Low-Speed Wind Tunnel

A photograph of a 2-m Darrieus wind turbine is shown in Figure 29 prior to tests in the wind tunnel. A complete matrix of Darrieus wind turbine tests were completed during the second series of tests which took place in October 1975 at LTV in Dallas. The test matrix, shown in Table I, includes two- and three-blade configurations and blade solidities ranging from 30 percent down to 13 percent. The blade solidity is defined as the outer surface blade area, $Nc\ell$, divided by the projected swept area, A_s , of the turbine, where N is the number of blades, c is the blade chord length, and ℓ is the total length of the curved blade. The cross section on all the Darrieus blades was that of a NACA-0012 airfoil.

Two types of tests were performed with the Darrieus turbine. One type was with a constant wind velocity where the turbine rotational speed was varied over a tip speed ratio from two to turbine runaway. Runaway is the high-speed condition where the output torque is equal to the friction torque of the system and no power is produced. The second type of tests consisted of running the turbine at a fixed rotational rate and varying the wind velocity to span the range of tip speed ratios from two to runaway. The second mode of testing was chosen because that would best simulate an actual system operating at a fixed rotational speed and it also would give a more realistic Reynolds number effect on the blade performance. The actual wind velocity the blades see is a larger function of the turbine rotational speed than the free-stream air velocity, since the tip speed velocity is several times the wind velocity, i. e., operation of the turbine ranges from a tip speed ratio greater than two to runaway which may be a tip speed ratio in excess of ten.

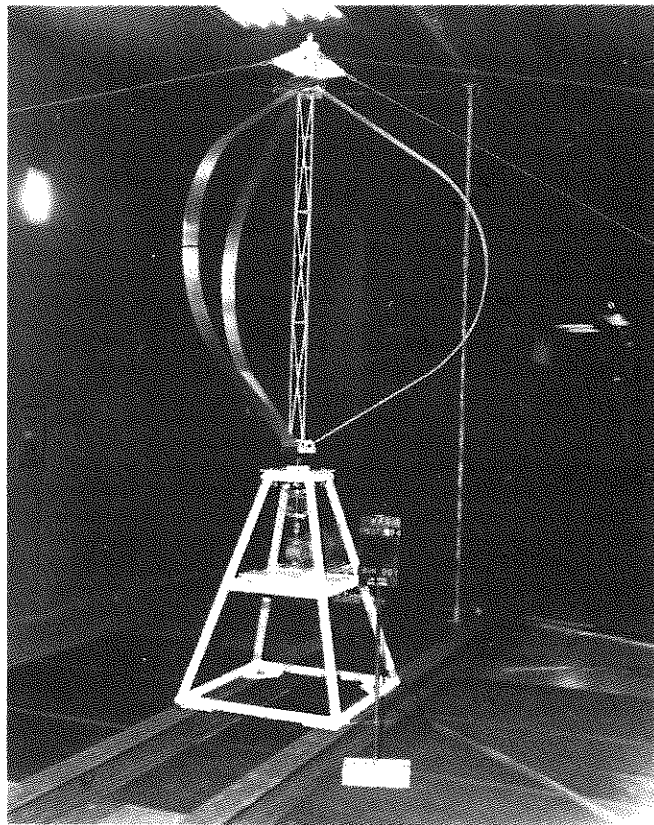


Figure 29. Photograph of a 3-Blade, 30-Percent Solidity Darrieus Model in the LTV 15- x 20-Foot Low-Speed Wind Tunnel

TABLE I

Darrieus Rotor Tests in the LTV LSWT

Run No.	No. of Blades	Solidity (%)	Rotor (RPM)	Wind Velocity (m/s)	Chord (cm)	Chord Reynolds Number	Configuration Number
1	3	30	180	Variable	8.815	104,000	1
2	3	30	267	Variable	8.815	150,000	1
3	3	30	500	Variable	8.815	290,000	1
5	3	30	Variable	11	8.815	Variable	1
6	3	30	Variable	9	8.815	Variable	1
7	3	25	216	Variable	7.346	101,000	2
8	3	25	320	Variable	7.346	151,000	2
9	3	25	600	Variable	7.346	278,000	2
10	3	25	Variable	11	7.346	Variable	2
11	3	25	Variable	9	7.346	Variable	2
13	3	20	270	Variable	5.877	101,000	3
14	3	20	400	Variable	5.877	154,000	3
15	3	20	525	Variable	5.877	200,000	3
16	3	20	Variable	9	5.877	Variable	3
17	3	20	Variable	7	5.877	Variable	3
18	2	20	180	Variable	8.815	106,000	4
19	2	20	267	Variable	8.815	156,000	4
20	2	20	350	Variable	8.815	204,000	4
21	2	20	500	Variable	8.815	290,000	4
22	2	20	Variable	9	8.815	Variable	4
23	2	20	Variable	11	8.815	Variable	4
24	2	13	Variable	7	5.877	104,000	5
25	2	13	270	Variable	5.877	155,000	5
26	2	13	400	Variable	5.877	200,000	5
27	2	13	525	Variable	5.877	Variable	5
28	2	13	Variable	9	5.877	Variable	5

$$A_s = 2.5944 \text{ m}^2$$

$$R = 0.9798 \text{ m}$$

For comparison purposes, the data for a constant RPM Darrieus test is shown in Figure 28 with a plot of Savonius rotor data. The Darrieus wind turbine data are for a three-blade, 25 percent solidity configuration operating at a chord Reynolds's number,

$$\frac{\rho R \omega c}{\mu}$$

of approximately 3×10^5 . The symbol, μ is the free-stream air viscosity. The peak power coefficient for that configuration is approximately 0.35 at a tip speed ratio of 4.7. This demonstrates that the Darrieus turbine, a lifting device, is more efficient than a Savonius rotor, a drag device.

A representative set of data for the Darrieus wind turbine tests is shown in Figure 30 for all five solidities tested at a common chord Reynolds number of approximately 1.5×10^5 . This figure shows the effect of solidity on turbine performance. It can be seen that, for this Reynolds number, a solidity of approximately 25 percent produces the maximum peak power coefficient. Decreasing solidity widens the operational tip speed ratio range as can be seen by examining the 13 percent solidity data.

It should be noticed when comparing Figures 28 and 30 that the peak power coefficient increases from 0.32 to 0.35 when the chord Reynolds number is increased from 1.5×10^5 to 3×10^5 .

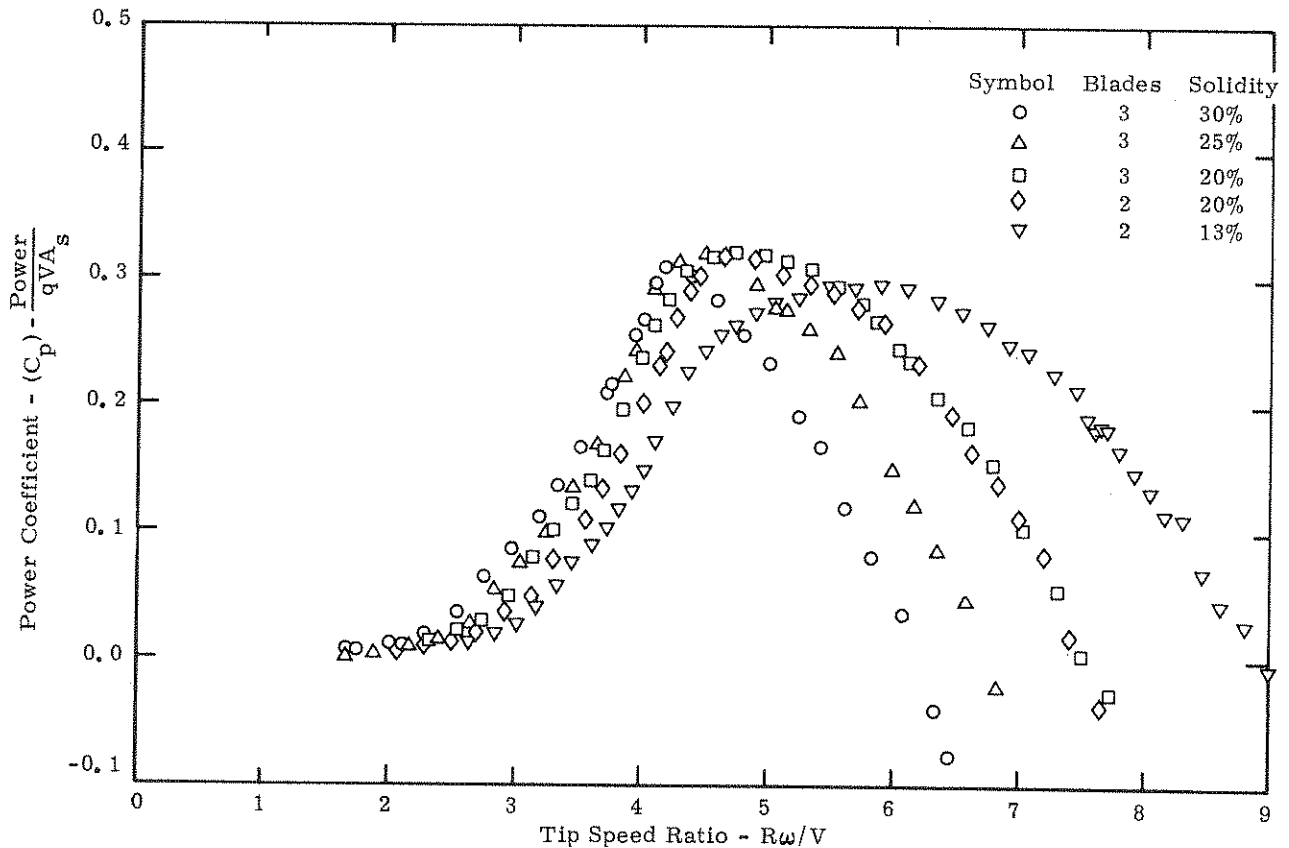


Figure 30. 2-m Darrieus Turbine Power Coefficients for Five Configurations at an Approximate Chord Reynolds No. of 150,000 w/NACA-0012 Blades

PART II
SPECIFIC APPLICATIONS EFFORTS

The 17-m Turbine

Introduction

The design and construction of the 17-m vertical-axis wind turbine, which will be the largest of its type in the U. S., is one of the primary FY 76 goals of the Sandia Vertical-Axis Wind Turbine Program. The main purpose of this device will be to serve as a research tool which is large enough to approach the economically optimum sizes suggested by our systems studies. It is only through the exercise of design, construction, and operation of such a turbine that an accurate realization can be made of the advantages, disadvantages, and technical problems associated with vertical-axis power generation systems.

It is believed that the design approach adapted for the 17-m turbine will yield an operational unit which will fulfill the fundamental objectives of the program. There is no illusion, however, that this turbine represents an optimum wind energy system. Indeed, the knowledge necessary to define optima depends on experience which is only beginning to be accumulated.

As regards the construction of turbine components, the most unusual components, the blades, have received the most attention this quarter. An effort has been made to utilize the resources of private industry and to promote industrial involvement for the problem of blade design. A blade request-for-quotation (RFQ) (see Appendix A) was sent to 58 manufacturers in early fall 1975. This RFQ specified mainly the geometrical and structural requirements of the blades and left the actual analysis, design, and construction of the blades open to the manufacturer. Kaman Aerospace Corp. of Bloomfield, Connecticut, offered a design and analysis approach using helicopter technology, which was felt to have a high probability of success. A contract will be placed with Kaman for an expected blade delivery date of fall 1976. The Sandia designed tower, tie-downs, and electrical equipment will be completed at that time so that the turbine can be assembled and erected immediately.

While the RFQ approach to blade procurement was successful in that operational blades within the program time scales will be obtained, this approach is not without difficulties. For example, response to the RFQ was quite limited, apparently because private industry was uncertain about how to analyze and design these unique blades. Also, the helicopter-type blade construction methods selected are expensive, the blade costs being the order of \$50/lb, even for high production units. To alleviate these problems, an in-house blade design program is being pursued. This design effort will proceed in parallel with the Kaman effort, but with longer time scales. The

in-house design, which will be discussed in more detail next quarter, will emphasize low-cost construction methods and utilize the latest information on turbine loads, structural analysis, and aerodynamic requirements, as it is generated by the overall wind power program. This program, together with the experience accumulated by Kaman in their design and manufacturing program, should yield a much improved basis for obtaining low-cost blades on subsequent turbines.

The following sections will document the specific activities that Sandia has initiated in support of the 17-m turbine program as of December 31, 1975. These studies include system performance predictions, structural analyses, turbine load characterization, component mechanical design, and the electrical system design.

Performance Predictions

Early in the program a matrix of potential turbine sizes and maximum output power levels was defined. This matrix was suggested by an overall system design philosophy of constructing a system which is large enough to generate significant power levels and to present design problems associated with large systems yet small enough to have a reasonable probability of success. These considerations led to the selection of a 17-m diameter turbine, using troposkien or troposkien-approximation blades.⁸ Corresponding to each point in the matrix was a required turbine rotational speed. These were calculated using the NRC experimental turbine performance data,⁶ the only data available at that time. The data base has been extended by wind tunnel testing and aerodynamic code development. This section describes the utilization of those data along with models for the other system components to better estimate the performance of the 17-m turbine system, leading to selection of the generator capacity and the gear ratios for the speed increaser.

Input/output relationships for the components are combined to estimate maximum system output power as a function of turbine rotational speed. In addition, the percentages of time that wind speed would be expected to exceed the wind speeds required for positive output power are calculated.

The basic system components are the synchronous generator, the speed increaser, and the wind turbine. Generator capacities of 30 kW and 60 kW are considered for comparative purposes.

Generator -- The generator rotational speed is chosen to be 1800 RPM. Although lower speeds are available, step-up to 1800 RPM will require gear ratios appropriate to larger systems. Representative efficiencies under various load conditions are shown in Table II.

TABLE II
Percent Efficiencies of Synchronous Generators
(1800 rpm)

Rating	Load		
	4/4	3/4	2/4
30 kW	88.9	87.2	83.0
60 kW	90.6	89.3	85.9

A linear relationship between input and output power can be used to approximate these efficiency characteristics which are given by

$$P_{out} = 0.957 P_{in} - 2.30 \text{ kW (30-kW generator)}$$

$$P_{out} = 0.958 P_{in} - 3.47 \text{ kW (60-kW generator)}$$

where P_{in} and P_{out} are in units of kilowatts.

Speed Increaser -- Losses at rated load in a 6-to-1 transmission stage amount to about 2 percent of rated load. The assumption is made that this loss is approximately constant. Since the speed increaser for the 17-m system will involve a stepup of approximately 36 to 1, the losses are 4 percent of rated load which is dependent upon the generator size. The input/output power relationship for the speed increaser is given by

$$P_{out} = P_{in} - 1.35 \text{ kW (30-kW generator)}$$

$$P_{out} = P_{in} - 2.65 \text{ kW (60-kW generator)}$$

where P_{in} and P_{out} are in units of kilowatts.

Wind Turbine -- The wind turbine performance characteristic of interest for the synchronous (i. e., constant rotational speed) application is the variation of power with wind speed. Turbine power is usually expressed by

$$P = 1/2 \rho A V^3 C_p \left[\frac{R\omega}{V} \right],$$

where the power coefficient, C_p is a function of the tip speed to wind speed ratio, $R\omega/V$. Although

the required performance characteristic can be generated from this equation, a more useful form is given by

$$P = 1/2 \rho A (R\omega)^3 K \left[\frac{V}{R\omega} \right] ,$$

where

$$K = \frac{C_p \left[\frac{R\omega}{V} \right]}{\left(\frac{R\omega}{V} \right)^3} .$$

The function K depends on the advance ratio, $V/R\omega$ and also on the properties of the wind turbine and the flow. For example, Figure 31 shows the variation of K with advance ratio derived from wind-tunnel test data for a Darrieus turbine with a solidity of 0.2 and 3 blades of NACA-0012 cross section. As is most appropriate for constant rotational speed operation, the Reynolds number is based on tip speed and chord length.

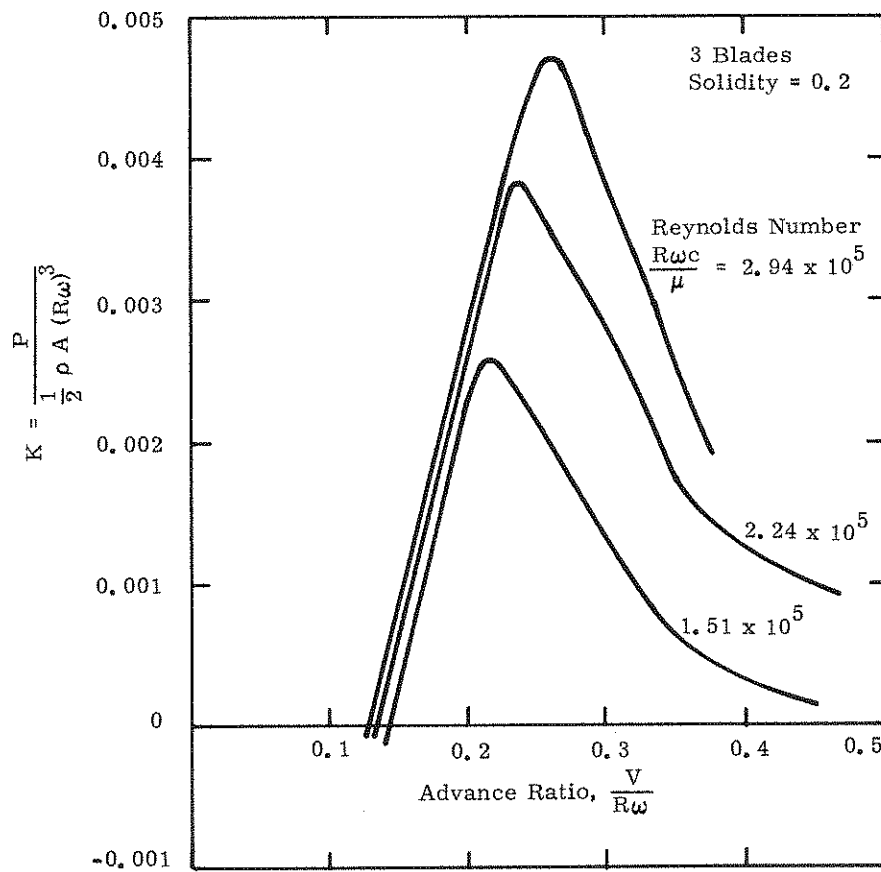


Figure 31. Wind Turbine Performance Characteristics

For a given value of Reynolds number, Figure 31 indicates that K achieves a maximum with respect to advance ratio; that is, power achieves a maximum with respect to wind speed. The advance ratio at which $K = K_{\max}$ is related to the wind speed for maximum power. The advance ratio at which $K = 0$ is the inverse of the "runaway" tip speed ratio; for a system with no losses, this value of advance ratio is related to the wind speed above which positive power is generated. These three parameters are used to estimate the performance of the 17-m system. The curves in Figure 31 further indicate a substantial Reynolds number dependence. Figures 32 through 34 show the variation of K_{\max} ,

$$\left(\frac{V}{R\omega}\right)_{K=K_{\max}}, \text{ and } \left(\frac{V}{R\omega}\right)_{K=0}$$

with Reynolds number for the wind tunnel test data. These figures also show predictions from the single streamtube and multiple streamtube aerodynamic codes. The codes currently neglect Reynolds number variations along the turbine blade. Even with this limitation, however, the trends agree well with experimental data. Thus, there is reasonable confidence at this time of extrapolation to Reynolds numbers association with the 17-m system; i. e., $Re \sim 1.3 \times 10^6$.

Due to structural considerations, the 17-m turbine will include struts which extend from the turbine axis to the blade. Parametric studies were performed to investigate the influence of struts on aerodynamic performance. Consideration was given to cylindrical and NACA-0012 cross sections of various chord lengths. Since a cylinder experiences only drag, this type of strut causes a decrease in power coefficient at all tip speed ratios; in fact, because the drag coefficient is of the order of 1.0, a cylinder of 1-inch diameter can lower the efficiency by 50 percent. With a NACA-0012 cross section, the struts degrade performance only slightly at high tip speed ratios due to a small additional drag from the struts; at intermediate values of tip speed ratio, turbine efficiency can be increased since the struts can act to produce positive torques.

Results -- Figure 35 shows maximum system output power as a function of turbine rotational speed. With a 30-kW generator, rated output power corresponds to a turbine rotational speed of 36 rpm and a wind speed of 22 mph. With a 60-kW generator, rated output power corresponds to a turbine rotational speed of 43.5 rpm and a wind speed of 28 mph.

At selected points on the curves of Figure 35 are noted two percentages. These are percentages of time for which the wind speed exceeds certain values and are based on yearly wind statistics for Albuquerque at a height of 48 feet above the ground. The larger is the percentage of time for which the wind speed exceeds the value for positive output power at the given turbine rotational speed. The smaller is the percentage of time for which the wind speed exceeds the value for maximum output power at the given turbine rotational speed; this percentage can be approximately doubled for the windiest month and halved for the calmest month. Thus, the numbers indicate that, for fractions of time exceeding 25 percent, positive system output power would be generated, while for fractions of time of the order of a few percent, maximum system output power would be generated. Additional

calculations show, however, that at a 12-mph average wind speed site, the latter percentage is increased by about a factor of 5, which gives an indication of 17-m system performance at a potential operational site.

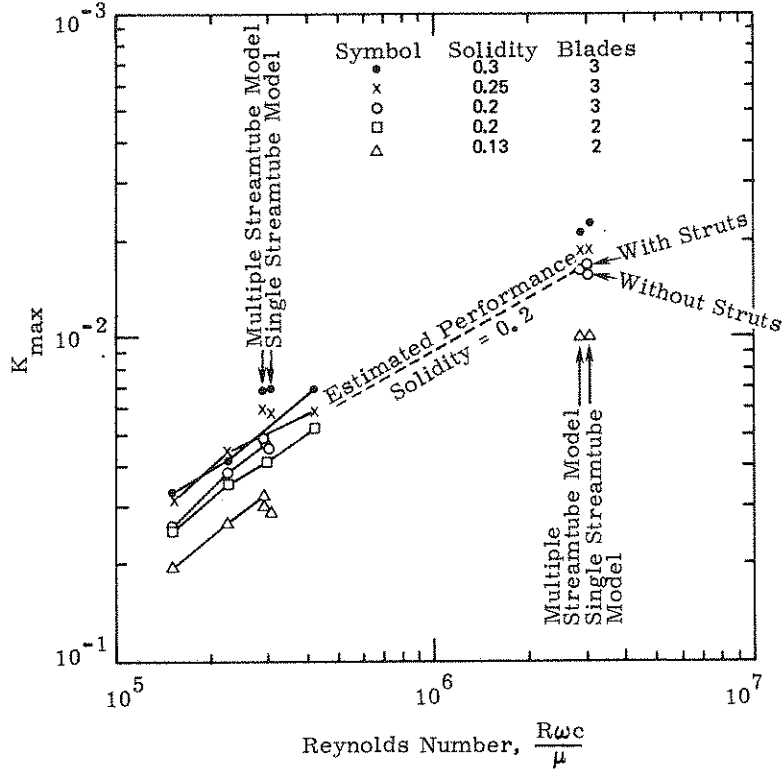


Figure 32. Variation of K_{max} with Re

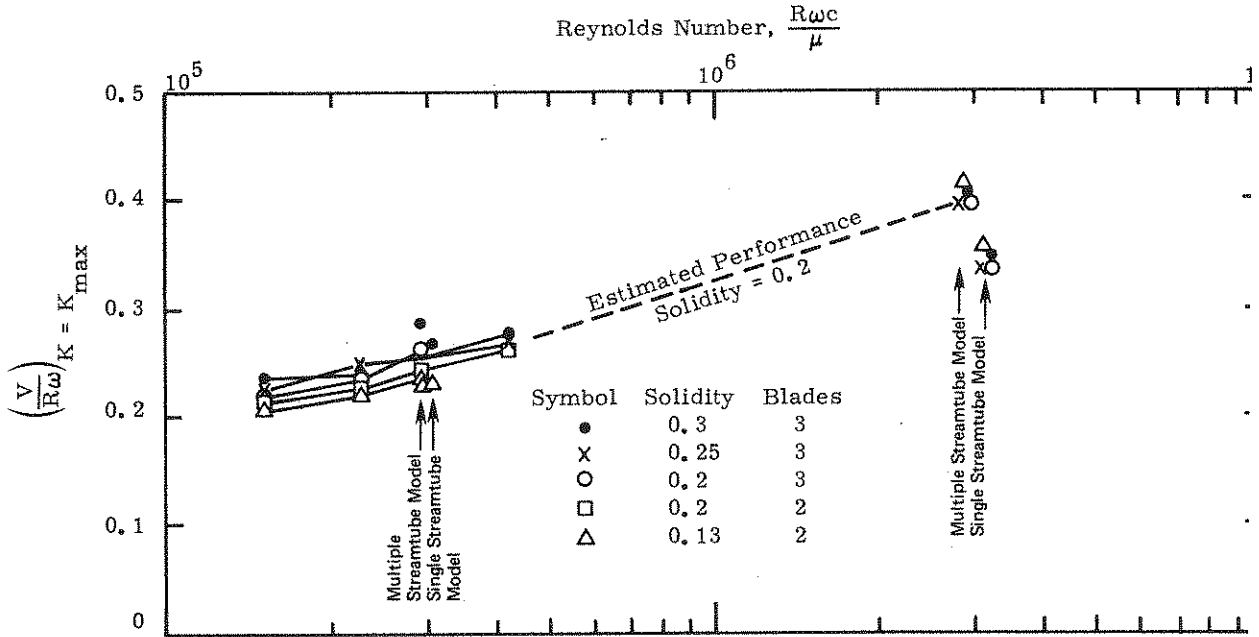


Figure 33. Variation of $\left(\frac{V}{R\omega}\right)K = K_{max}$ with Re

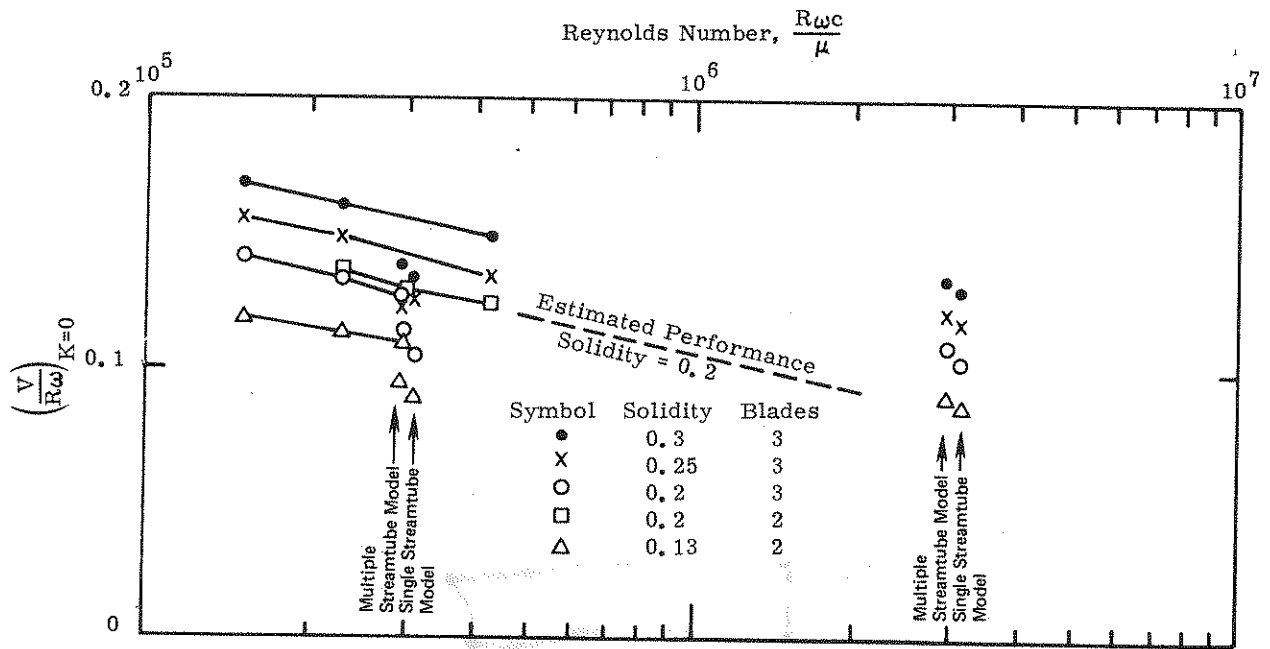


Figure 34. Variation of $\left(\frac{V}{R\omega}\right)_{K=0}$ with Re

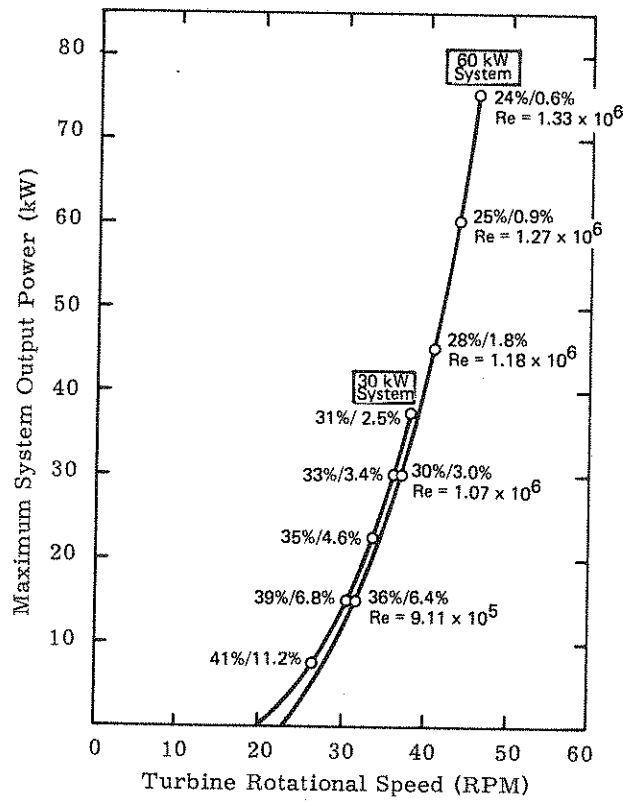


Figure 35. Performance of the 17-m System

Consideration should be given to the 17-m system as a potentially interesting application unit. The economic model indicates that a 17-m turbine should be coupled to a 90-kW generator at a 12-mph average wind speed site. While the absolute size is subject to some doubt due to the questioned adequacy of the model, use of a 60-kW generator rather than a 30-kW generator is probably in the right direction. Furthermore, the difference in efficiencies of the 30-kW and 60-kW generator are not large.

Perhaps more importantly, the system will be used to deduce turbine performance characteristics in anticipation of scale-up. Turbine rotational speeds should be selected to cover a wide range of Reynolds numbers, since both the wind-tunnel test data and the aerodynamic codes indicate a strong dependence of performance on Reynolds number. Figure 36 shows the intervals of Re spanned by experimental data from wind tunnel tests and proposed 5-m turbine tests. In order to provide some overlap, a speed of 23 rpm corresponding to an Re of 6.65×10^5 appears attractive. To hedge against a bad guess on performance, speeds of 41 rpm, 44 rpm, and 46 rpm are suggested. Thus, as indicated in Figure 36, the interval $6.65 \times 10^5 < Re < 1.33 \times 10^6$ would be covered.

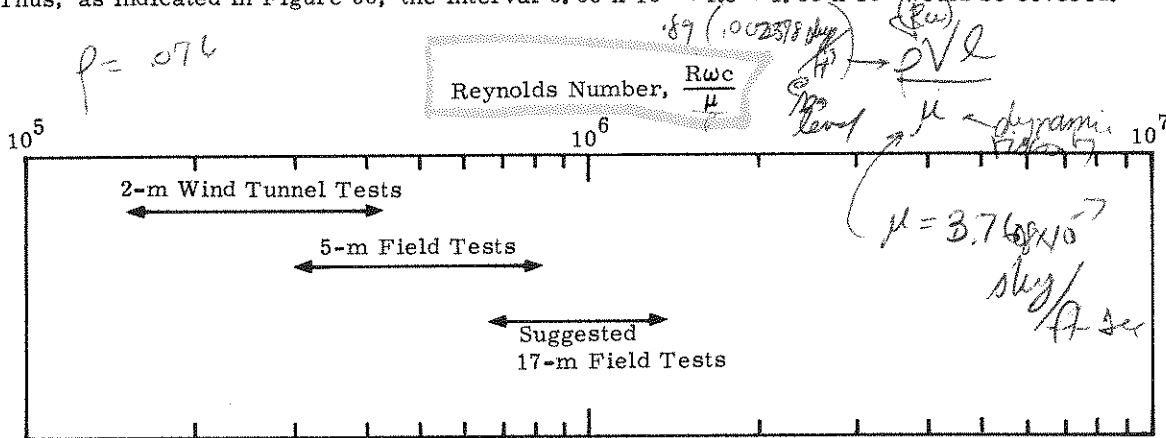


Figure 36. Reynolds Number Intervals for Experimental Data

Structural Analysis

Blade Analysis -- The major effort in blade analysis involved evaluating the proposals received from the design and fabrication RFQ (see Appendix A). The major structural blade requirements may be simply summarized: the blades are to survive the loads imposed by gravitational, centrifugal, and aerodynamic forces for a maximum turbine speed of 75 RPM; and the lowest blade resonant frequency should exceed 3 per revolution plus 20 percent at 75 RPM (4.5 Hz). The extra 20 percent is included so that a resonant response is not centered about the turbine maximum speed.

The results of a preliminary analysis carried out on the Kaman blades will be discussed. The basic geometry is shown schematically in Figure 37. This proposal includes support struts (NACA 0012 sections). The analysis was conducted both with and without the struts included, so that the stiffening provided by these supports could be quantified.

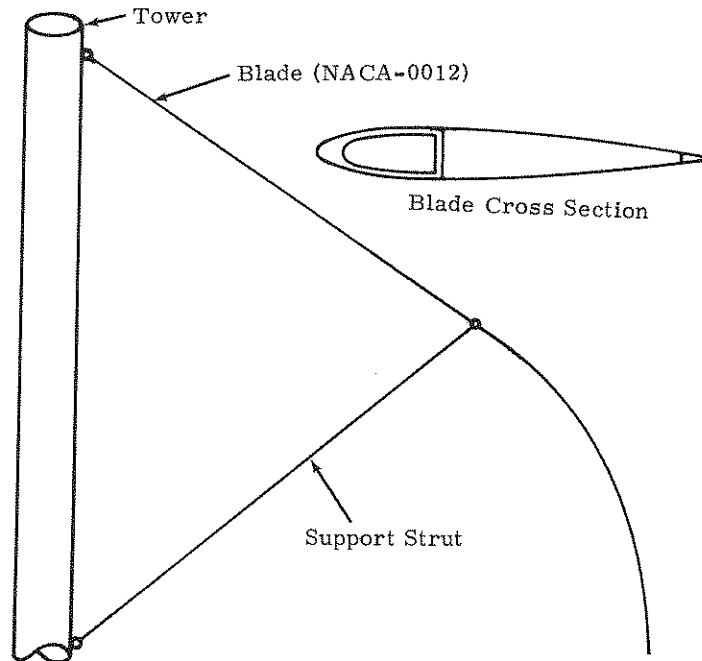


Figure 37. Kaman Blade

Figures 38 and 39 depict the deflection (magnified 10 times) and lowest frequency mode shape, respectively, under the influence of gravitational and centrifugal forces at 75 RPM. This case does not include the support struts. The maximum blade stresses were found to be the order of 10,000 psi for this loading. On Figure 39, the eigenvalue (natural frequency) corresponding to the mode shape is 1.931 Hz. This is much lower than the 4.5-Hz requirement stipulated in the blade design and fabrication RFQ.

To simulate the effect of struts on the structure, the displacements were restricted normal to the blade at the point of strut attachment. Maximum stresses at 75 RPM were approximately the same, though stresses at 0 RPM were reduced. The deflection (magnified 10 times) and lowest natural frequency are shown in Figures 40 and 41, respectively, for 75 RPM. Due to the struts, the natural frequency is raised to 5.352 Hz, which is above the 4.5-Hz requirement.

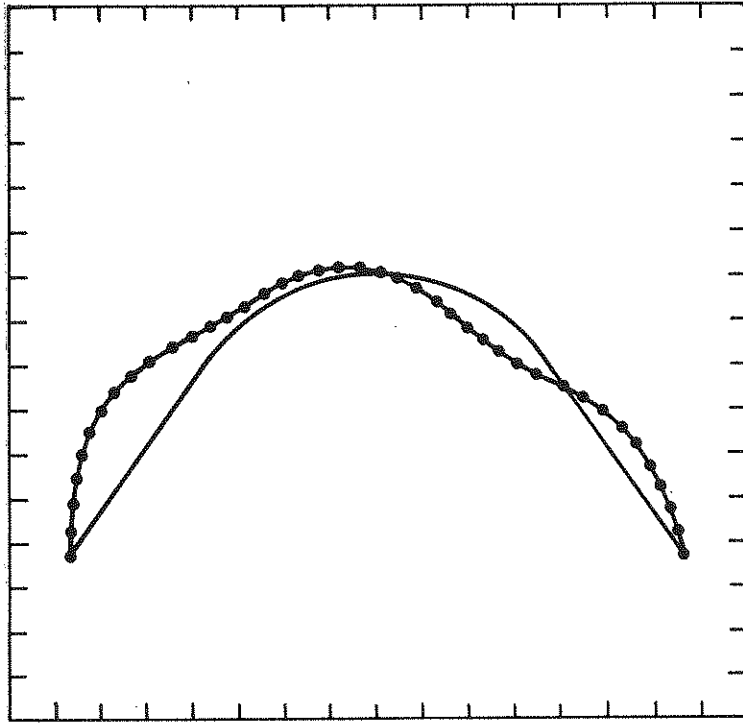


Figure 38. Deflection (10X) at 75 RPM - Kaman Blade

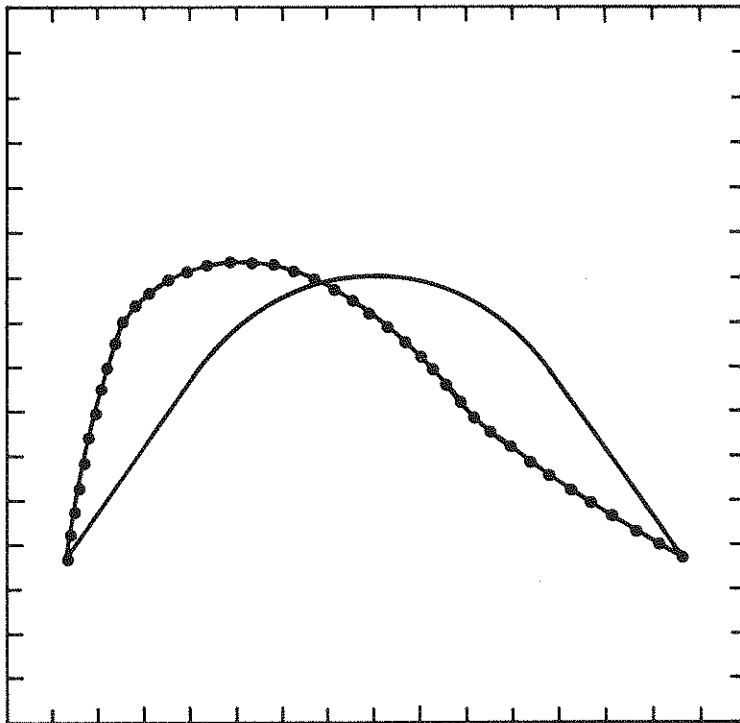


Figure 39. Lowest Eigen Function at 75 RPM - Kaman Blade (1.931 Hz)

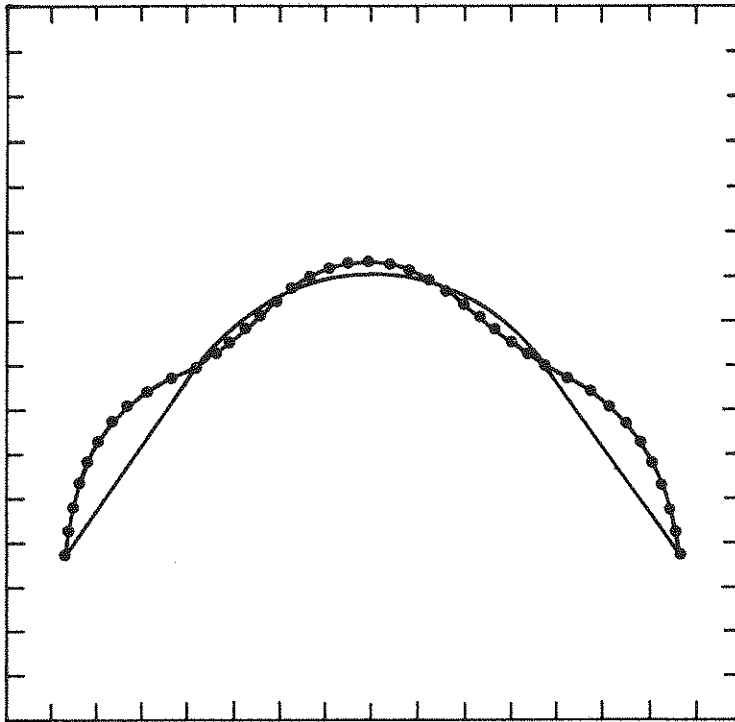


Figure 40. Deflection (10X) at 75 RPM Kaman Blade with Struts

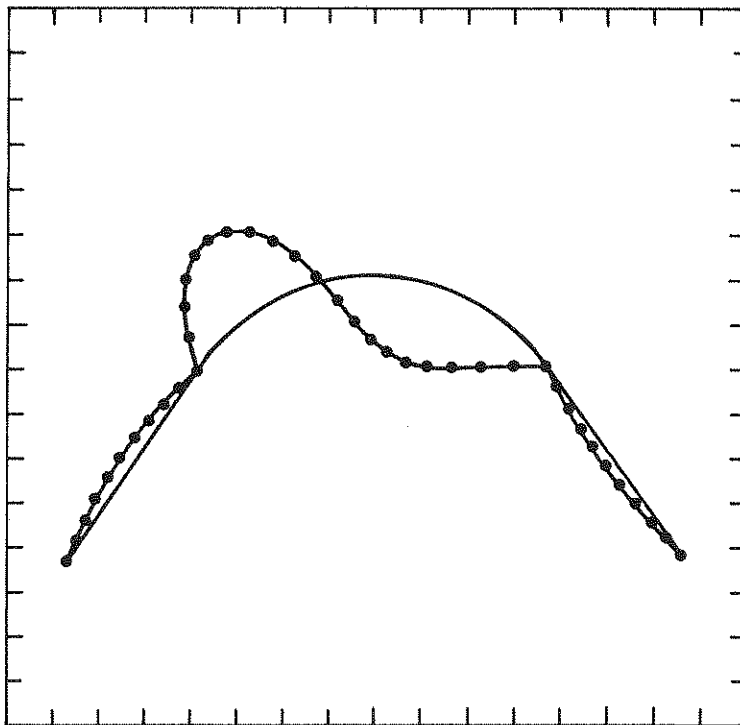


Figure 41. Lowest Eigen Function at 75 RPM Kaman Blade with Struts (5.352 Hz)

The effect of the large flapwise aerodynamic forces on the blade structure have also been examined. These loads, in extreme operating conditions are comparable to the centrifugal forces. During each cycle, a blade experiences a maximum outward (from the tower) flap aerodynamic force and a maximum inward force of approximately the same magnitude. Figures 42 through 47 show the effect of this force on stresses and deformations for a 60 RPM turbine speed in a 100-mph wind. Admittedly, this is not a condition to be seen frequently, but the turbine may have to withstand environments of this order. Figures 42 and 44 show the outer and inner fiber flapwise bending stresses (in psi) with an outward and inward directed 100-mph flap aerodynamic force. Figure 43 is the condition seen halfway between points in the cycle corresponding to Figures 42 and 44. There is effectively no flap aerodynamic force at this point. Figures 45 through 47 show the corresponding results for the actual deflections. The S coordinate used in the stress plots is a meridional blade coordinate. There are three points to be made with these results. First, the addition of the flap aerodynamic force at 60 RPM increases the maximum stresses almost a factor of two. Second, the variation of resultant stresses during a cycle can be as high as 17,000 psi, which indicates a need to consider fatigue if such environments are frequently encountered. Third, the deformation during each cycle as seen in Figures 45 through 47 may degrade aerodynamic performance. Though not studied yet, the effect of struts is anticipated to reduce the oscillations and stresses during the cycle.

In conclusion, this preliminary structural analysis suggests that the Kaman blade design, particularly when using support struts, will be suitable for use on the 17-m turbine. Analysis will continue to examine more aspects of this problem in particular, the lead-lag behavior of the blades and the effect of support struts.

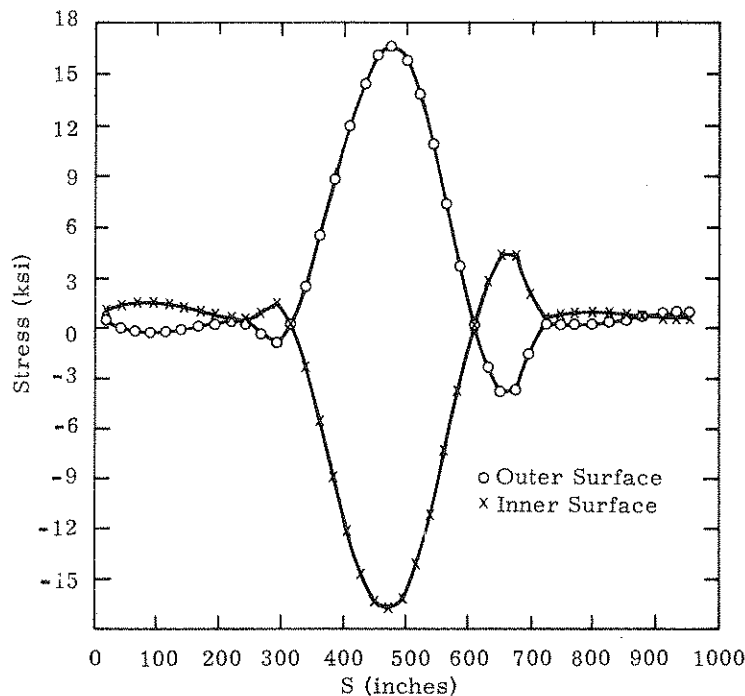


Figure 42. Stresses at 60 RPM with Inward-Directed 100-mph Wind - Kaman Blade

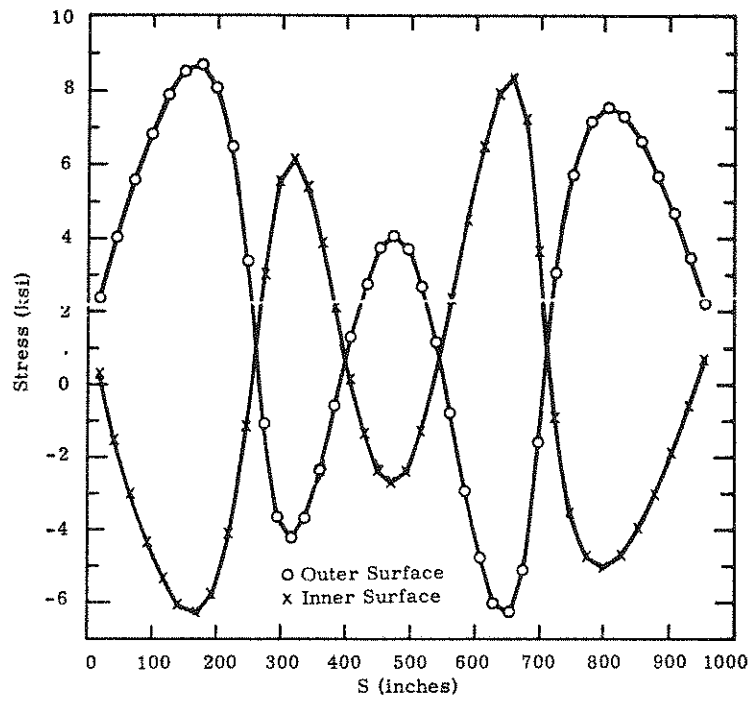


Figure 43. Stresses at 60 RPM with No Wind Loading - Kaman Blade

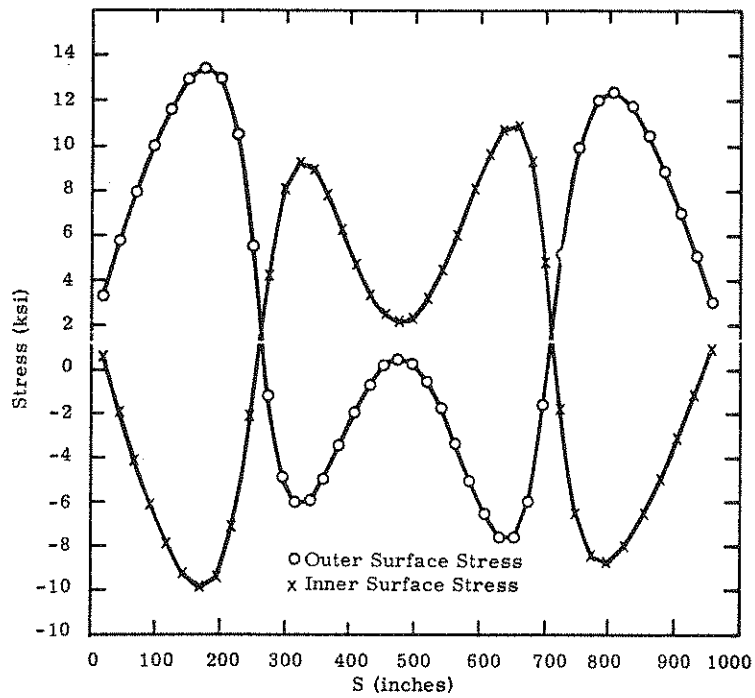


Figure 44. Stresses at 60 RPM with Outward-Directed 100-mph Wind - Kaman Blade

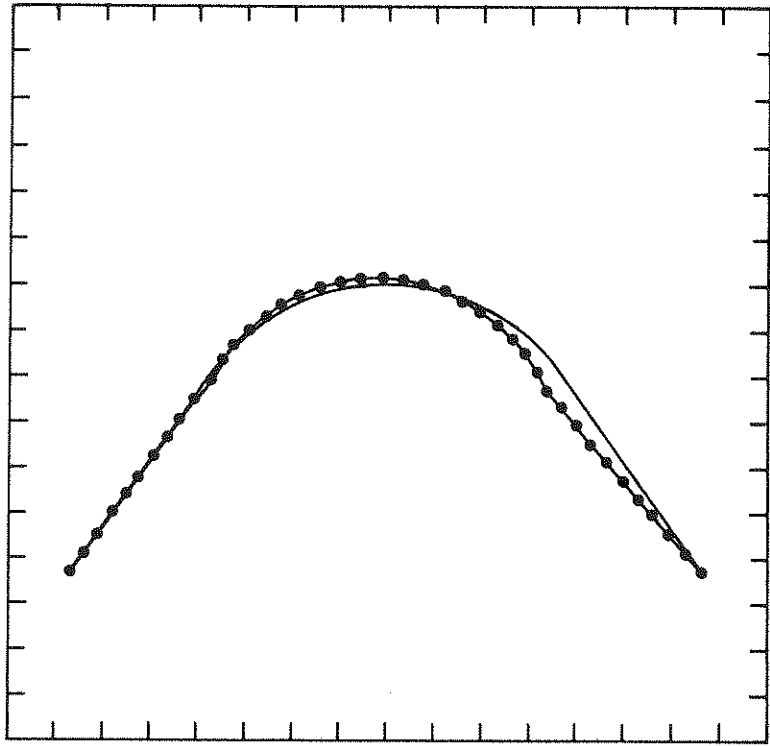


Figure 45. Deflections at 60 RPM with Inward-Directed 100-mph Wind - Kaman Blade

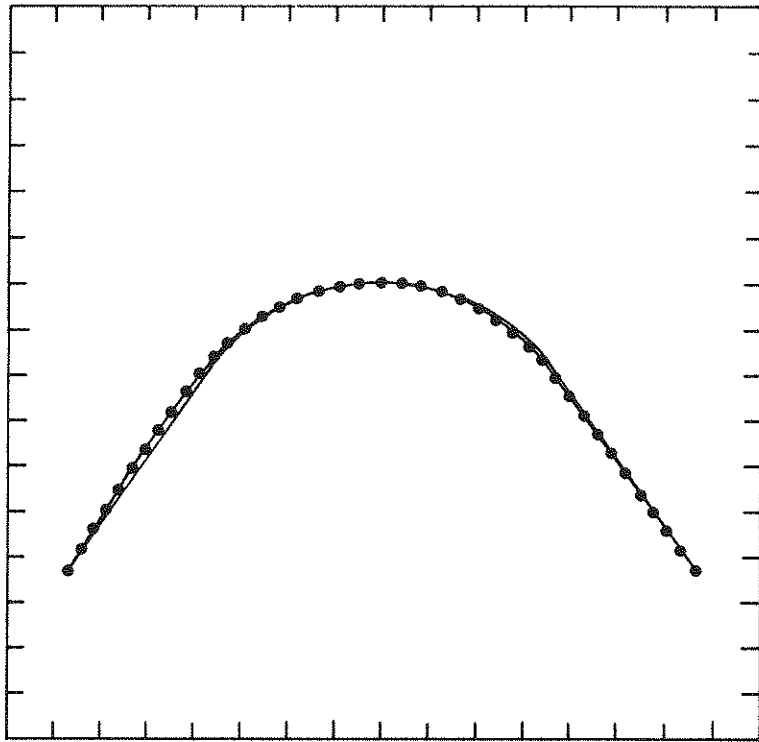


Figure 46. Deflections at 60 RPM with No Wind Loading - Kaman Blade

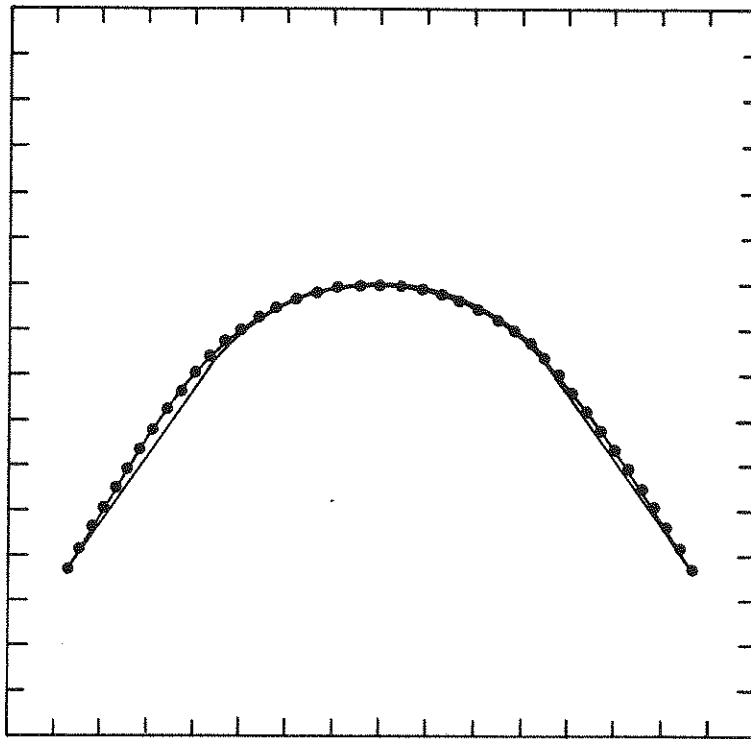


Figure 47. Deflections at 60 RPM with Outward-Directed 100-mph Wind - Kaman Blade

Tower Analysis -- The tower for the 17-m turbine must be designed to withstand axial loads due to the tie-down, axial components of the blade root loads, and turbine weight. It must also withstand torsional loads due to blade root moments resulting from aerodynamic torques and turbine inertial loads, as well as flexural loads due to radial components of the blade root loads and aerodynamic drag. Finally, the resonant frequencies of the tower, or those which involve the tower, should be above 4.5 Hz which is three times the turbine runaway speed of 75 RPM, plus 20 percent. All of these conditions place requirements on the tower which can be characterized by axial, torsional, and flexural stiffnesses; buckling resistance; and load-carrying capabilities. Design curves for these requirements, or properties, are being developed, using analyses mentioned in the General Applications Section, which cover wide ranges of truss parameter values. Examples are provided in Figures 48 through 50 where element buckling resistance and torsional bay stiffness are presented for triangular cross-section, single cross-brace truss towers. Figure 48 illustrates the dependence of minimum truss element diameter on bay length for various critical axial loads. Figures 49 and 50 illustrate the dependence of torsional stiffness of a bay on bay length for various truss radii and element diameters, as indicated. Torsional stiffnesses of the bays must be added in series to obtain a torsional stiffness for the entire tower.

Similar design curves exist for all design parameters. In general the tower stiffnesses will be determined by allowable resonant frequencies and the load-carrying capability will be determined by loads applied to the tower at the blade attachment points. The use of these design curves to select an appropriate tower design is continuing and results will be presented next quarter.

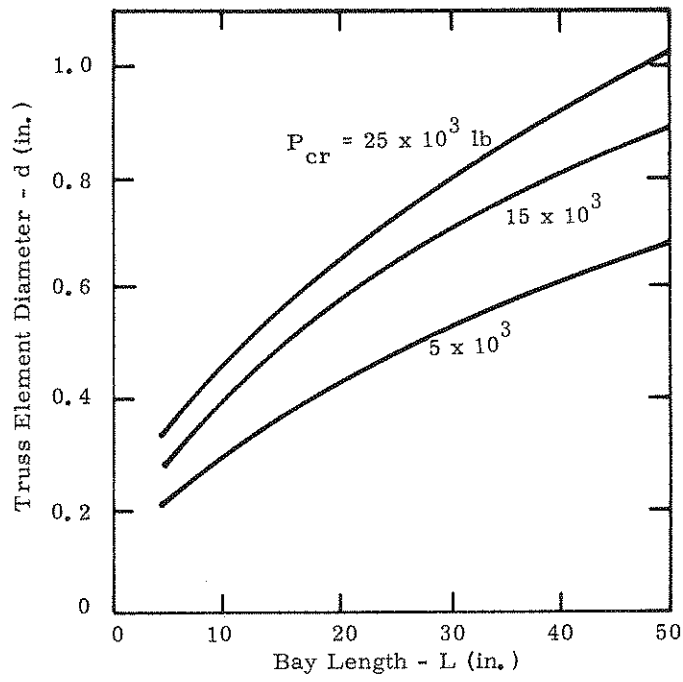


Figure 48. Truss Element Buckling Resistance

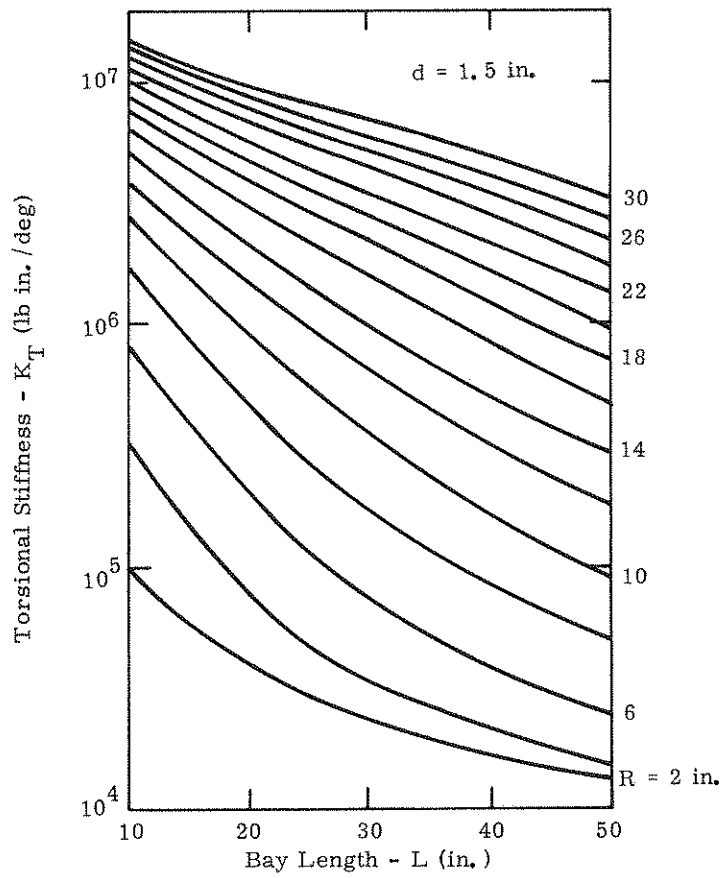


Figure 49. Torsional Stiffness of Truss Tower Bays ($d = 1.5 \text{ in.}$)

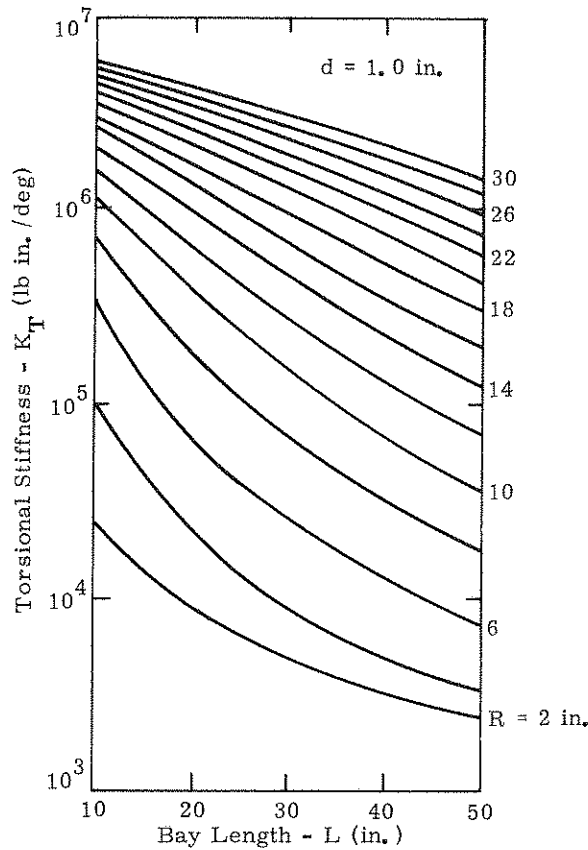


Figure 50. Torsional Stiffness of Truss Tower Bays ($d = 1.0$ in.)

Structural Load Requirements

An attempt has been made in the last quarter to quantify the basic structural loads that the 17-m turbine components must withstand. The analysis to date has focused on the loads distributed along each blade, the resultants of these loads at the blade root, and the net effect of the root loads on the tower. Except where noted, the current results include the effects of aerodynamic,* centrifugal, and gravitational forces.

In calculating the loads, the turbine blades and tower are assumed to behave as rigid bodies. It is believed that this simplification does not compromise the results for use as engineering design guides. The legitimacy of this approximation will be examined in the future by applying the calculated loads to a finite element model of the structure to see if deflections are large enough to significantly change the aerodynamic loading. Should the deflections be large, an attempt will be made to iterate the loads so that they are compatible with the structural deformation.

* The single streamtube model discussed in the General Applications Section was used to evaluate aerodynamic blade loads.

The bulk of the analyses completed so far has concentrated on normal operating conditions, i. e., the operation of the turbine at constant RPM for wind speeds less than 60 mph. These conditions are expected to occur for indefinite periods of time, and the structure should survive the resulting loads without fatiguing and without excess deformations of the blades which might degrade performance. There are, however, potentially more severe abnormal conditions which the turbine must also survive, although not on a high cycle basis. These conditions include startup, runaway, emergency braking, and operation in unusually high winds. Of these a preliminary analysis of the emergency brake has been completed.

The following sections will briefly summarize the calculated loads on the blades, the blade roots, and the net effect on the tower. Finally, the preliminary emergency brake design analysis is discussed. Except when noted otherwise, all the results are for a straight-circular-straight troposkien approximation blade with a solidity of 0.2 and no support struts. The NACA-0012 blade section is used along the entire length of blade, and three blades are used.

Distributed Blade Loadings -- Figure 51 summarizes the results for distributed loads on the blades due to aerodynamic and centrifugal effects. The magnitudes represented in this figure are for the portion of the blade at the maximum radius position from the axis of rotation. To estimate loads at other radial positions, a reasonable approximation is to assume the load to decay linearly with distance from the turbine axis.

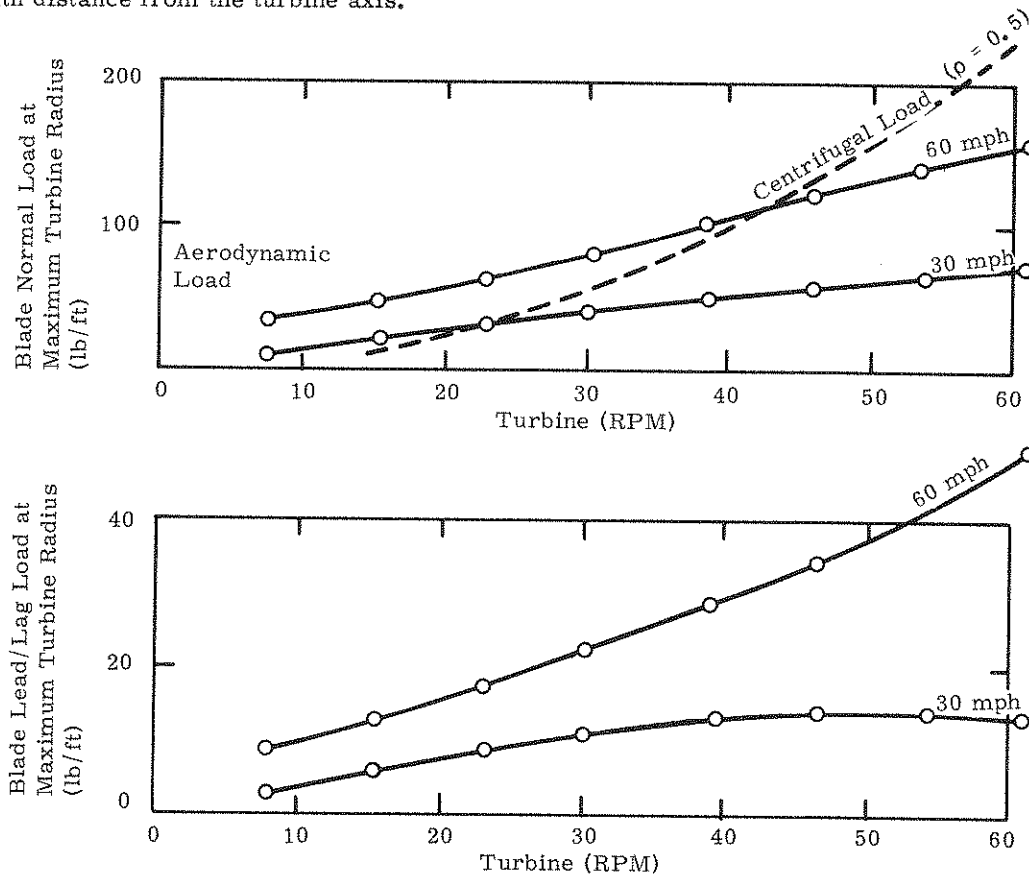


Figure 51. Aerodynamic and Centrifugal Blade Loads

The aerodynamic loads vary as the turbine rotates through a complete revolution. The magnitudes in Figure 51 represent the maxima which occur over a cycle. The direction of the "normal" force is taken to be normal to the flatwise plane of the blade for the aerodynamic forces and normal to the turbine axis for the centrifugal loads.

It is apparent from Figure 51 that the blade loading is most severe in the high wind, high RPM operating condition. The lead/lag aerodynamic forces are lower in magnitude than the normal forces by a factor of 3 to 4. The centrifugal forces are evidently the same order of magnitude as the aerodynamic forces for the relatively light blades (approximately 7 lb/ft) used in the 17-m turbine.

Blade Root Loads -- The various resultants at the root from the applied loads on the blades are shown in Figure 52, which refers to the lower root of a particular blade.

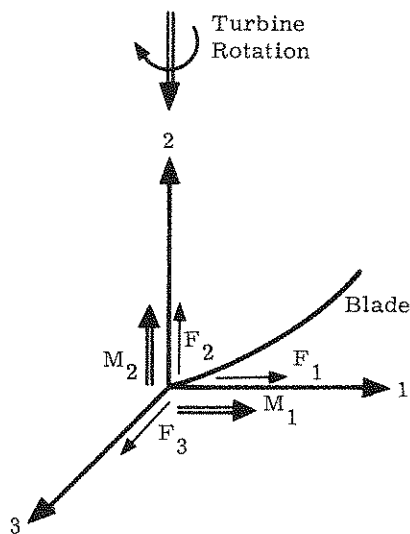


Figure 52. Root Load Nomenclature

The 1-2-3 coordinate system is fixed to the blade, with the blade in the 1-2 plane and the turbine axis coincident with the 2 axis. Three forces (F_1 , F_2 , and F_3) and two moments (M_1 and M_2) are considered to apply at the root. The root is assumed to be a single-degree-of-freedom hinge with unrestricted rotation possible only about the 3 axis. The loads given are treated as reactions from the tower applied to the blades.

The aerodynamic model used neglects wind shear, so the aerodynamic portion of the loads at the upper root are related to lower root loads by symmetry. These symmetry arguments show that all the loads except F_2 and M_1 have the same magnitude and direction at the upper root. The loads F_2 and M_1 , alternatively, are of opposite sign at the upper and lower roots.

The following numerical results do not include the loads at the blade root due to centrifugal or gravitational forces. These forces may be accounted for by adding the incremental loads F_1^* , F_{2B}^* , and F_{2T}^* (see Table III) to the aerodynamic resultants F_1 and F_2 . The subscripts B and T

refer to the bottom and top of the turbine, respectively, as the addition of load to F_2 is not symmetrical due to the effect of blade weight.

TABLE III
Load Adjustments for Centrifugal and Gravitational Effects

Turbine (RPM)	F_1^* (lb)	F_2^* (lb)	F_{2B}^* (lb)
0	0	264	+ 264
10	-148	364	+ 164
20	-591	663	- 135
30	-1331	1161	- 633
40	-2366	1860	- 1332
50	-3697	2757	- 2229
60	-5323	3853	- 3325
70	-7245	5149	- 4621
75	-8317	5872	- 5344

Figures 53 and 54 show the variation of the moment M_2 and Force F_1 with the azimuthal angle θ and various tip speed ratios. These curves are normalized such that the maximum value over a cycle is unity. With this normalization, the shapes of the curves are a function of only the tip speed ratio. The erratic behavior of both loads at low tip speed ratios (corresponding to high wind speeds) is due to the aerodynamic stalling of the blades. For tip speed ratios above 3, angles of attack are low enough to eliminate blade stall. In this case, the moment M_2 approaches the classical two-per-revolution characterization, while F_1 approaches one per revolution. The behavior of loads F_3 and M_1 are essentially identical (although of opposite sign) to that of M_2 when the normalized coordinates of Figures 53 and 55 are used. The same correspondence applies to the loads F_2 and F_1 .

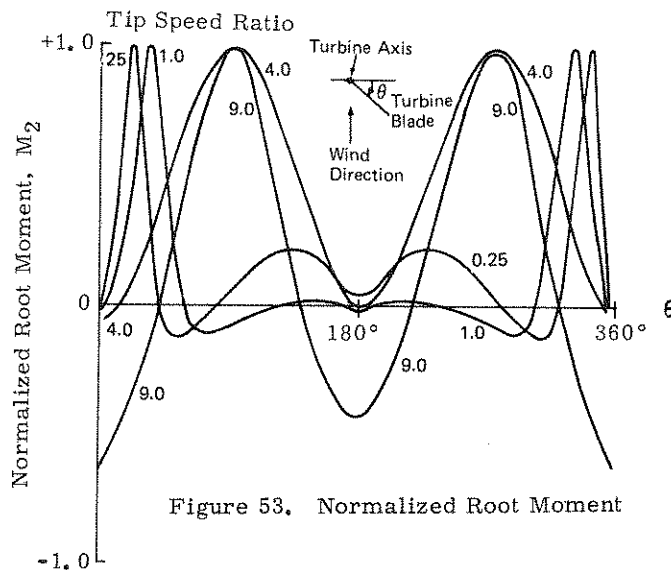


Figure 53. Normalized Root Moment

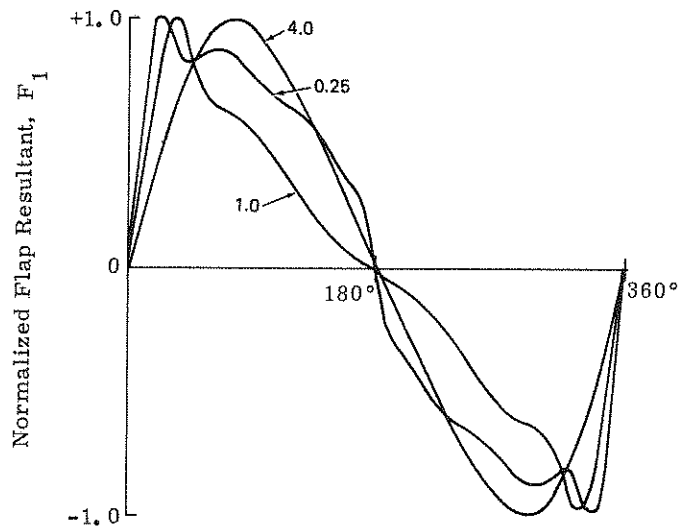


Figure 54. Normalized Flap Resultant

The peak magnitudes of the various loads which occur over a cycle are shown in Figures 55 through 57, as a function of RPM and wind speed. As might be expected, the loads are most severe in high winds at high rotational speeds.

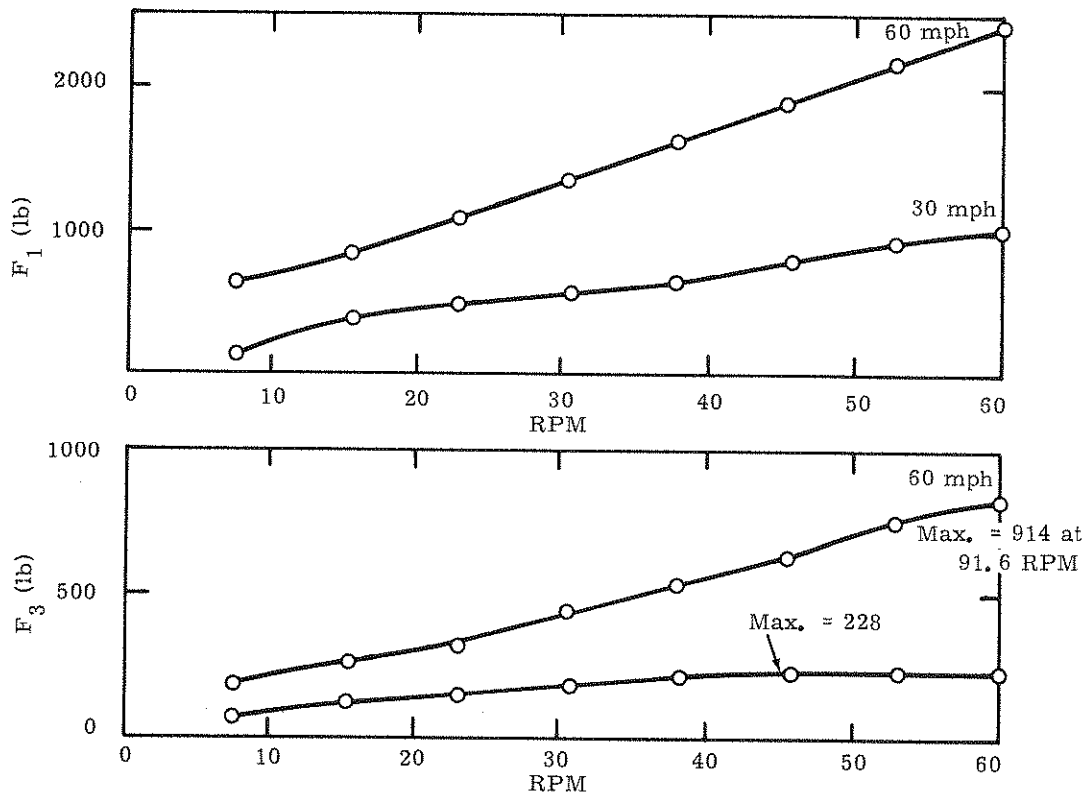


Figure 55. Flap and Lead/Lag Resultant Magnitude

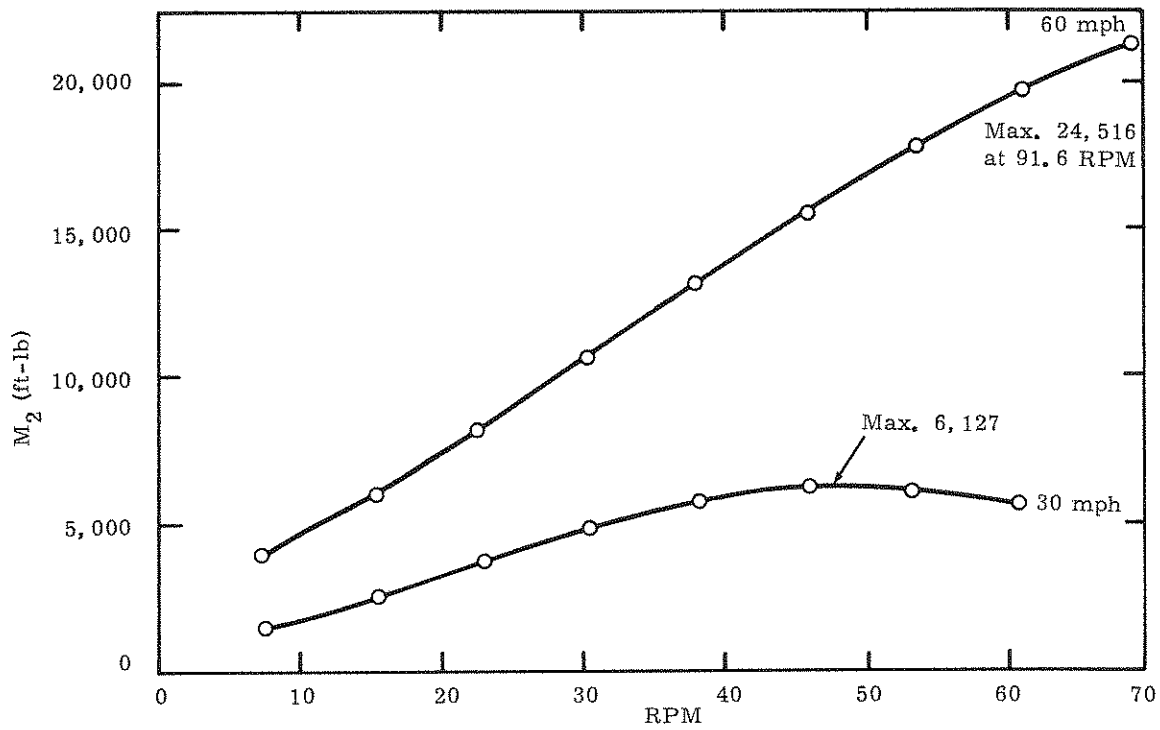


Figure 56. Root Moment (M_2) Magnitude

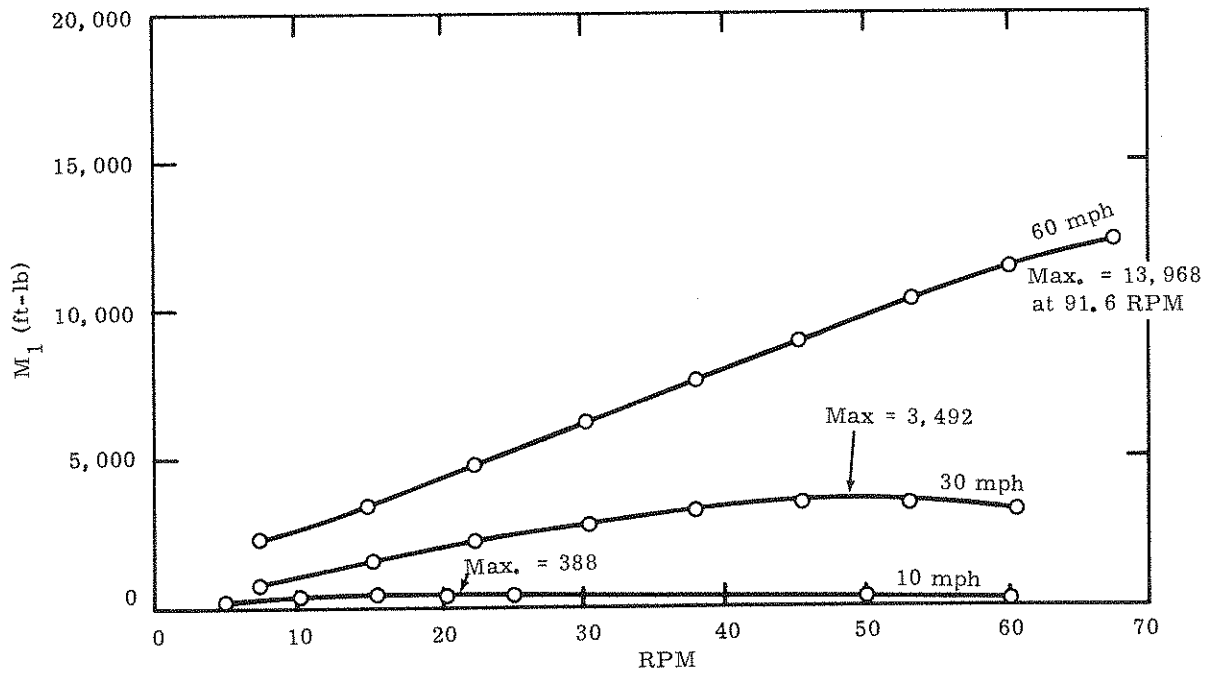


Figure 57. Root Moment (M_1) Magnitude

Tower Force Resultants -- The aerodynamic loading on each blade of the Darrieus turbine will lead to a net unbalanced horizontal force on the tower directed principally in the downwind direction. The nature of this horizontal force will govern the design of the tower tie-down system.

The downwind force is calculated by resolving the individual blade root forces at the blade/tower connection point. It was found that the nature of the resultant depends strongly on the number of blades used, so both two- and three-bladed rotors are considered. As the centrifugal and gravitational loads do not contribute to the net horizontal load on the tower, only the aerodynamic portion of the root loads are used in the analysis.

The net horizontal load does not always act exactly in the downwind direction, as shown by the polar plot of Figure 58. The radial coordinate on these polars represents the normalized horizontal force resultant on a single blade/tower connection point as the rotor turns in the direction shown.

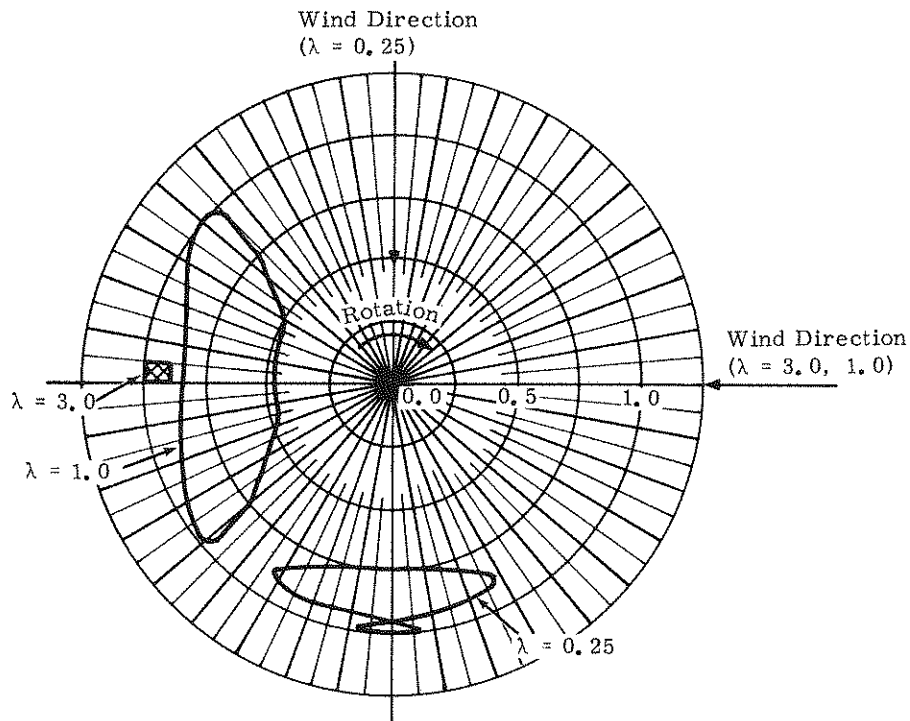


Figure 58. Force Polars for Three-Bladed Rotor

The normalization is selected to yield a maximum force of one unit over a cycle. This normalization is convenient, as the resulting shape of the polars depends primarily on the tip speed ratio, and not the absolute size of the rotor, or the wind speed and RPM.

Figure 58 shows polars for a three-bladed rotor. It is noteworthy that for low tip speed ratios (< 2.5), the resultant vector varies considerably in magnitude and direction, an effect caused by the periodic stall of the blades. The cycles shown repeat every 120 degrees of tower rotation due to symmetry, and so the tower excitation is fundamentally a 3-per-revolution type. As the tip speed

ratio increases above about 2.5, the horizontal force varies only slightly in magnitude and is directed within 3 degrees of downwind.

Figure 59 shows a different character for two-bladed rotors. The force polars show a generally wider variation in magnitude and direction. The most significant difference occurs at relatively high tip speed ratios (> 2.5), where the two-bladed force polar approaches a circle passing through the origin. Also, since the cycle repeats every 180 degrees of tower rotation, the excitation is fundamentally of a 2-per-revolution character.

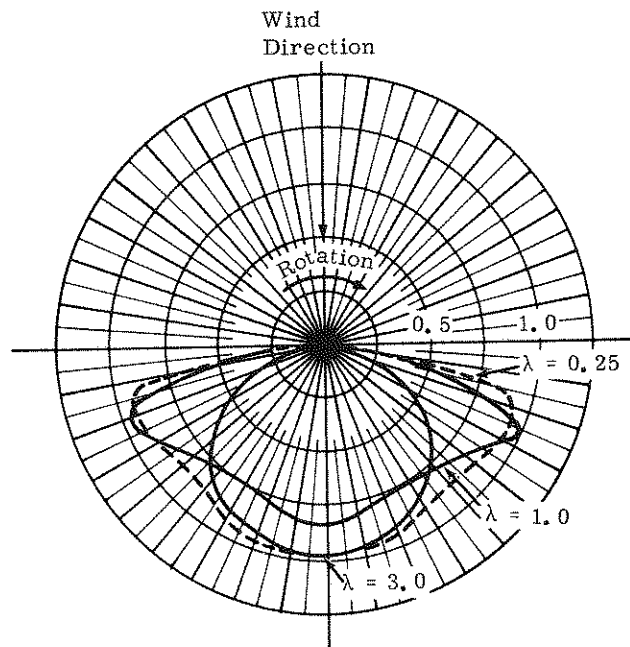


Figure 59. Force Polars for Two-Bladed Rotor

Figure 60 shows the maximum amplitude of the horizontal resultant for the 17-m turbine. The two-bladed rotor yields higher forces because of the opportunity for this geometry to add root loads constructively at certain portions of the cycle.

The net torque produced at the blade/tower connection influences the sizing of the tower and other torque transmitting shafts. The overall shaft torque could be determined in an analogous manner to the horizontal forces by summing the appropriate root moments. However, this calculation has not been completed at this time. An alternative method, based on the turbine power coefficient, is used here for an order-of-magnitude estimate of the torque. This analysis is an approximation in that the maximum average torque which can be produced will not necessarily be realized normally, and the fluctuating component of the torque could yield peak shaft torques above this average.

TABLE IV

Average Aerodynamic Torque

Turbine RPM	30	40	50	60	75
Aerodynamic Torque (ft. -lbs.)	6300	11,200	17,600	25,200	39,400
Wind Speed at Maximum Torque (mph)	19.6	26.2	32.7	39.3	49.1

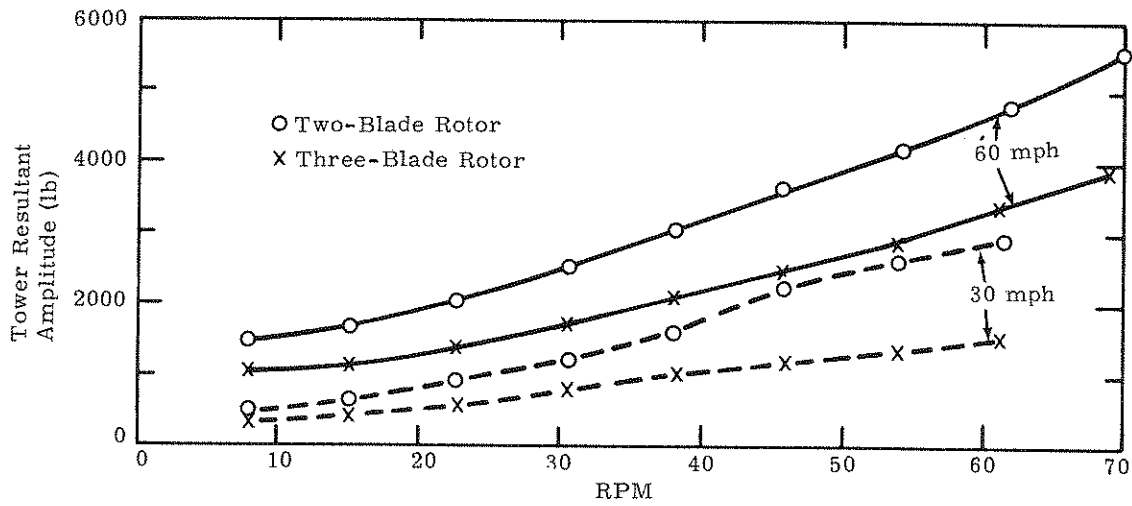


Figure 60. Tower Resultant Magnitude

Emergency Brake Loading -- The deceleration of the turbine due to application of an emergency brake leads to effective body forces applied to the blades in the lead/lag direction. The magnitudes of these inertial loads have been estimated for a particular type of brake, a simple constant torque type applied automatically at some preselected RPM limit. The selection of required torque for such a brake is dominated by the need to overcome the maximum wind torque that can be produced by the turbine at the RPM limit. Although the actual turbine deceleration will depend upon the prevailing winds during braking, it is possible to put an upper bound on the deceleration by considering a no wind condition.

Table V summarizes the upper bound decelerations along with required braking torques and blade inertial loads. The results are for a blade specific gravity of 0.5 (7 lbm/ft) which is representative of the blades under consideration for the 17-m unit. The inertial blade loads refer to that portion of the blade at the maximum radius from the turbine axis; for other positions of the blade, the loads should be reduced in proportion to the distance from the turbine axis.

TABLE V
Emergency Brake Loading

<u>Turbine Limit (RPM)</u>	<u>Brake Torque (ft-lbs)</u>	<u>Maximum Deceleration (rad/sec²)</u>	<u>Inertial Load (lbs/ft)</u>
75	49,000	2.9	17.3
70	43,000	2.4	14.3
60	31,000	1.8	10.7
50	22,000	1.2	7.2

Concluding Remarks -- The major loads acting on the 17-m Darrieus turbine have been defined and form a reasonable quantitative starting point for the structural design of the machine. The loads given in this summary are, of course, approximate. It is a goal of this program to continuously update the loads analysis as improved methods are developed, as physical experience is accumulated, and to account for changes in the turbine geometry.

Most of the effort next quarter will probably be directed toward mathematically applying these loads to the 17-m structure to examine its adequacy. In the long term, by considering the response of hypothetical structures to the loads, it should be possible to identify what minimum structural properties are required to ensure adequate performance. It is through this longer term effort that future blade designs can be properly matched to the loads imposed by the turbine, thereby avoiding costly excess structural capacity.

Mechanical Design

The Sandia responsibilities for mechanical components on the 17-m turbine include the support tower and tie-downs, the blade-to-tower connecting hubs, the in-house blade design, and the turbine base. This section will discuss primarily the turbine base, as the base has received the most detailed design consideration this quarter. The major effort for the other mechanical components has gone into design tools which are discussed in other sections of this report. The actual design of these other components is proceeding and will be covered in the next quarterly report.

The turbine base contains the means for axial support of the turbine, the power train (consisting of a speed increaser, synchronous generator, and an inductive starter), and a braking system. A schematic layout of the base (Figure 61) illustrates the major features of the design. Most striking is the right-angle drive, which permits installing the generator/starter system on a horizontal axis. This feature, which is admittedly more complex and less efficient than a straight drive, does offer important advantages when used in this prototype. For example, the horizontal components can be easily removed and changed due to their accessibility; and the constraint of compactness (to avoid excess base height) is relieved by having two rotational axes. This will simplify making any modification to the drive train once it is installed. These advantages are believed to be much less important for production machines, and a production-oriented design would probably have a straight drive.

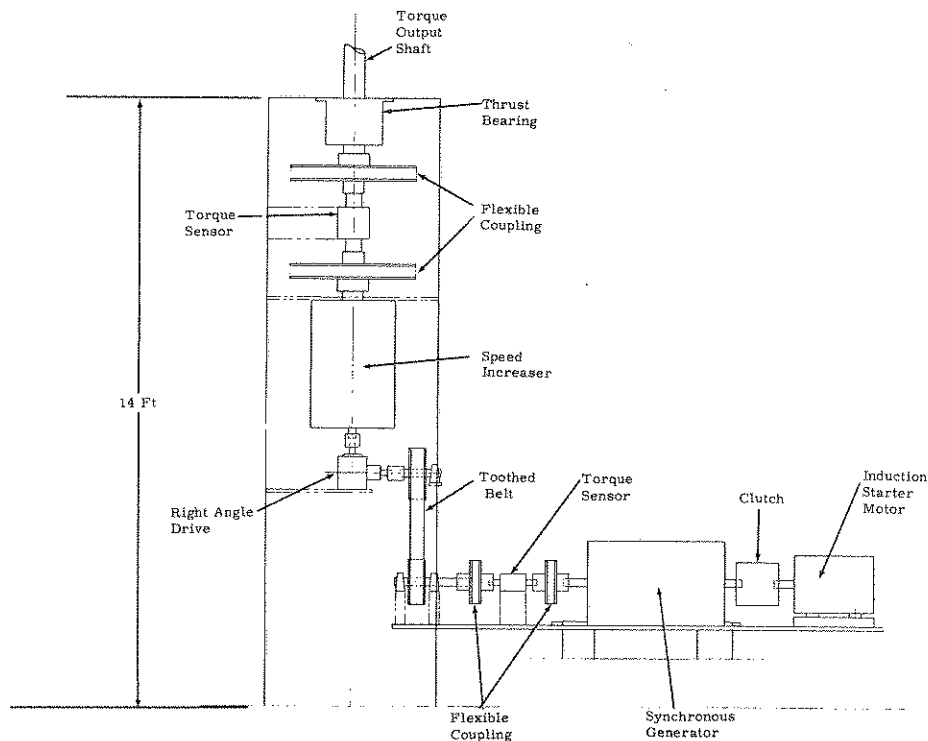


Figure 61. Turbine Base Design Schematic

The turbine output shaft will be equipped with a torque transducer protected from mechanical shock by flexible couplings. A second torque transducer is located on the high-speed side of the power train. This meter will be used to measure the transmission losses. Both torque meters are manufactured by Lebow Associates, Inc., and are the strain-gage type.

The design of the speed increaser and the brake system is now complete and will be discussed in detail.

Speed Increaser Design -- The speed increaser system for the turbine has been selected and the various hardware components have been ordered. Each of the components selected is available as a stock item, although slight modification of the primary increaser is required to accommodate the desired vertical shaft mounting orientation.

The essential drive components are: (1) triple planetary gear reducer (series 1, 200 - 1, 200 - 20, 000) manufactured by the Crichton Manufacturing Co.; (2) right-angle spiral bevel gear drive (series 800) manufactured by Safeguard Industries, Inc.; (3) final stage timing belt drive utilizing 1-1/4-inch pitch, 4-inch-wide belts. Standard and interchangeable components are available from several manufacturers.

The primary function of the gear train is to increase the shaft RPM from the turbine (approximately 40 to 45 RPM) to the synchronous shaft speed (1800 RPM) of the generator. The final drive stage will use timing belts. With the use of four different size drive sprockets, a wide range of discrete turbine rotational speeds can be accommodated. These ratio changes can be carried out relatively quickly, since only a single belt and two sprockets are involved. The primary speed increaser, located on the vertical shaft, consists of a planetary gear reducer. The speed increase is carried out in three stages, although two-stage transmissions were also considered. The maximum ratio per stage in a planetary gear box is about ^{*} 6:1, restricting a two-stage gear box to an overall ratio of 36:1. This ratio is not sufficient for the 17-m turbine without an increase in the final drive ratio. While the final drive ratio could be increased, it seems preferable to use a three-stage primary gear box instead, as the high ratio is more representative of larger turbine systems.

The lowest ratio available in a three-stage Crichton gear box is 42.87:1. For an output shaft RPM of 1800, the turbine RPM is approximately 42, which is in the range of operational RPM planned for the 17-m turbine. Thus, this gear box could be connected directly to the generator for demonstration of how a production system could be configured. The removal of the right-angle drive and the final drive would improve efficiency by an estimated 3 percent. More typically, however,

^{*} This restriction also applies to helical, nonplanetary gear boxes.

the timing belt drive will be used to vary the ratio for experimental purposes. Standard sprockets will be purchased with 34, 30, 26, and 24 teeth. By using appropriate combinations of these sprockets, the following discrete turbine operating RPM's are obtained: 29.6, 32.1, 33.6, 36.4, 37.0, 38.7, 42.0, 45.4, 47.5, 48.4, and 52.5.

The torque and horsepower ratings for the planetary speed increaser are shown in Figure 62, along with the requirements for both of these parameters. It should be noted that there has not been included a service factor to the torque and horsepower requirements. A reasonable number might be 1.2 or lower. With the inclusion of a service factor greater than 1.1, it can be noted that the torque requirements are not met. However, the drive is still considered adequate for the following reasons:

- a. The unit will seldom undergo these extreme conditions;
- b. There is some conservatism in both the torque requirements estimate and in the rating of the gear box;
- c. The uniformity and normal durations of the loads indicate the selection of a low service factor;
- d. If operated at these limits (including the appropriate service factor), the unit would theoretically have an infinite life.

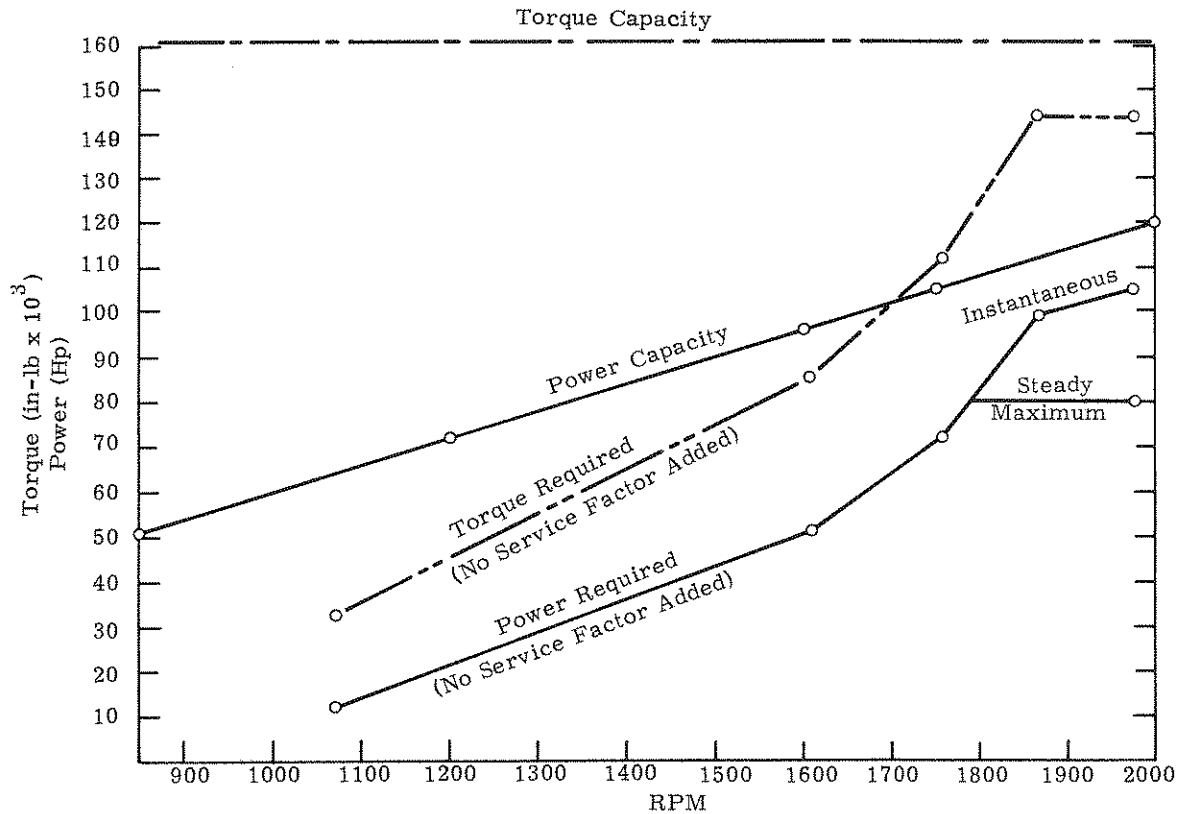


Figure 62. Transmission Loading

Other gear systems were also considered, including a parallel axis, helical-gear three-stage system, which is manufactured in the capacity ranges desired by several established companies. It is probable that a gear box of this type will have a slightly better efficiency than the planetary drive selected. Such units, however, weigh considerably more, cost two to three times more, and do not have the convenience of in-line shafting. Furthermore, the best delivery time promised was from 10 to 12 months. A unit as described above may be purchased for testing of its efficiency at a later time, and the cost of the expected slight performance increase will be accurately determined.

Two other systems should also be mentioned. Both are "toothless" gear drives employing rollers and eccentrics: the Sumitomo SM Cyclo Drive and the Compudrive Corporation systems. The latter of these is usually of smaller capacity than is required for a large wind system, although the factory stated that the system could be designed for any capacity, that performance would be better, and that weight and cost would be about the same as those of the planetary system. The SM drive is manufactured in the capacity range required but is limited to only 1165 RPM on the high-speed shaft. With a reduction of the generator RPM to this value, the SM drive should again be considered. It offered the lowest weight and cost for the intended application. Both of the above transmissions, because of their unique "gearing" arrangements, can obtain the ratios desired for large wind turbines in a single stage. Efficiencies of these units, when used as speed increasers, are not certain but are believed by factory representatives to be above 93 percent.

In summary, the planetary gear box with right-angle drive and toothed belts is best suited for immediate application in the 17-m turbine. Other gear-box types, with more development and manufacturing time available, may be applied to future turbine systems.

Emergency Brake Design -- The braking system will use hydraulically actuated disc brakes placed directly on the output shaft of the turbine above the base unit. This placement permits open-air cooling of the brake disc and allows the brakes to function without relying on intermediate shafts or transmissions.

Two identical brake discs are to be used. One disc is devoted to emergency use, and the other is to aid in synchronizing the turbine to the electrical network and for routine stopping of the turbine. The synchronizing brake will have a means for proportional application, while the emergency brake will be automatically applied at a preset RPM limit by connecting a pressure reservoir to the calipers. The two brakes are otherwise identical, for the sake of simplicity, although the sizing of the brake is governed by the emergency brake requirements.

For the sizing of the brakes, the torque and energy dissipation requirements must be determined. The maximum design RPM of the turbine is 75 RPM, so the brake should be able to stop the machine effectively from this RPM and overcome any wind-applied torques which may be present during this operation. The maximum torque output of the turbine is 40,000 ft-lbs at 75 RPM, with optimum wind conditions. Thus, a brake capacity of 50,000 ft-lbs has been selected. The energy input to the brake depends on the wind loading, which may be present during braking. An upper

bound may be calculated by assuming that the wind torque is at the turbine maximum throughout the deceleration cycle. These upper bound dissipation requirements are summarized in Table VI, along with torque requirements for RPM limits of 75, 70, 60, and 50 RPM.

TABLE VI
Brake Torque and Dissipation Requirements

<u>RPM Limit</u>	<u>Torque Required (ft-lbs)</u>	<u>Energy Dissipation (ft-lbs)</u>
75	50,000	2.0×10^6
70	43,000	1.7×10^6
60	31,000	1.3×10^6
50	22,000	$.9 \times 10^6$

A stock brake has been selected which will meet the requirements for 75-RPM operation. A set of four Kelsley-Hayes calipers (Model 2500H) will provide 53,000 ft-lbs of torque when used with a 30-inch disc and 2000-psi hydraulic pressure. This arrangement is capable of removing approximately 3×10^6 ft-lbs of energy in a single stop. These specifications are well in excess of the requirements for 75-RPM operations.

Electrical Analysis and Design

The objectives of this effort are to provide a cost-effective design and supporting analyses to establish component requirements and to procure the hardware necessary for the electrical subsystem.

As shown in Figure 63, the electrical subsystem consists of the following major components:

1. Electric motor - to start the turbine and bring it up to an operating speed close to synchronism with the three-phase AC utility line.
2. Synchronous generator - to convert the mechanical power extracted from the wind by the turbine to electrical power in synchronism with the AC line.
3. Electrical controls and interfacing - these components consist of the reactor starter for the motor, the synchronizer, voltage regulator, main generator contactor, and operator controls and monitors.

Achievements to date are:

Generator requirements established,
Synchronization analysis completed,
Starter analysis completed, and
Starter hardware requirements established.

A summary of each achievement is given in the following sections.

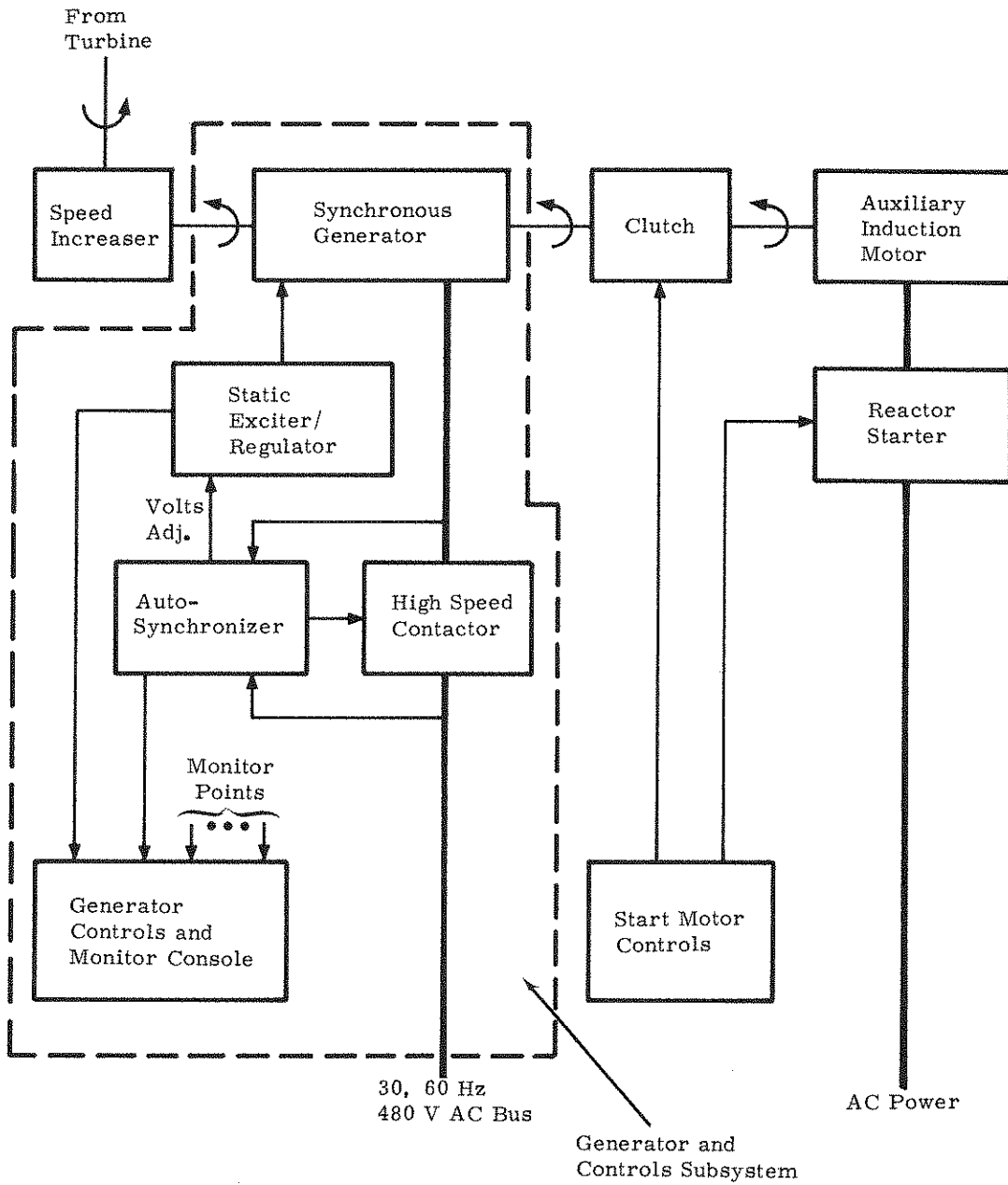


Figure 63. Electrical Block Diagram for VAWT System

Generator Requirements -- A ground rule for establishing the generator requirements is that industry-accepted standards and state of the art should be followed as closely as possible to minimize cost and assure the performance of the hardware, as well as to stimulate industry involvement and participation. The basic characteristics of the generator are:

- Type - Brushless synchronous
- Speed - 1800 RPM
- Electrical - 60-kW, 3-phase, 60-Hertz, 0.8 power factor, 277/480-volt output
Y connected
- Mechanical - Two-bearing, horizontal-mount, dripproof guarded enclosure
- Protective Services - Ground fault protection, overcurrent, overvoltage, loss of phase,
loss of synchronization

Six representative electrical machinery manufacturers were contacted and desired to respond to a request for quotation (RFQ) covering the synchronous generator and associated hardware as a completely wired and tested subsystem. Appendix B contains a copy of the generator RFQ.

Synchronization Analysis -- The process of matching the wind turbine's synchronous generator output with the electric utility in frequency, phase, and voltage is called synchronization. If proper synchronization is obtained, the turbine will be smoothly coupled to the utility power, when the generator's output is connected to the line. However, if there is a mismatch in frequency, phase, or voltage at the instant connection is made, potentially damaging electrical and mechanical transients can occur.

From the point of view of synchronization, the most severe conditions occur when the mechanical and aerodynamical losses are negligible and where the wind's speed history is such as to give maximum turbine torque at each particular instantaneous turbine RPM. For these conditions, the turbine will rapidly come up to operating speed and pass through synchronization in minimum time. Also, maintenance of the turbine's speed at the synchronous value will require maximum power to be absorbed in any brake or regenerative equipment.

The principal results of this analysis are:

1. Under worst-case wind conditions, a commercially available automatic synchronizer will probably be successful in synchronizing "on the fly" as the turbine is spinning up.
2. Near synchronous speed, the auxiliary induction machine will assist synchronization by providing oscillatory damping, but it will not prevent overspeed in the worst-case wind.
3. A 50-HP motor is sufficient and is recommended for both starting (in series with a reactor starter) and regenerative braking under maximum rated load, but not in worst-case winds.

4. In worst-case winds, at least a 75-HP induction machine is necessary for regenerative braking.
5. To assure sufficient time for synchronization, in the worst case, a speed control system using a mechanical braking torque of 40,000 ft-lb maximum at the turbine shaft is required.

Based on this analysis, the following recommendations are made:

1. Procure a commercially available automatic synchronizer for the generator. Typical specifications are contactor closure of 0.1 second or better, within ± 0.5 Hz and ± 15 electrical degrees of perfect synchronism.
2. Procure a 50-HP motor for the first experimental version of the 17-m VAWT system. Smaller motors can then be used after gaining operating experience and eliminating some uncertainty in the system's design and performance.
3. Design a feedback controller for the mechanical brake to control the turbine's speed until synchronization has been completed. The controller should use tachometer input and should limit applied braking torques to safe values while smoothly controlling turbine speed. Maximum braking torque for control should be 40,000 ft-lb. The speed controller should hold the generator's angular acceleration to within ± 21 rad/sec² while dithering the speed about 1800 RPM to assure ample opportunity for synchronization without having to precisely control the speed.
4. If synchronization is not achieved within a reasonable time (to be determined by the heating of the brakes) the VAWT system should be braked completely and shut down.
5. The 50-HP motor should be equipped with thermal cutout to prevent overheating damage if sustained operation is experienced under regenerative braking conditions.

Starter Analysis -- The purpose of this analysis is to establish the requirements for the induction motor start system that will bring the 17-m VAWT up to operating speed. The goal of this effort is to eventually integrate the separate start motor into the induction damper windings of the synchronous generator to minimize the total system cost and complexity. In the near term, the starter system is being designed to provide sufficient power and flexibility to permit a wide variety of experimental tests to be performed on the VAWT system as well as operational simulation of various types of starter, synchronizer, and braking systems. The following are the salient results of this analysis:

1. To spin up the 17-m VAWT from 0 to 41 RPM in 30 seconds, a 40-HP, 3-phase induction motor should be used as an auxiliary starter. This size starter motor assures sufficient starting torque to investigate the VAWT's dynamics without wind. The 30 seconds is arbitrarily selected as a compromise that is relatively short mechanically and relatively long electrically. Longer time would involve

derating or auxiliary cooling of the motor and, if any mechanical resonances were encountered, a longer time to excite undesirable vibrational modes. Shorter time would result in proportionately higher motor rating and starting torque which may exceed the design limit of the VAWT or its drive train components.

2. A reactor starter should be placed in series with the start induction motor to provide a limit on the starting torque and a smooth acceleration of the VAWT up to operating speed.
3. To simulate various starting, synchronizing, and braking systems, a 40-kVA steady-state variable-speed drive for the start motor should be used. With 100 percent regeneration and controlled acceleration, this state-of-the-art speed drive will provide a flexible tool for investigating the performance of the 17-m VAWT with alternative subsystems.

Starter Hardware -- Although the starting analysis indicated a 40-HP induction motor would be sufficient for VAWT startup, a 50-HP motor will meet both the needs of startup and synchronization. The higher horsepower motor will provide the extra pullout torque required for stable synchronization even under worst-case wind conditions. It is felt that this starter size is conservatively large, and reduction in size is anticipated for future turbines pending the accumulation of more operating and design experience.

Based on the above motor requirement, a 50-HP, 3-phase, 1800-RPM, 277/480-volt, drip-proof, fan-cooled motor is being ordered. Also, a completely wired and tested reactor pack for limiting inrush current and smoothing the initial torque surge has been ordered as an interface between the induction motor and the AC line.

The 5-m Turbine

ction

The Sandia-designed and -constructed 5-m turbine* is now operational at the wind turbine test facility (Figure 64). This turbine was first assembled in the spring of 1974 and has been operated intermittently since that time.

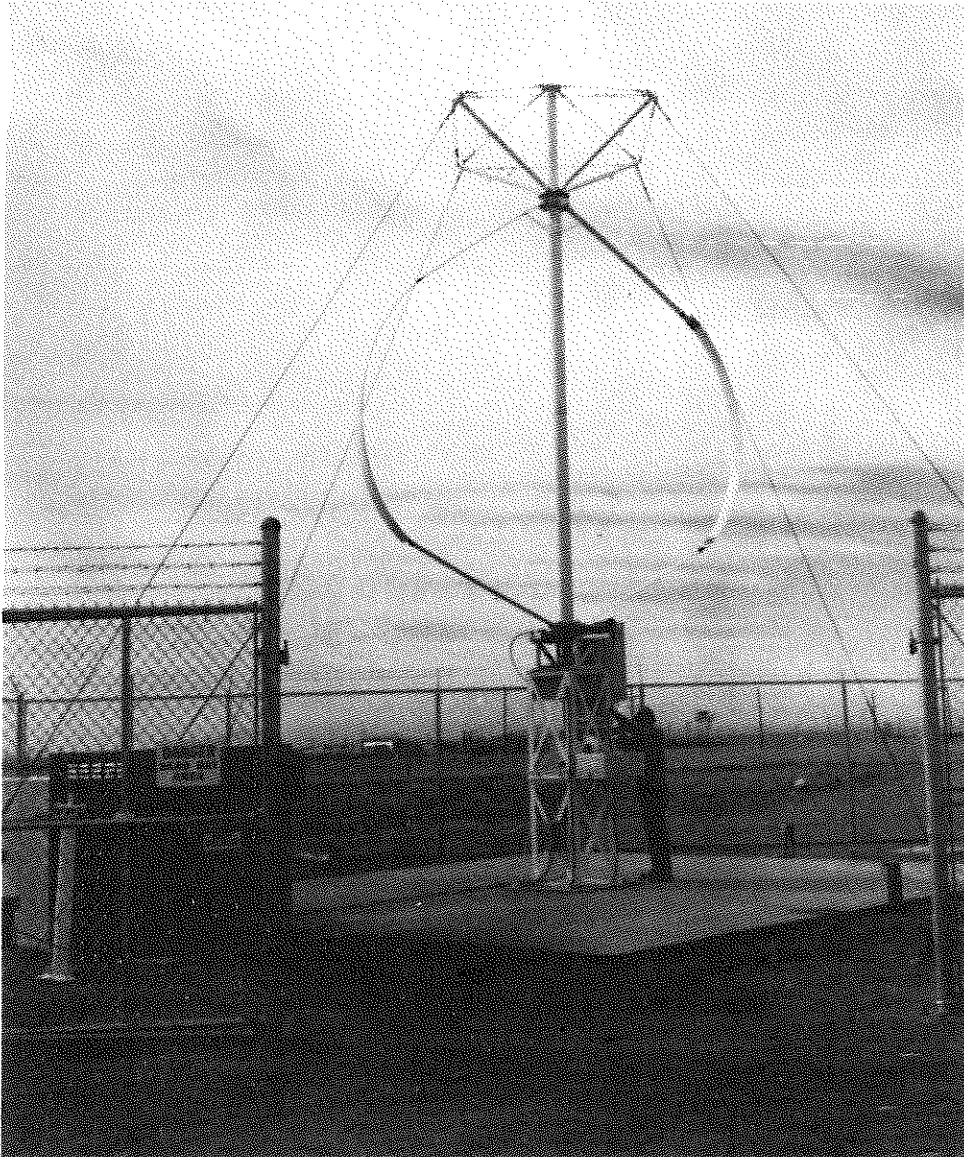


Figure 64. The Sandia 5-m Turbine

* This turbine was originally designed as a 15-foot diameter unit. In the interest of using consistent units in this report, it will be referred to as the 5-m turbine.

The machine was moved in the fall of 1975 from a rooftop location in the Sandia technical area to the test facility. During this move, the turbine structure was inspected and the bearings maintained. The inspection revealed small surface cracks in one of the blades. The major blade loads are carried by a steel strap within the blades, which X-ray inspection revealed to be sound. However, the cracks prevent sealing the blade from water penetration, so the cracked blade is no longer being used.

The 5-m turbine has accumulated approximately 16 hours of running time since being moved to the test facility. The unit serves as a flexible test bed for checking out instrumentation and as a model for structural analysis. The following sections will summarize the major features of the structural analysis and the synchronous (constant RPM) and asynchronous (variable RPM) test programs which have developed for the 5-m turbine.

Blade Structural Analysis

The finite element model of the blade described in Part I was utilized to analyze the blade of the 5-m wind turbine. Figures 65 and 66, picture the blade deformation and stresses due to centrifugal forces at 40 rad/sec (382 RPM). This is approximately the highest speed at which the device was operated. In Figure 66, the meridional coordinate, s , is nondimensionalized with respect to the half-blade length, S . Of particular importance is the fact that the stresses in the blade are not purely tensile as seen in a troposkien-type blade shape. The effect of the straight-circular arc design is to incorporate bending in the blades. The largest stress in the blade for 40 rad/sec is 40,000 psi, which is greater than the yield stress (30 to 35,000 psi) of the low-carbon steel used. This should produce a small amount of yielding in the straight section of the blade. Consequent examination of the blade indicated a small permanent deflection in the straight section with a maximum at $s/S \approx 0.35$. Figure 67 shows the outer fiber meridional stress versus angular velocity at $s/S = 0.37$. This is the location of the maximum stress at high angular velocities. This figure shows that the turbine speed should be less than about 300 RPM in order to avoid exceeding the yield stress of the steel.

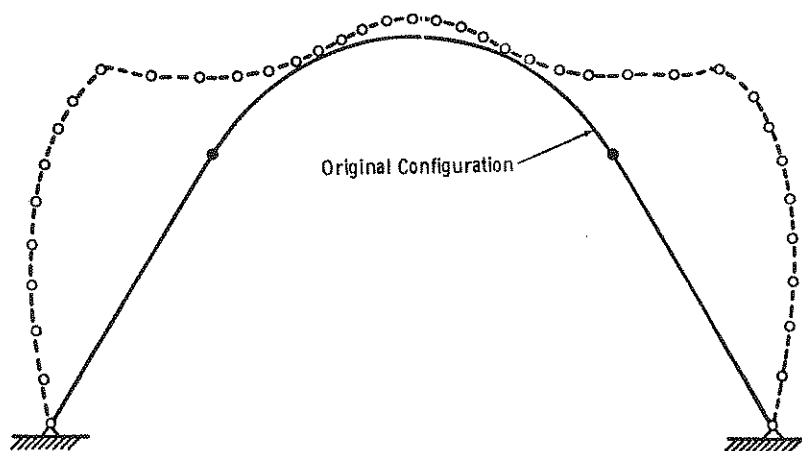


Figure 65. Deflected Shape (10X) of Blade at a Rotational Speed of 40 rad/sec for the 5-m Darrieus Turbine

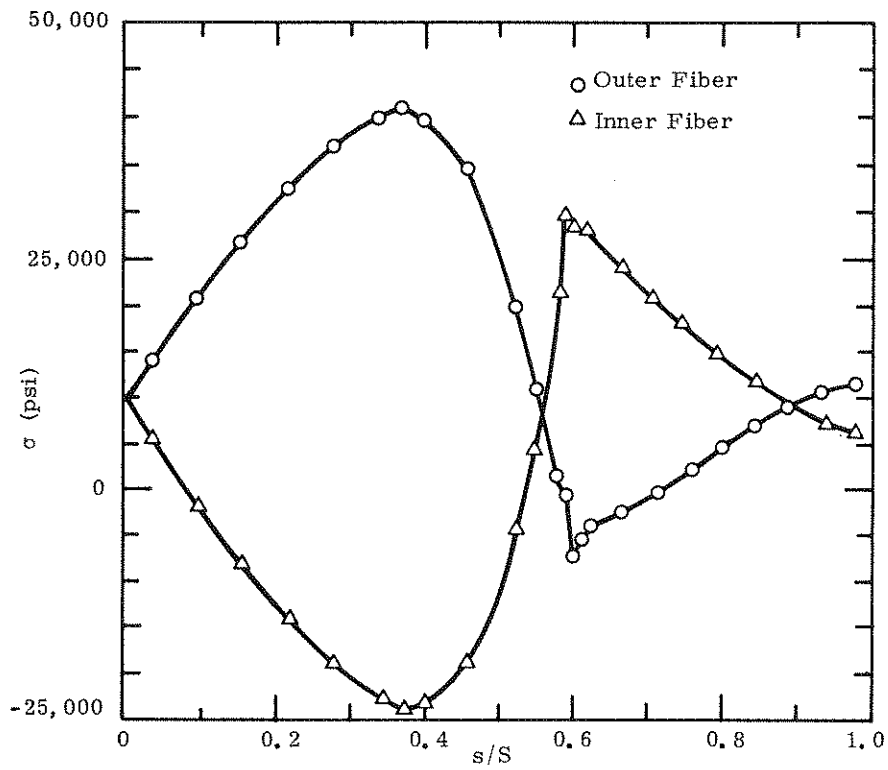


Figure 66. Meridional Stress, σ , versus Meridional Coordinate, s/S

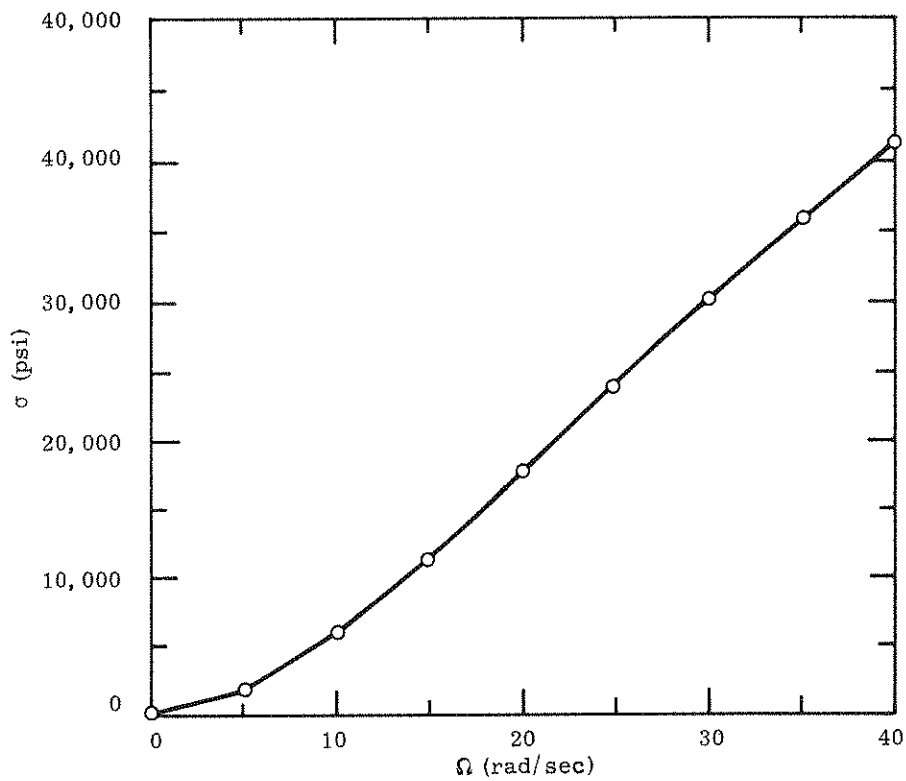


Figure 67. Outer Fiber Meridional Stress, σ , versus Angular Velocity, Ω , at $s/S = 0.37$. (This is maximum stress at high angular velocities.)

The resonant frequencies for the first two flap modes have been calculated for the 5-m turbine. These frequencies are shown in Figure 68 as a function of turbine RPM.

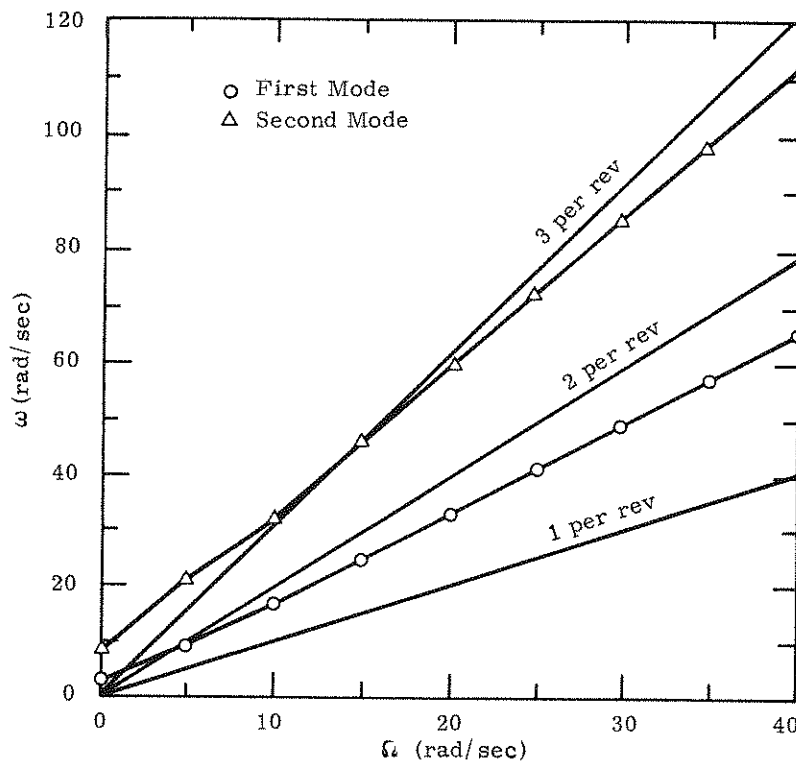


Figure 68. Natural Frequency Spectrum (first two modes), ω , versus Angular Velocity, Ω

It is noteworthy that the 5-m turbine is a "soft" system, in that the first flap mode has characteristic frequencies between the one- and two-per-revolution lines. Operation of the turbine (generally in the range of 10 to 40 rad/sec) has revealed no obvious blade resonances. This is probably due to the fact that the crossings of the two- and three-per-revolution lines with the first mode are at low RPM, where there is very little rotational energy in the turbine to amplify blade resonances. There have been, however, substantial resonances observed in smaller wind tunnel models which have a similar flap resonant frequency characteristic. These difficulties with "soft" blade systems have led to a conservative approach on the 17-m turbine where the lowest flap resonant frequency is put above the three-per-revolution line. This is consistent with the expectation to operate the turbine over a wide range of rotational speeds without structural anomalies.

Synchronous Test Program

The 5-m turbine is currently configured to operate in a nearly synchronous mode by connecting its output shaft to an induction motor/generator. With the induction machine connected to an AC line, the result is essentially constant RPM operation of the turbine, although the "slip" of the

machine does permit fluctuations of the order of 1 RPM about the turbine's nominal speed (175 RPM). Starting of the turbine is accomplished by using the induction machine as a motor.

The major goal of the 5-m turbine synchronous test program is to provide an experimental base in preparation for testing the 17-m system. In particular, it is desired to use the smaller, more manageable unit to verify the ability of the Darrieus to self-regulate in high winds, and to select appropriate instrumentation. For example, there is considerable interest in using automated or semiautomated schemes for measuring the turbine power coefficient based on field data. Various means for accomplishing such a measurement will be examined with the 5-m turbine.

A very limited amount of testing has been completed to date, due primarily to lack of wind. There have, however, been several windy days recently and data have been collected which are now being analyzed. The following sections will briefly examine certain aspects of these data directly related to the goals of the test program. The reader should be cautioned that these data are preliminary and have not as yet been fully verified.

Self-Regulating Output of the Darrieus Turbine -- The 5-m turbine, based on power coefficient data from the National Research Council of Canada,⁶ is predicted to produce a maximum output of 3 kW at a constant rotational speed of 175 RPM. Figure 69 shows a typical output trace from the turbine where wind speeds exceeding 35 mph are recorded. It is clear that the output does not exceed the 3-kW line,* even for these severe wind conditions. These initial data appear to confirm the ability of the 5-m turbine to be self-regulating, as was the case for the 2-m turbine used in the wind tunnel test series.

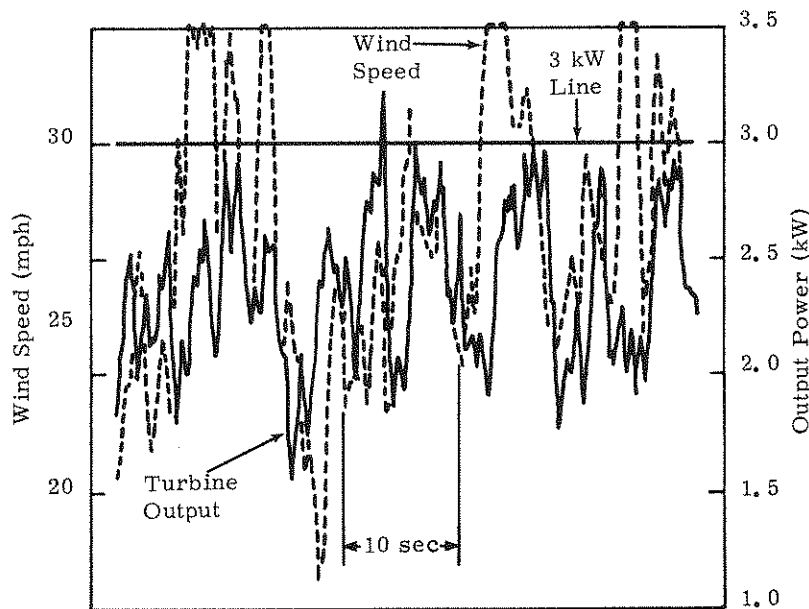


Figure 69. Output Trace Showing Self-Regulation of the 5-m Turbine

* There are certain peak outputs which do exceed the 3-kW line momentarily. This effect is believed due to RPM changes to be discussed subsequently.

Instrumentation Requirements -- Testing has shown that anemometer location is apparently quite critical if it is desired to correlate wind speed with turbine output. This is demonstrated by Figure 70, showing the output of two anemometers located at 10 m and 100 m horizontally from the turbine axis. While both instrument outputs are statistically similar, they do diverge considerably at any particular time. It has been observed that a portable anemometer located horizontally about one turbine diameter upstream and vertically at the turbine midpoint yields a reasonable correlation between anemometer output and turbine response. Conversely, the 100-m anemometer is only vaguely correlated to turbine output. The search for optimal anemometer locations will continue into the next quarter. The major conclusion at this time is that anemometer location is an important factor to consider in any data collection program.

The other major instrumentation used in this early test series, such as torque meters, RPM counters, and monitoring equipment, has performed adequately and should be usable on the 17-m turbine.

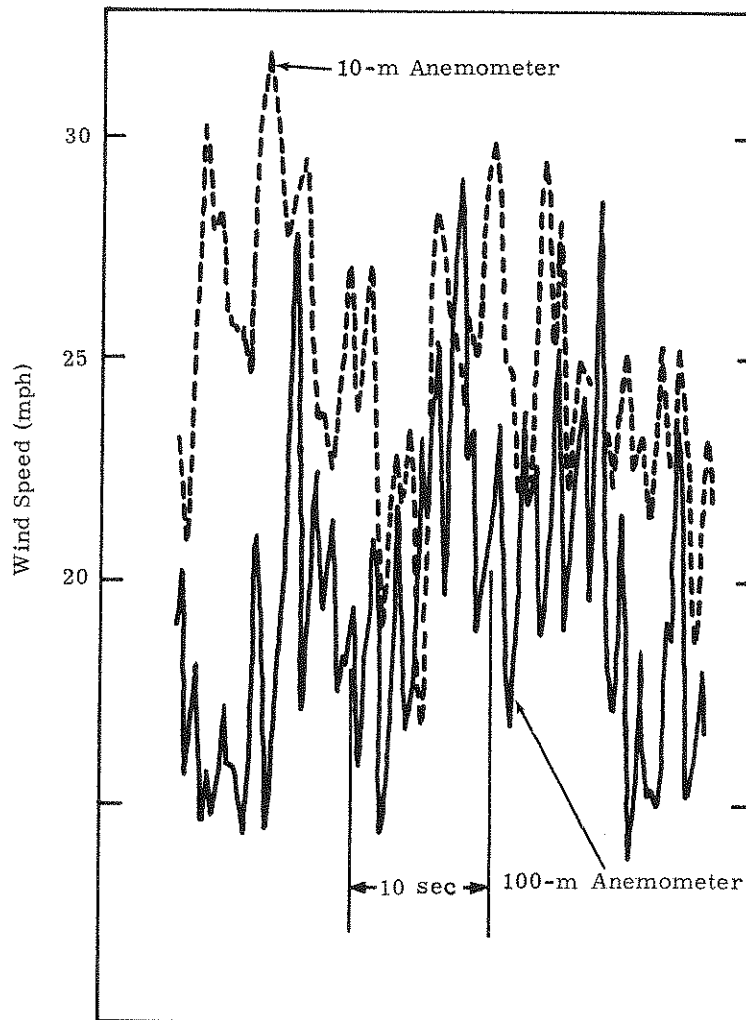


Figure 70. Time Traces of 10-m and 100-m Anemometer

Field Measurement of the Turbine Power Coefficient -- In the synchronous, constant RPM mode of operation, the fundamental turbine performance curve is the wind-applied torque versus wind speed. From this curve, other performance measures, such as the power coefficient, can be derived. In principle, if a time-varying wind speed through the turbine is measured along with the torque on the output shaft, the torque versus wind speed curve can be constructed. In practice, the small RPM fluctuations in an induction motor drive cause the output shaft torque to differ from the wind-applied torque due to the inertia of the rotor. The errors induced by these RPM fluctuations have been examined with a transient model of the induction motor/turbine system. In this model, the wind speed profile of Figure 70 is input, and the shaft output torque for a specified power coefficient turbine is calculated. The calculated output torque and wind speed are sampled at discrete times and plotted as points in Figure 71. Note that the RPM fluctuations lead to scatter of these points about the wind-applied torque versus wind speed characteristic. It is clear, however, that the average is apparently representative of the wind-applied torque and, if enough points are collected, it should be possible to define the performance curve.

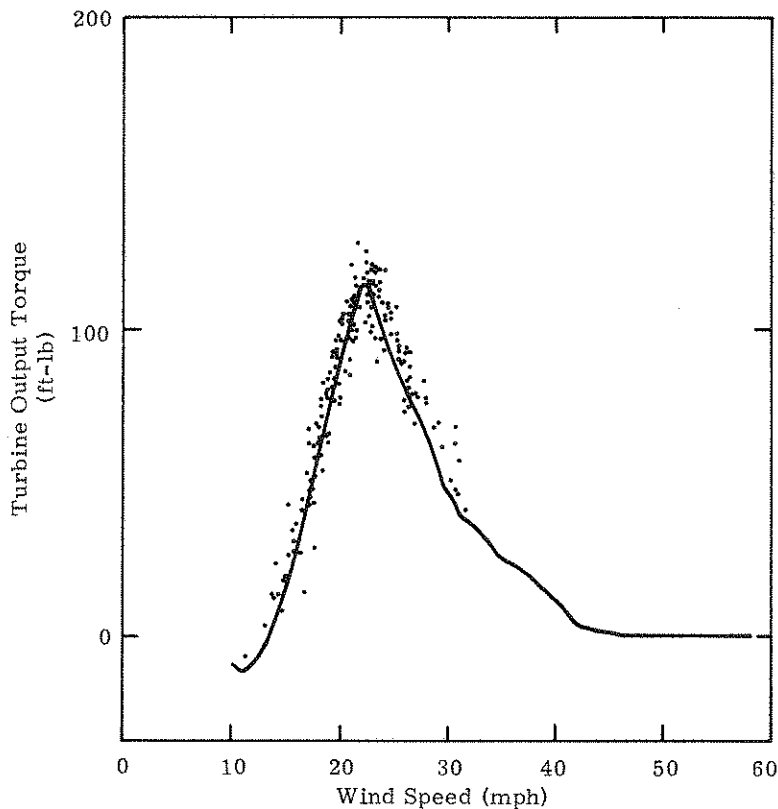


Figure 71. Transient Effects on Measured Torque

There are, of course, many other sources of scatter besides RPM fluctuations, including transient instrument error, anemometer location problems, or fluctuations in velocity across the turbine disc. It is believed at this time that appropriate sampling methods can reduce these errors. Experiments in sampling methods are now being conducted with the 5-m turbine and will be reported in the next quarter.

Asynchronous Test Program

The main thrust of the Sandia VAWT Program is the synchronous power grid application. Constant rotational speed is achieved by connecting the VAWT through a synchronous generator to an established AC electrical network. A number of potential remote site applications for the VAWT, however, can be identified in which no source of AC electrical power is available. These applications include small-scale electrical power systems and water pumping systems. System operation would be in an asynchronous mode, that is, variable rotational speed. Therefore, a portion of the Specific Applications Efforts will utilize the 5-m turbine as a test bed for a selection of variable-speed electrical systems. Additionally, analytic models will be developed to perform parameter studies leading to systems definitions for possible demonstration projects. This section briefly summarizes efforts to date in these areas.

Three variable-speed electrical power generation systems are shown schematically in Figures 72 through 74. The first system uses a 210-ampere, 14-volt DC Leece Neville alternator feeding power to a variable-resistance load bank; such a load will allow investigation of control strategies which achieve maximum performance from the turbine in a changing wind environment. The second system uses an induction generator in conjunction with a resonant exciter which provides a controllable source of excitation to the generator; a cycloconverter is then used to provide AC electrical power at a constant frequency. The third system uses an AC generator feeding a rectifier and a Gemini synchronous inverter to achieve constant output frequency. A portion of this hardware has been procured and is presently being installed in the wind energy test facility. Other techniques using, for example, the AC commutator generator and the field modulated generator will also be investigated for possible testing with the 5-m turbine.

The vertical-axis wind turbine coupled to a speed-dependent load has a potential problem of stalling during transient wind conditions. A sudden increase in wind speed of sufficient magnitude can lead to a reduction in torque and a slowing down of the turbine. This stalling effect is difficult to generalize, as it depends on many factors, including the gustiness of the wind, the system inertia, and the specific nature of the load. To examine the stalling problem, computer models of the real-time response of the turbine to time-varying winds are being developed. The code is in modular form so that a variety of load control strategies can be studied. Work to date has indicated that, in order to achieve maximum energy extraction, the load must occasionally drive the turbine to maintain favorable operating conditions. This suggests that consideration be given to energy storage mechanisms. Further effort is needed to model various generator systems and to establish requirements for energy storage.

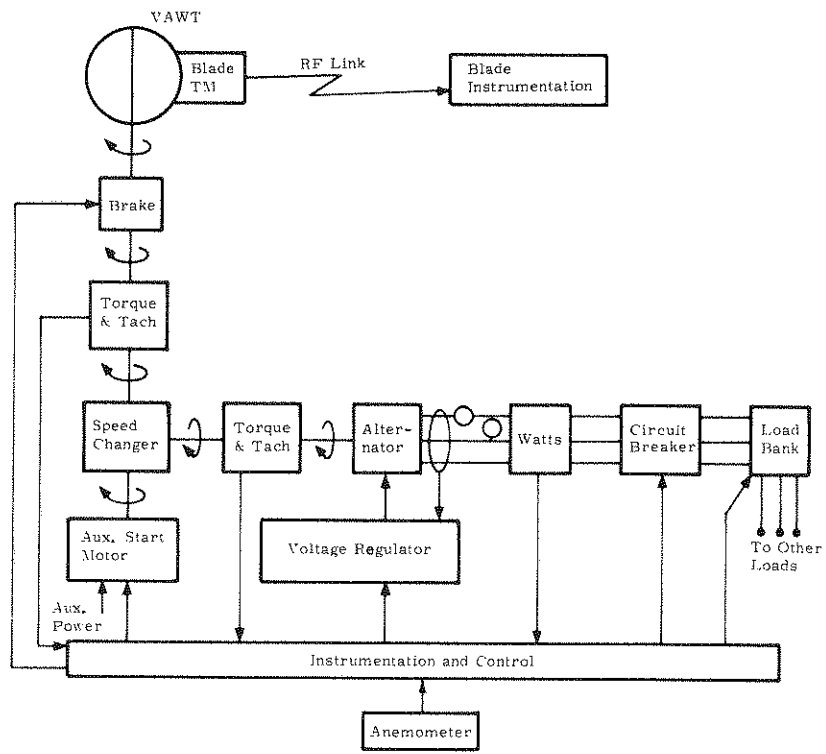


Figure 72. Asynchronous Wind Power System I

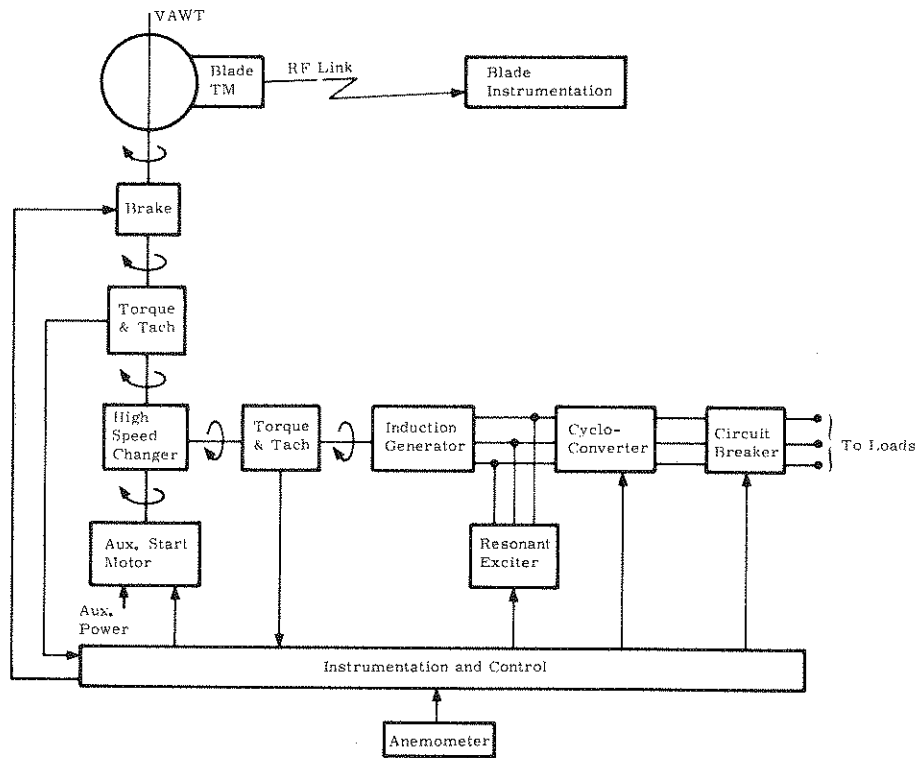


Figure 73. Asynchronous Windpower System II

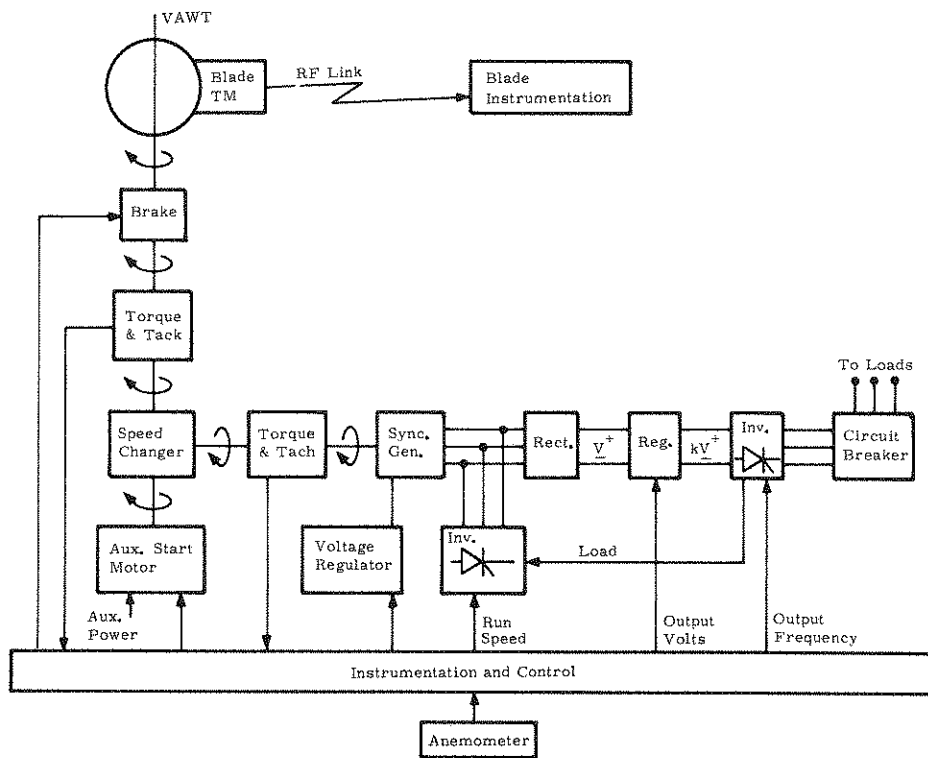


Figure 74. Asynchronous Windpower System III

References

1. B. F. Blackwell, The Vertical-Axis Wind Turbine - How it Works, SLA-74-0160, April 1974.
2. B. F. Blackwell and L. V. Feltz, Wind Energy - A Revitalized Pursuit, SAND75-0166, March 1975.
3. J. F. Banas, E. G. Kadlec, and W. N. Sullivan, Application of the Darrieus Vertical-Axis Wind Turbine to Synchronous Electrical Power Generation, SAND75-0204, April 1975.
4. J. F. Banas, E. G. Kadlec, and W. N. Sullivan, Methods for Performance Evaluation of Synchronous Power Systems Utilizing the Darrieus Vertical-Axis Wind Turbine, SAND75-0165, April 1975.
5. J. H. Strickland (Texas Tech University, Lubbock, Texas), The Darrieus Turbine - A Performance Prediction Model Using Multiple Streamtubes, SAND75-0431, October 1975.
6. R. J. Templin, National Research Council of Canada, Aerodynamic Performance Theory for the NRC Vertical-Axis Wind Turbine, Report LTR-LA-160, June 1974.
7. Program for Conceptual Design, Parametric Analysis and Preliminary Designs for Low Power (50-250 kW) and High Power (500-3000 kW) Wind Generator Systems - General Electric Company, NASA Contract NASA - 19403, April 1975.
8. B. F. Blackwell and G. E. Reis, Blade Shape for a Troposkien Type of Vertical-Axis Wind Turbine, SLA-74-0154, April 1974.

APPENDIX A

17-m Turbine Blade Request-For-Quotation (RFQ)

I. SCOPE OF WORK

A. Objective

The primary objective of this project is to have a set of three or more airfoil blades for a vertical-axis wind turbine designed, fabricated, and delivered to a location in Albuquerque, New Mexico, to be specified by Sandia Laboratories. An artist's drawing of the turbine is provided in Figure A-1.

B. Description of Project

The project consists of three tasks. Major tasks designated Phase 1 and Phase 2 call for the structural design and fabrication of a set of three or more blades for a vertical-axis wind turbine. This turbine will be part of an intermediate-sized ($\sim 30 \text{ kW}_e$, 17-m diameter), synchronous, wind power system that will serve as a research facility for experimentally verifying aerodynamic, structural, and system design concepts. Design of the wind power system will permit synchronous operation at three turbine rotational speeds for a broad experimental capability. The turbine will rotate counterclockwise when viewed from the top. Design and fabrication of the blades should take into account, wherever possible, advanced or future concepts such as special requirements of larger blades, mass production and unattended, automated turbine operation.

Phase 3 consists of delivery of the blades to a specified location. Execution of Phases 2 and 3 of the project will be contingent upon successfully completing Phase 1 in conformity with the design guidelines discussed in Section C below. The project scope covers only blade design development and optimization based on structural performance as specified by the guidelines furnished; it does not cover other system studies. Design changes due to aerodynamic performance optimization are not encouraged except where structural response is involved as in the case of aerodynamic loading and blade flutter.

C. Phase 1 - Structural Design

The following is an itemized discussion of guidelines to be followed for successful completion of the structural design phase of the project. Specific numerical values related to turbine blade size, shape, and performance may be changed moderately by the contractor when suggested by design iteration and optimization. These changes are subject to approval by Sandia Laboratories.

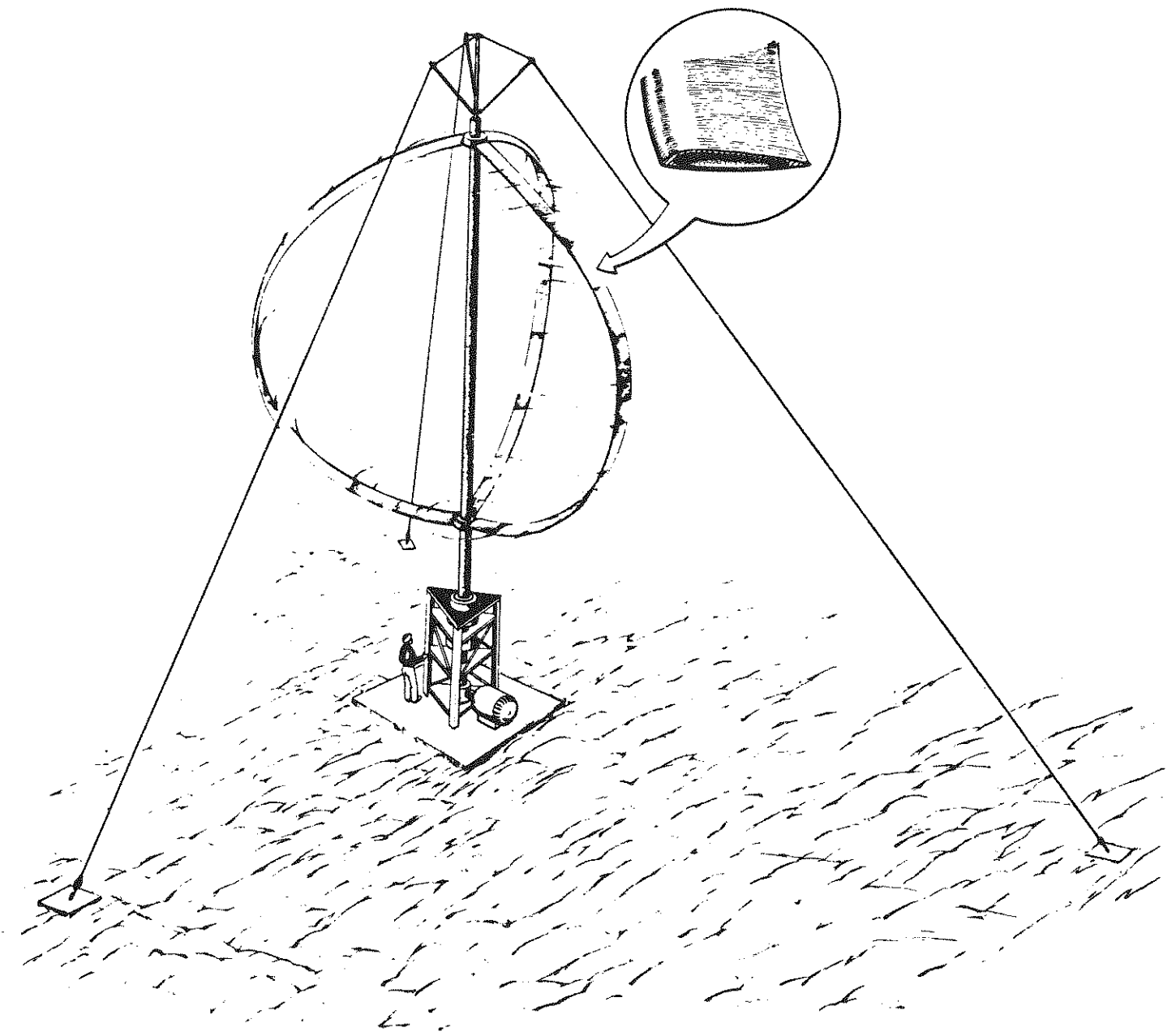


Figure A-1

Blade Size and Shape -- The wind turbine for which blade design, fabrication, and delivery are required is identified, by its size, as the Seventeen Meter Turbine. This dimension is approximately equal to the maximum diameter of the area swept by the turbine. The shape of the blade is its profile as viewed normal to a plane containing the turbine's axis of rotation and the locus of points described by the quarter chords of the blade's cross sections. The theoretical optimum blade shape is called a troposkien.* This is the shape assumed by a rope, in the absence of gravity, which is supported at its ends and is spinning about an axis containing these end points. While the troposkien is most desirable from a structural standpoint, other factors, such as cost, may suggest that an approximation to this shape be made. An acceptable approximation to the troposkien shape is defined by two straight segments connected to one circular arc segment. Relative sizes and locations of these three blade segments are specified in Figure 2.

Blade Cross Section -- The entire length of all blade segments will have a cross section specified by NACA-0012 and a chord length of 0.5 meter. With the center of pressure located at the quarter-chord point, the center of gravity of the cross section will be within 3 percent of the chord length forward of the quarter-chord point and the center of twist of the cross section will be within 3 percent of the chord length aft of the quarter-chord point. This requirement is made to reduce coupling between bending and torsional motions of the blade.

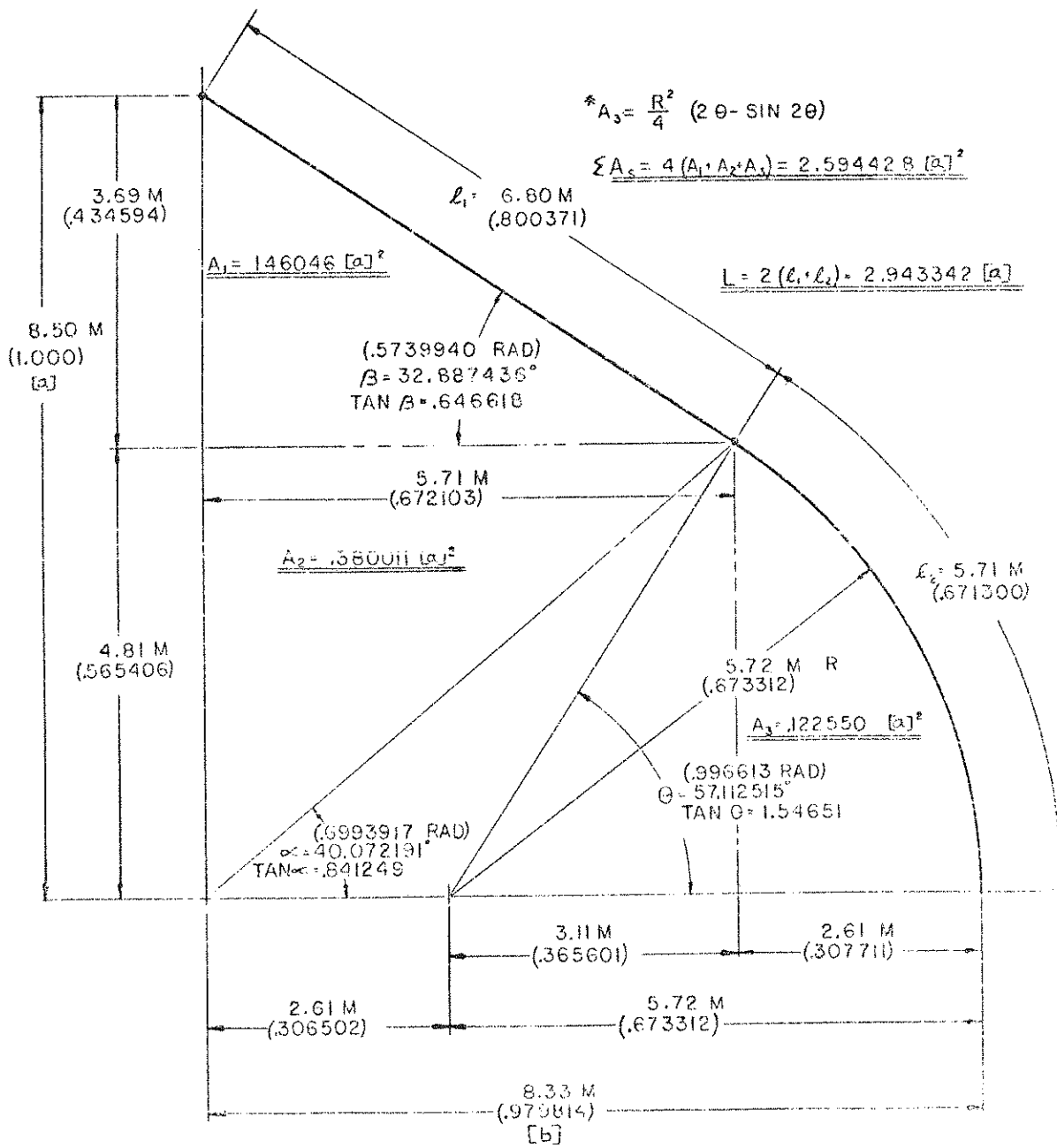
Additional Requirements --

1. Design of the blades must include consideration of the natural frequencies of lead-lag, flap, and torsion (linear motion in a plane tangent to the blade and rotational motion about the blade axis). The maximum rotational speed of the turbine is 75 RPM (1.25 Hz). All blade natural frequencies must be above 4.5 Hz when the turbine is rotating at 75 RPM in order to avoid two- and three-per-revolution excitation. Aerodynamic blade flutter must not occur at rotational speeds below 90 RPM. These rotational speeds are considerably higher than those planned for synchronous operation of the turbine. The overspecification is made to accommodate a runaway condition and to extend operation of the turbine to possible asynchronous applications. Because of the tentative nature of the asynchronous applications and present uncertainties associated with turbine braking, it is important to understand the dependence of program cost and program schedule on blade resonant

*Blackwell, B. F. and Reis, G. E., Blade Shape for a Troposkien Type of Vertical-Axis Wind Turbine, Sandia Laboratories, Albuquerque, NM, SLA-74-0154, March 1975.

Reis, G. E., and Blackwell, B. F., Practical Approximations to a Troposkien by Straight-Line and Circular-Arc Segments, Sandia Laboratories, Albuquerque, NM, SAND74-0100, March 1975.

Blackwell, B. F. and Reis, G. E., Some Geometrical Aspects of Troposkiens as Applied Vertical-Axis Wind Turbines, Sandia Laboratories, Albuquerque, NM, SAND74-0177, May 1975.



STRAIGHT-LINE/CIRCULAR ARC FIT
 TO A TROPOSKIEN $\rightarrow [B/A]_{TRP} = 0.9458568$

- a. Half of the turbine height
- b. Half of the turbine diameter

NOTE: Numbers in parentheses represent dimensions based on a unit value for a.

Figure A-2. 17-m Turbine Geometry Information Drawing

frequency requirements imposed by the specified rotational speed. If the resonant frequency requirements are difficult to achieve and excessively time consuming and costly, sufficient justification may exist for relaxing these requirements.

2. Blades must be designed to withstand aerodynamic, centrifugal, and gravitational loads under operating conditions up to a maximum rotational speed of 75 RPM in a free-stream wind velocity of 60 mph, with gusts up to 80 mph without permanent deformation. Blades must also withstand gravitational loads and aerodynamic loads due to an ambient wind velocity of 120 mph, with gusts up to 150 mph under a nonoperating status (see Item 10 below). These ambient wind and gust velocity values were selected to maximize the number of future turbine site possibilities with a minimum of future design changes. If these values are unreasonable from a cost and time standpoint, it will be necessary to demonstrate the dependence of program cost and duration on design wind velocities in order to establish more cost- and time-effective guidelines. Additional blade support may be included in order to (1) achieve sufficient blade stiffness for minimization of sag due to gravity and (2) fulfill the aforementioned natural frequency requirement. This additional support or restraint, if necessary, must consist of straight, NACA-0012 struts with chords of approximately 20 inches or less. These struts must be located so that the turbine remains symmetric with respect to a horizontal plane through its midpoint. Natural frequencies of the struts must be above 4.5 Hz, as with the blades.
3. Blades must be designed to withstand repeated angular accelerations and decelerations of the order of 0.26 rad/sec/sec (a preliminary figure) during free run and braking.
4. Total blade design must be conducted in such a way as to interface with the turbine support tower design to be conducted at Sandia. Of particular importance is attachment joint design and static and dynamic elastic coupling between tower and blades. The tower will be designed to meet the same natural frequency requirement as the blades. Whenever possible, blade design will dominate tower design.
5. Contractor must make provisions for static balancing of the blades prior to delivery, as specified under Phase 2 - Fabrication, and for dynamic balancing of the blades by Sandia after installation.
6. Preliminary and final physical and mechanical blade properties are to be determined and made available to Sandia as they evolve. These properties must include:
 - a. Linear densities of blade section.
 - b. Locations of the centers of gravity and twist of blade sections.

- c. Dimensions of blade components.
 - d. Axial, bending, and torsional stiffnesses with respect to principal blade axes.
 - e. Axial and torsional stiffnesses of the blades with respect to the tower axis.
 - f. Principal moments of inertia of blade sections.
 - g. Mass moments of inertia of the blades about the turbine axis.
7. Contractor must determine the location and type of strain gages necessary to monitor blade stresses in critical load-carrying blade components. Strain gages must be compatible with either telemetry or slip-ring signal transmission. The contractor must supply the gages, mount them, and check their continuity.
8. If the design is based on multiple-segment blades, all blade joints must be shrouded or otherwise streamlined to minimize drag and noise during operation, and to minimize any disruption of a continuous airfoil surface. Joints, if present, must be field detectable.
9. Airfoil surfaces will be smooth with a surface roughness not to exceed 63. Steps of up to 0.025 cm are allowed at surface joints. Surfaces must be able to withstand year-round exposure to the environmental conditions described below. Blades must be made as watertight as possible and must contain provisions for drainage of water in the event of rain leakage. Life expectancy of the blades must exceed 20 years when operated an average of 50 percent of the time.
10. Blades must survive environmental conditions specified in MIL-STD-210B, 15 December 1973, under Detailed Requirements-Ground Environment (Paragraph 5.1), with the following exceptions:
- a. Design criteria for high temperature:
 - Operations 110°F (43°C)
 - Withstanding 120°F (40°C)
 - b. Design criteria for low temperature:
 - Operations -20°F (-29°C)
 - Withstanding -30°F (-34°C)
 - c. Design criteria for high relative humidity with low temperature:
 - Operations 100% at -20°F (-29°C)
 - Withstanding 100% at -30°F (-34°C)
 - d. Wind speed:
 - Operations 60 mph with gusts up to 80 mph
 - Withstanding 120 mph with gusts up to 150 mph

e. Hail size:

Operations 0.5 in. dia.

Withstanding 1.0 in. dia.

Additional exceptions may be imposed by Sandia if necessary.

In addition to these requirements, the blades must withstand a maximum solar radiation heat flux at 120°F of 350 Btu/hr-ft² and salinity criteria defined by ERDA/DOD, Environmental Data Bank Nos. 273 and 274, and Area I of ERDA/DOD Environmental Data Bank No. 1008.

11. Wind turbines larger than the Seventeen Meter Turbine may be constructed in the future. It is therefore desirable to use design concepts which would be appropriate for larger turbine blades whenever possible.
12. At the conclusion of Phase 1, the contractor must furnish Sandia with a complete set of engineering drawings of the blades. Units and drawing specifications may be determined by the contractor; however, drawing specifications must be complete and of standard form. At this time the contractor must also furnish Sandia with documentation of design rationale and a synopsis of analytical methods used. Discussion should be complete but to the point so that documentation length is kept to a minimum.

D. Phase 2 - Fabrication

Three or more identical blades are to be fabricated upon approval of the final blade design by Sandia Laboratories. Fabrication methods should be determined primarily by those which minimize costs, and, whenever possible, those which mimic mass production of turbine blades and those appropriate for fabrication of larger blades. Prior to delivery, blades must be statically balanced so that the weight of each blade is within 0.3 percent of the weights of the other blades. Magnitudes of geometric tolerances related to blade shape, blade twist, and the location of the complete blade center of gravity must be determined by the contractor. Effects of these tolerances on blade structural performance and blade cost must be included in this determination. Sandia reserves the right to have representatives present when the tolerance requirements are actually fulfilled.

E. Phase 3 - Delivery

Delivery of the blades will be made by a specified date to a specified location in Albuquerque, New Mexico. Shipping containers or supports will be retained by Sandia and must be designed to permit blade storage at the delivery site. Modes of transportation for the blades may be selected by the contractor.

F. Reports and Schedules

The following reports are required:

1. Monthly letter reports
2. Preliminary design Review
3. Phase I Final Report
4. Phase II Final Report
5. Final Report

Verbal communication between the Contractor and Sandia must be permitted at all times. Sandia reserves the right to visit the Contractor at any time and will give no greater than a five-day notice. The Contractor will collaborate with Sandia insofar as required by blade support-tower integration.

Phase 1 should be completed by February 28, 1976, and Phase 2 by May 31, 1976. Blades must be delivered by June 11, 1976. In addition, the Contractor may bid on a time schedule which deviates from the above provided that it is specified and justified.

II. CONTENTS OF PROPOSAL

A. Design

In this portion of the proposal, describe concepts to be used in designing the blades to conform with the specified guidelines. Attention should be directed toward details of blade construction with emphasis on blade cross-section geometry and methods of achieving sufficiently high stiffness-to-density ratios.

Describe relative advantages and disadvantages of designs considered, and enumerate criteria for design selection. Discuss dependence of program cost and duration of specified resonant frequency requirements in sufficient depth to influence a decision regarding resonant frequency specifications.

Describe provisions to be made for dynamic balancing of blades after their installation on the tower.

Describe analytical methods to be used in support of blade design in sufficient detail to make clear the intended approach and degree of rigor. Discuss analyses for static loads due to gravity, aerodynamic loads during nonoperating and operating status, and centrifugal loads during operation. Also include a discussion of methods of analysis for vibrations, flutter, wind gust transients, fatigue, and environmental resistance.

B. Fabrication

Describe general fabrication methods to be used and estimate production time and cost for a set of three blades, a set of four blades, and groups of twelve, twenty-four, thirty-six, and seventy-two blades.

C. Delivery

Describe methods of supporting blades during shipping and the portability and handling requirements of the blades after delivery. Discuss methods of transporting the blades from the fabrication site to the installation site.

D. Cost Estimate

Provide detailed cost estimate of each phase of this request.

E. Organization

Provide a project organization chart showing the names and functions of key personnel. Discuss company and personnel qualifications. Limit this portion of the proposal to five pages or less.

APPENDIX B

Synchronous Generator Request-For-Quotation (RFQ)

Requirements for Synchronous Generator and Controls

Application

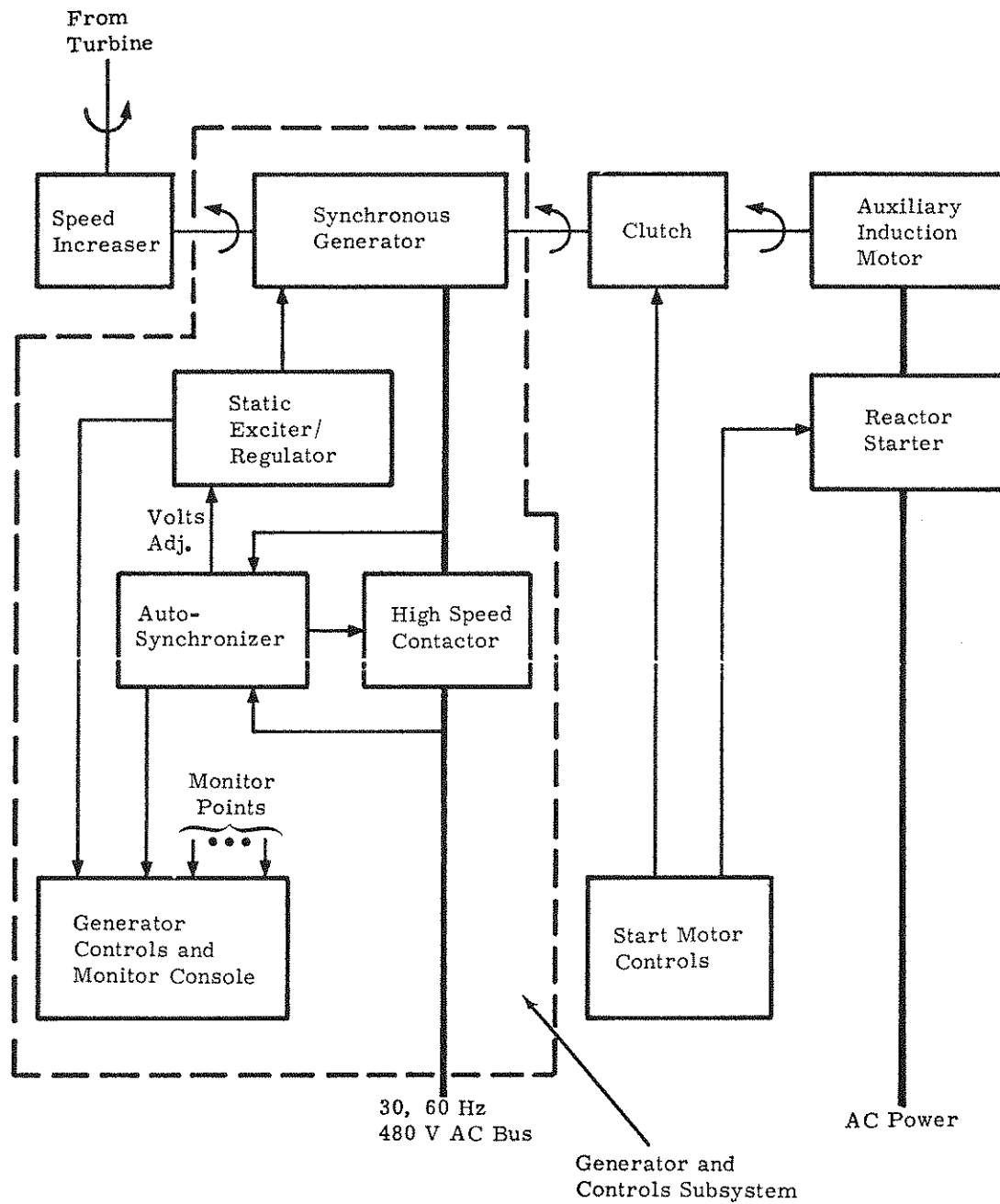
General -- This synchronous generator is to be used in Sandia Laboratories' experimental Vertical Axis Wind Turbine (VAWT) system to convert the power from the rotating shaft of the turbine to synchronous electrical power fed directly to the 3-phase utility lines. A block diagram of the generator and generator controls is shown in Figure B-1. This request covers the following items:

1. Generator
2. Static exciter/regulator
3. Autosynchronizer and power contactor
4. Generator system operator controls and monitors
5. Electrical protective devices, wiring, and switch gear necessary to conform to the latest NEMA, ASA, and ASME standards
6. Wiring the above components together into a completely packaged and tested operational system.

To permit Sandia Laboratories to accommodate the mounting and mechanical interfacing of this generator in its facility, the manufacturer will supply to Sandia at least one set of drawings which mechanically define the outline, mounting, and interface details of the generator with double shaft extensions within 3 weeks of approval and acceptance of this procurement. Within 12 weeks, the manufacturer will supply a complete set of electrical schematics and mechanical outline drawings.

Start-Up and Run Sequence -- A typical start-up and run sequence proceeds as follows:

1. The clutch to the auxiliary motor is engaged.
2. The auxiliary induction motor is started through the reactor starter.
3. The auxiliary motor spins the generator and turbine up to a speed sufficient for the turbine to extract energy from the wind.
4. The turbine drives the generator to a speed close to synchronous speed, the autosynchronizer is activated such that the generator's output voltage is regulated close to the 3-phase line's voltage, and, when the generator's output frequency and phase are sufficiently close to the line's values, the high-speed contactor is energized and the generator is smoothly brought into synchronism with the AC line and continues to run in parallel with the line. The power to or from the generator is controlled by the exciter/regulator to provide smooth transitions and prevent mechanical shocks to the system attached to the generator's shaft.
5. If synchronization is not achieved and the speed exceeds the synchronous value, the auxiliary induction motor automatically becomes a generator and limits the turbine's speed until either the wind dies down or a mechanical brake is actuated to reduce the speed to a value for synchronization to be attempted again.
6. If, while in synchronous operation, the wind speed should decrease, the synchronous generator will run as a synchronous motor maintaining constant turbine speed, within the rating of the generator.
7. After a suitably long period of time to assure proper synchronous operation of the system, the auxiliary motor is deenergized and the clutch is disengaged.



Shutdown -- If synchronization is lost or if the generator overheats, overcurrents, overvoltages, or otherwise faults, the generator is taken off line and deenergized, and an automatic brake (not shown) is activated to prevent turbine overspeed.

If the wind dies down sufficiently long, the generator is taken off line and deenergized, and the turbine is braked to a stop.

Generator Requirements

Type: Brushless synchronous

Speed: 1800 rpm

Electrical: 60 kW
3-phase
60 Hertz
0.8 power factor
277/480 volt output, Y connection
12 lead specific voltage

Insulation: Class F rated for Class B temperatures per NEMA standard

Temperature Rise: 70°C in 40°C ambient

Mechanical: Two-bearing horizontally mounted

Dripproof guarded enclosure

Overspeed: The generator must be capable of withstanding with no damage 3000-rpm shaft speed with no field excitation.

Modifications:

1. Double shaft extension
2. Temperature monitoring thermocouples: at least two to monitor stator winding temperature.
3. Exciter/rectifier/field winding protection to allow operation of the generator as a synchronous motor with across-the-line induction starting under a no-load condition.
4. Overcurrent protection shall consist of time overcurrent sensing on each phase and operation of the power contactor on overcurrent.

Optional Starting -- A cost estimate of the following optional feature is requested as a part of the reply to this request:

It may be desired to start the synchronous generator as a synchronous motor with an applied inertia load equal to 450 lb ft². A reactor starter, reduced voltage starter, or other similar device may be used to limit the in-rush current and torque on start-up.

Generator Controls

1. Static exciter/regulator for above generator having $\pm 1\%$ regulation, steady state, no load to full load with constant ambient temperature, $\pm 1\%$ thermal drift over design range.
Current boost capability to provide 200% or more short-circuit current capability for clearing faults and allowing return to normal system voltage.
Remote voltage adjustment to operate with the autosynchronizer to automatically bring the generator on line in parallel with the AC 3-phase line.
2. 3-phase sensing on regulator
3. Cross current or droop compensation for paralleling across AC line
4. Ground fault protection
5. High-speed power contactor having a maximum closing time of 0.10 second to operate in conjunction with autosynchronizer and sized for the full-load current of the 60-kW generator.
6. Autosynchronizer to provide automatic paralleling of the generator and AC 3-phase bus when the generator is within ± 15 electrical degrees and within 0.5 Hertz of the 3-phase bus. The autosynchronizer will also function with the exciter/regulator to control the generator's output voltage to within $\pm 5\%$ of the line for synchronization to occur.
7. Generator control panel for packaged units on or near generator. Sandia Laboratories will supply a suitably sized control console within which is to be mounted the following meters and controls:
 - a. Ammeter
 - b. Two voltmeters (one on generator and one on line)
 - c. Switch for ammeter and voltmeter to select each of the three phases
 - d. Frequency (dial type)
 - e. Running time
 - f. Kilowatts
 - g. Kilowatt hours
 - h. Power factor
 - i. Reverse power indication
 - j. Synchroscope and manual synchronizing switch as backup to the autosynchronizer
 - k. Manual override on volts adjust

Sandia Laboratories will supply the console and pay the shipping charges to and from the manufacturer's facility.

Tests

The following factory tests on the generator and the generator's controls and operating system are required:

1. Cold resistance of all windings.
2. Insulation resistance of all windings.
3. High potential on all windings.
4. Open-circuit saturation.

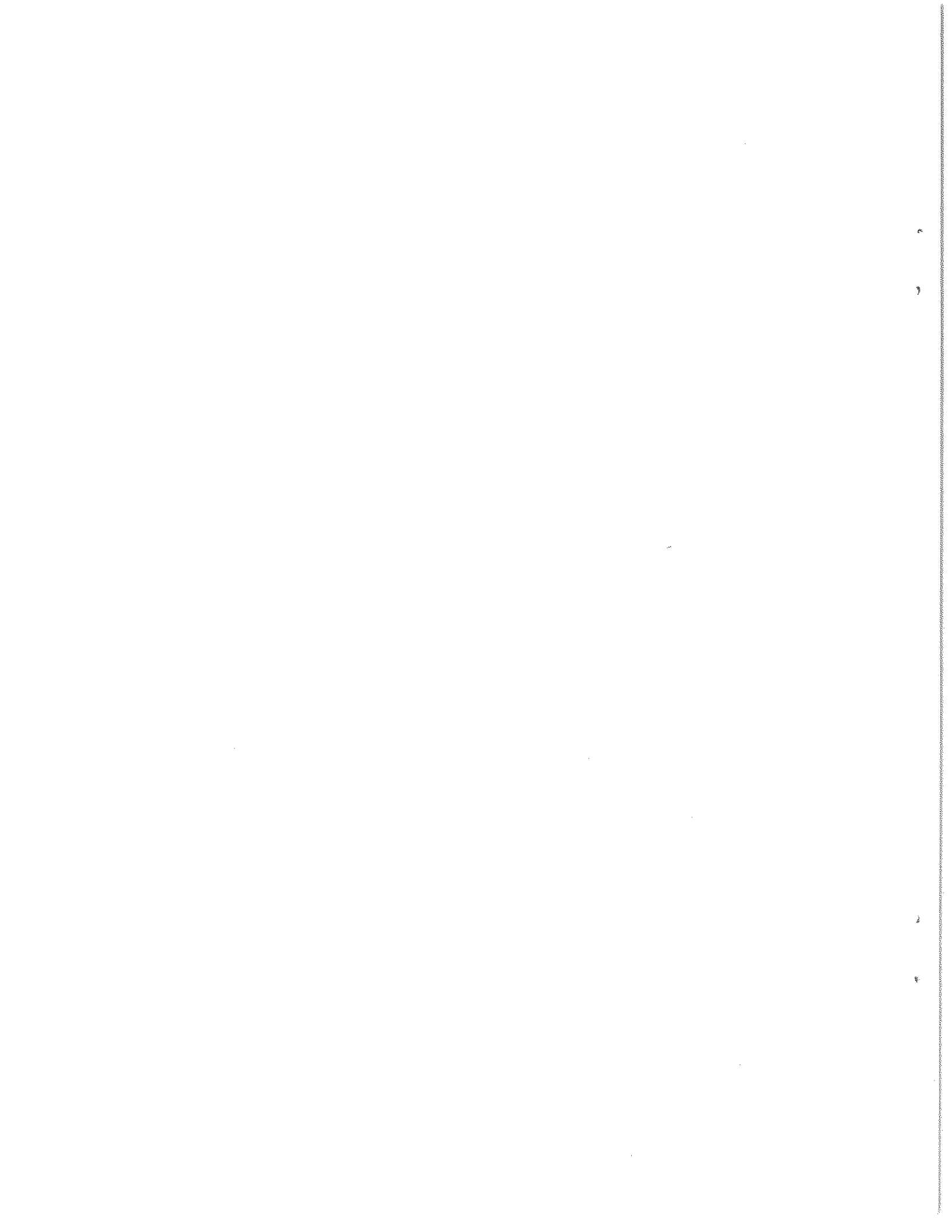
5. Voltage balance on windings.
6. Current balance on windings.
7. Regulation with regulator to be supplied with generator.
8. Voltage adjustment range of regulator.
9. Phase sequence.

Special Tests to Mil-Std-705:

1. Synchronous impedance curve.
2. Zero-power factor saturation curve.
3. Rated load current saturation curve.
4. Summation of losses.
5. Short-circuit ratio.
6. Direct-axis synchronous reactance.
7. Negative sequence reactance.
8. Zero sequence reactance.
9. Direct-axis transient reactance.
10. Direct-axis subtransient reactance.
11. Direct-axis transient open-circuit time constant.
12. Direct-axis transient short-circuit time constant.
13. Short-circuit time constant of armature windings.
14. Exciter nominal ceiling voltage.
15. Voltage waveform (harmonic analysis).
16. Regulator stability and transient response (generator only).
17. Voltage droop with regulator (generator only).
18. Inherent voltage droop (generator only).
19. Voltage regulation with regulator (generator only).
20. Inherent voltage regulation (generator only).
21. Voltage unbalance with unbalanced load line to neutral load.
22. Voltage unbalance with unbalanced load line to line load.
23. Short-circuit test (mechanical strength).
24. Shaft current.

Complete System Tests -- With the generator, exciter/regulator, autosynchronizer, power contactor, and operator monitors and controls in place, a complete system test will be performed by the manufacturer, prior to delivery to Sandia, to verify proper manual and automatic operation of the generator system from start-up through autosynchronization, parallel operation across the line, and manual shutdown. For this test the generator may be driven by a suitable engine or electric motor. Sandia Laboratories personnel may be present during this test to gain familiarity with operating the hardware.

APPENDIX C
Sandia Publications and Presentations



PREVIOUS SANDIA PUBLICATIONS AND
PRESENTATIONS

Sandia Publications

- SAND74-0071 Wind Energy Potential in New Mexico, J. W. Reed, R. C. Maydew, B. F. Blackwell, July 1974.
- SAND74-0100 Practical Approximations to a Troposkien by Straight-Line and Circular-Arc Segments, G. E. Reis, B. F. Blackwell, March 1975.
- SAND74-0105 An Electrical System for Extracting Maximum Power from the Wind, A. F. Veneruso, December 1974.
- SLA-74-0154 Blade Shape for a Troposkien Type of Vertical-Axis Wind Turbine, B. F. Blackwell, G. E. Reis, April 1974.
- SLA-74-0160 The Vertical-Axis Wind Turbine - How it Works, B. F. Blackwell, April 1974.
- SAND74-0177 Some Geometrical Aspects of Troposkiens as Applied to Vertical-Axis Wind Turbines, B. F. Blackwell, G. E. Reis, March 1975.
- SLA-74-0298 A Wind-Powered Fresh Water Condensation Air Conditioning, Mariculture, and Aquiculture Integrated System for Pacific Atolls, D. B. Shuster, V. L. Dugan, R. H. Richards, June 1974.
- SAND74-0348 Wind Power Climatology of the United States, J. W. Reed, May 1975.
- SAND74-0378 Nonlinear Stress Analysis of Vertical-Axis Wind Turbine Blades, L. L. Weingarten, R. E. Nickell, April 1975.
- SAND74-0379 An Investigation of Rotation-Induced Stresses of Straight and of Curved Vertical-Axis Wind Turbine Blades, L. V. Feltz, B. F. Blackwell, March 1975.
- SAND74-0435 Wind Power Climatology, J. W. Reed, December 1974.
- SAND75-0165 Application of the Darrieus Vertical-Axis Wind Turbine to Synchronous Electrical Power Generation, J. F. Banas, E. G. Kadlec, W. N. Sullivan, March 1975.
- SAND75-0166 Wind Energy - A Revitalized Pursuit, B. F. Blackwell, L. V. Feltz, March 1975.
- SAND75-0204 Methods for Performance Evaluation of Synchronous Power Systems Utilizing the Darrieus Vertical-Axis Wind Turbine, J. F. Banas, E. G. Kadlec, W. N. Sullivan, April 1975.
- SAND75-0431 The Darrieus Turbine: A Performance Prediction Model Using Multiple Streamtubes, J. H. Strickland, October 1975.
- SAND75-0530 Engineering of Wind Energy Systems, J. F. Banas, W. N. Sullivan, January 1976.
- SAND76-0130 Wind Tunnel Performance Data for the Darrieus Wind Turbine with NACA-0012 Blades, B. F. Blackwell, L. V. Feltz, R. E. Sheldahl, to be published.
- SAND76-0131 Wind Tunnel Performance Data for Two- and Three-Cup Savonius Rotors, B. F. Blackwell, L. V. Feltz, R. E. Sheldahl, to be published.

External Publications

- U. S. Patent Number 3,918,839, "Wind Turbine," 16 Claims, B. F. Blackwell, L. V. Feltz, R. C. Maydew, November 11, 1975.
- J. W. Reed, "Wind Power Climatology," Weatherwise, 27, 6, December 1974, and SAND74-0435, Sandia Laboratories, December 1974.
- J. W. Reed, R. C. Maydew, and B. F. Blackwell, A Report of the Governor's Select Committee on Wind Energy, "Wind Energy Potential in New Mexico," Santa Fe, NM, June 7, 1975.
- L. L. Weingarten and R. E. Nickell, "Nonlinear Stress Analysis of Vertical-Axis Wind Turbine Blades," Journal of Engineering for Industry, Transactions ASME, Vol. 97, Series B, No. 4, November 1975, pp. 1234-1237.

Presentations

- J. W. Reed, "Some Notes on Wind Power Climatology," American Meteorological Society Climatology Conference, Asheville, NC, October 8-11, 1974.
- L. V. Feltz, "Wind Power - A Revitalized Pursuit," Heights Lions Club, Albuquerque, NM February 13, 1975.
- B. F. Blackwell, "Wind Energy - A Revitalized Pursuit," ASME Resource Recovery Symposium, Albuquerque, NM, March 6-7, 1975.
- R. C. Maydew, "Wind Energy," New Mexico State University, Las Cruces, NM, March 14, 1975.
- L. V. Feltz, "Wind Power - A Revitalized Pursuit," Sierra Club, University of Colorado, Boulder, CO, March 22, 1975.
- J. W. Reed, "Wind Energy Potential in the Southwest," Southwestern Technology Utilization Conference, Albuquerque, NM, April 16-17, 1975.
- L. V. Feltz, "Wind Power - A Revitalized Pursuit," New Mexico IEEE Spring Symposium on Energy Research in New Mexico, Albuquerque, NM, April 17-18, 1975.
- J. W. Reed, "Wind Power Climatology," New Mexico IEEE Spring Symposium on Energy Research in New Mexico, Albuquerque, NM, April 17-18, 1975.
- J. W. Reed, "Wind Power Climatology Research at Sandia Laboratories," 51st Annual American Association for the Advancement of Science Southwestern Division Meeting, Energy Resources Symposium, Los Alamos, NM, April 23-26, 1975.
- R. H. Braasch, "Power Generation with a Vertical Axis Wind Turbine," Wind Workshop II, Washington, DC, June 9-11, 1975.
- J. W. Reed, "Wind Climatology," ERDA-NSF Wind Energy Conversion Symposium Workshop, Washington, DC, June 9-11, 1975.
- J. W. Reed and B. F. Blackwell, "Some Climatological Estimates of Wind Power Availability," 2nd U. S. National Conference on Wind Engineering Research, Ft. Collins, CO, June 23-25, 1975.
- B. F. Blackwell and G. E. Reis, "Geometrical Aspects of the Troposphere as Applied to the Darrieus Vertical-Axis Wind Turbine," ASME Paper 75-DET-42, ASME Design Engineering Technical Conference, Washington, DC, September 1975
- A. F. Veneruso, "VAWT Technology," New York Ocean Science Laboratory, Montauk, Long Island, NY, August 20, 1975.
- L. V. Feltz, "Wind Energy Potential," Bureau of Indian Affairs, Juneau, Alaska, September 11, 1975.
- A. F. Veneruso, "VAWT Technology," United Nations Office of Technical Cooperation, UN Hdqs, NY, September 25, 1975.
- L. L. Weingarten, "Nonlinear Stress Analysis of Vertical-Axis Wind Turbine Blades," ASME Paper 75-DET-35, ASME Design Engineering Technical Conference, Washington, DC, September 1975.
- R. C. Reuter, "Wind Power," Rio Grande Lions Club, Albuquerque, NM, October 10, 1975.
- E. G. Kadlec, "Sandia Wind Power Program," American Wind Energy Association, Santa Rosa, CA, October 11, 1975.
- E. G. Kadlec, "Sandia Wind Power Program," Iowa 2000 Conference, Ames, Iowa, October 12, 1975.
- A. F. Veneruso, "VAWT Technology and Electrical Considerations for Utilities," Public Service Company of NM, Albuquerque, NM, October 23, 1975
- L. L. Weingarten and L. V. Feltz, "Material and Manufacturing Considerations for the Vertical-Axis Wind Turbine," Seventh National Society for the Advancement of Material and Process Engineering Technical Conference, Albuquerque, NM, October 1975.
- E. G. Kadlec, "Sandia Wind Power Program," Industrial College of the Armed Forces, Albuquerque, NM, December 8, 1975.

DISTRIBUTION:

TID-4500-R64, UC-60 (249)

R. J. Templin
Low Speed Aerodynamics Section
NRC-National Aeronautical Establishment
Ottawa 7, Ontario, Canada K1A0R6

A. Robb
Memorial Univ. of Newfoundland
Faculty of Eng. & Applied Sciences
St. John's, Newfoundland
Canada A1C 5S7

H. Sevier
Rocket and Space Division
Bristol Aerospace Ltd.
P. O. Box 874
Winnipeg, Manitoba
R3C 2S4 Canada

V. A. L. Chasteau
Department of Mech. Engineering
The University of Auckland
Private Bag
Auckland, New Zealand

G. Herrera
Jet Propulsion Lab
4800 Oak Grove Drive
Pasadena, CA 91103

NASA Langley Research Center
Hampton, VA 23665
Attn: R. Muraca, MS 317

NASA Lewis Research Center (2)
2100 Brookpark Road
Cleveland, OH 44135
Attn: J. Savino, MS 500-201
R. L. Thomas

ERDA (3)
1800 G. Street NW
Washington, DC 20550
Attn: L. Divone

University of New Mexico (2)
Albuquerque, NM 87106
Attn: K. T. Feldman
Energy Research Center
V. Skoglund
ME Department

A. N. L. Chiu
Wind Engineering Research Digest
Spalding Hall 357
University of Hawaii
Honolulu, HI 96822

R. N. Meroney
Colorado State University
Dept. of Civil Engineering
Fort Collins, CO 80523

A. G. Vacroux
Illinois Institute of Technology
Dept. of Electrical Engineering
Chicago, IL 60616

New Mexico State University
P. O. Box 3450
Las Cruces, NM 88003
Attn: M. M. Sluyter

Oklahoma State University (2)
Stillwater, OK 74074
Attn: W. L. Hughes
EE Department
D. K. McLaughlin
ME Department

Oregon State University (2)
Corvallis, OR 97331
Attn: R. Wilson
ME Department
R. W. Thresher
ME Department

Texas Tech University (2)
P. O. Box 4289
Lubbock, TX 79409
Attn: K. C. Mehta
CE Department
J. Strickland
ME Department

R. G. Watts
Tulane University
Dept. of Mechanical Engineering
New Orleans, LA 70018

M. Snyder
Aero Engineering Department
Wichita State University
Wichita, KS 67208

ERDA
Nevada Operations Office (2)
P. O. Box 14100
Las Vegas, NV 89114
Attn: R. Ray, Operations
H. Mueller, ARL

DISTRIBUTION (cont):

Los Alamos Scientific Lab (7)
P. O. Box 1663

Los Alamos, NM 87544

Attn: R. R. Brownlee, J-9
J. R. Bartlit, Qu-26
J. D. Balcomb, Q-DO-T
R. G. Wagner, P-5
J. Nachamkin, T-DO-TEC
S. W. Depp, E-DO
H. Deinken, ADWP-1

ERDA/ALO (3)

Kirtland AFB East
Albuquerque, NM 87115

Attn: D. K. Knowlin
D. C. Graves
D. W. King

R. Camarero
Faculty of Applied Science
University of Sherbrooke
Sherbrooke, Quebec
Canada J1K 2R1

American Wind Energy Association
21243 Grand River
Detroit, MI 48219

E. E. Anderson
Dept. of Mechanical Engineering
South Dakota School of Mines & Tech.
Rapid City, SD 57701

E. S. Takle
Climatology and Meteorology
312 Curtiss Hall
Iowa State University
Ames, IA 50010

P. B. S. Lissaman
Aeroenvironment, Inc.
660 South Arroyo Parkway
Pasadena, CA 91105

R. A. Parmelee
Department of Civil Engineering
Northwestern University
Evanston, IL 60201

J. Park
Helion
P. O. Box 4301
Sylmar, CA 91342

W. F. Foshag
Aerophysics Company
3500 Connecticut Avenue NW
Washington, DC 20008

W. L. Harris
Aero/Astro Department
MIT
Cambridge, MA 02139

K. Bergey
Aero Engineering Department
University of Oklahoma
Norman, OK 73069

J. Fischer
F. L. Smidth & Company A/S
Vigerslevalle 77
2500 Valby
Denmark

H. M. Busey
DMA, Safety and Facilities A-364
ERDA Headquarters
Washington, DC 20545

P. Bailey
P. O. Box 3
Kodiak, AK 99615

M. E. Beecher
Solar Energy Collection
Arizona State University
University Library
Tempe, AZ 85281

U. A. Coty
Lockheed - California Co.
Box 551-63A1
Burbank, CA 91520

Lawrence Livermore Laboratory (2)
P. O. Box 808 L-340
Livermore, CA 94550
Attn: D. W. Dorn
D. Hardy

J. A. Garate
General Electric Co.
Valley Forge Space Center
King of Prussia, PA 19406

O. Krauss
Division of Engineering Research
Michigan State University
East Lansing, MI 48824

A. H. Stodhart
Electrical Research Associates
Cleeve Road
Surrey, England

DISTRIBUTION (cont):

V. Nelson
Department of Physics
West Texas State University
P. O. Box 248
Canyon, TX 79016

E. Gilmore
Amarillo College
Amarillo, TX

R. K. Swanson
Southwest Research Institute
San Antonio, TX 78228

U. S. Department of Agriculture
Agriculture Research Center
Building 303
Beltsville, MD 20705
Attn: L. Lilj Dahl

University of Alaska
Geophysical Institute
Fairbanks, AK 99701
Attn: T. Wentink, Jr.

E. J. Warchol
Bonneville Power Administration
1002 NE Holladay
Portland, OR 97208

W. Batesole
Kaman Aerospace Corporation
Bloomfield, CT 06002

Stanford University
Stanford Electronics Laboratories
Radioscience Laboratory
Stanford, CA 94305
Attn: A. V. da Rosa

Dr. O. Ljungström
Sälgstigen 12, S-181 62
Lidingö 3
Sweden

H. Dörner
Institut Für Flugzeugbau Der
Universität Stuttgart
7000 Stuttgart 80, Pfaffenwaldring 31
Germany

Dr. A. Fritzsche
Manager, Mechanical Design and Systems
Dornier System GmbH
Postfach 1360
7990 Friedrichshafen
Germany

1000 G. A. Fowler
1200 W. A. Gardner
1280 T. B. Lane
1284 R. T. Othmer
1284 W. N. Sullivan
1284 L. I. Weingarten
1300 D. B. Shuster
1320 M. L. Kramm
1324 E. C. Rightley
1324 L. V. Feltz
1324 D. F. McNeill
1330 R. C. Maydew
1333 S. McAlees, Jr.
1333 B. F. Blackwell
1333 R. E. Sheldahl
1400 A. Y. Pope
3161 J. E. Mitchell (50)
5000 A. Narath
5431 D. W. Lobitz
5443 J. W. Reed
5700 J. H. Scott
5710 G. E. Brandvold
5715 R. H. Braasch
5715 E. G. Kadlec (100)
5715 C. E. Longfellow
5715 R. C. Reuter
5715 R. S. Rusk
5715 A. F. Veneruso
5740 V. L. Dugan
5742 S. G. Varnado
5742 J. F. Banas
8000 T. B. Cook, Jr.
8100 L. Gutierrez
8110 A. N. Blackwell
8300 B. F. Murphey
8320 T. S. Gold
9622 R. C. Anderson
9743 K. G. Grant
8266 E. A. Aas (2)
3141 C. A. Pepmueller (Actg.) (5)
3151 W. L. Garner (3)
For ERDA/TIC (Unlimited Release)

Reprinted January 1980

